Exploring the Biological Functions of AlkB Proteins and How They Relate to AAG

by

Chun-Yue Lee

B.S., Chemical Engineering (2002)
University of California, Berkeley

Submitted to the Department of Chemical Engineering
in Partial Fulfillment of the Requirements for the Degree of

Doctor of Philosophy in Chemical Engineering
at the
Massachusetts Institute of Technology

February 2009

Signature of Author .....
Department of Chemical Engineering
October 15, 2008

Certified by .....
Leona D. Samson
Professor of Biological Engineering and Biology
Thesis Supervisor

Certified by .....
Linda G. Griffith
Professor of Biological and Mechanical Engineering
Thesis Supervisor

Accepted by.....
William M. Deen
Professor of Chemical Engineering
Chairman, Committee for Graduate Students

TABLE OF CONTENTS

Acknowledgment

It's so hard to believe that I'm actually writing a thesis, near the end of the grad school tunnel! There are so many people I have to thank here. Without their help and support, this thesis would not have been possible. I would like to thank my advisors Leona Samson and Linda Griffith for their support, help, and guidance, and the opportunity to work on the project. I also thank my thesis committee, Profs. Doug Lauffenberger and Dane Wittrup, for their helpful comments over the years.

Also there are many research collaborators outside of the Samson lab I need to thank. I have to thank Jim Delaney for his extensive library of oligonucleotides, Sureshkumar Muthupalani for the histopathological scores of mouse colons, Cintyu Wong for the purified AlkB protein, Eric Campeau for letting me use his wonderful expression constructs, and Jose McFaline from the Dedon lab for his help on lesion measurement.

The Samson lab members have also been wonderful and very helpful. Lisiane Meira has been incredible. She has helped me tremendously and given me so much advice. The lab is never the same without her! Also I'm indebted to Catherine Moroski for all her help and encouragement, especially on the mouse work. Jennifer Calvo has been amazing in giving me advice and comments on my thesis. I also need to thank all the present and past Samson lab members for tolerating me!

My friends have also been very important to me throughout these many years. I don't know if I would be able to survive the frustration without the fun and entertainment provided by them. Even having dinner on the weekends is a fun activity to look forward to! Hiroyo Kawai, Yinthai Chan, Cha Kun Lee, Janet Tse, Jujin An, Chung Tin, Raymond Lam, Patrick Sit, and many others have provided wonderful friendships over the years. Of course, Leehom Wang must be acknowledged for providing me with inspiration and moral support. Even though he doesn't know me at all, his music has been a great source of motivation that keeps me company through the years.

Finally, I would like to thank my family, which is the most important part of my life. My parents, my sister, and my husband Louis Wong have given me unconditional love and support and I know they will always be there for me no matter what.

ABBREVIATIONS:

εA, 1,N^6-ethenoadenine;
εC, 3,N^4-ethenocytosine;
1,N^2-εG, 1,N^2-ethenoguanine;
1MeA, 1-methyladenine;
1MeG, 1-methylguanine;
3EtU, 3-ethyluracil;
3-MeA, 3-methyladenine;
3MeC, 3-methylcytosine;
3MeT, 3-methylthymine;
3MeU, 3-methyluracil;
8oxoG, 8-oxo-7,8-dihydroguanine;
AAG, human 3-methyladenine DNA glycosylase;
ABH, AlkB homolog;
AlkA, *E. coli* 3-methyladenine DNA glycosylase;
AOM, Azoxymethane;
AP, apurinic;
BCNU, 1,3-bis(2-chloroethyl)-1-nitrosourea;
BER, base excision repair;
BSA, bovine serum albumin;
COX2, cyclooxygenase-2;
CRC, colorectal cancer;
dRPase, 5'-deoxyribo-phosphodiesterase;
DSS, dextran sulfate sodium;
EA, 1,N^6-ethanoadenine;
EDTA, ethylenediaminetetraacetic acid;
EGTA, ethylene glycol-bis(2-aminoethylether)-*N,N,N',N'*-tetraacetic acid;
ER, endoplasmic reticulum;
H&E, Hematoxylin and Eosin;
HA, hemagglutinin;
HCC, hepatocellular carcinoma
Hx, hypoxanthine;
IBD, inflammatory bowel disease;
IL-10, interleukin-10;
M1G, pyrimido[1,2-α]purin-10(3*H*)one;
MeLex, methyl lexitropsin;
MGMT, O^6-methylguanine methyltransferase;
MMS, methyl methanesulfonate;
MNU, methyl nitrosourea;
NSAIDs, nonsteroidal anti-inflammatory drugs;
O^6-BG, O^6-benzylguanine;
PCNA, proliferating cell nuclear antigen;
Polβ, polymerase beta;
RONS, reactive oxygen and nitrogen species;
SMUG1, single-strand-selective monofunctional uracil-DNA glycosylase 1;

U, uracil;
UC, ulcerative colitis;
UDG, uracil DNA glycosylase;

Exploring the Biological Functions of AlkB Proteins and How They Relate to AAG

by

Chun-Yue Lee

Submitted to the Department of Chemical Engineering
on October 15, 2008 in Partial Fulfillment of the
Requirements for the degree of Doctor of Philosophy in
Chemical Engineering

ABSTRACT

Our DNA is constantly under the assault of DNA damaging agents that are ubiquitous in nature and unavoidable. Fortunately, our cells have evolved DNA repair mechanisms to maintain genomic integrity against this constant attack. An important type of DNA damage is alkylation damage, which has been the focus of this thesis, the major goal of which is to explore the biological role of a set of alkylation repair proteins, the *E. coli* AlkB and two human AlkB homologs (ABH2 and ABH3), and how they relate to the 3-methyladenine DNA glycosylase (AAG). AAG is a base excision repair (BER) protein that has been well-studied and is known to be involved in the repair of a wide variety of substrates. On the other hand, the direct reversal protein AlkB, and its human homologs, have not been so extensively characterized, but it is known that they can repair not only DNA, but also RNA. Although there are eight human AlkB homologs, attention was focused on ABH2 and ABH3 since they are the more well-characterized homologs and recently implicated in DNA repair.

In order to investigate the role of the AlkB proteins, particularly in mammalian cells, I expressed ABH2 and ABH3 in established human cell lines and investigated whether their expression would enhance cell survival after alkylation treatment. However, no detectable phenotype was observed in the cell lines upon treatment with the alkylating agent methyl methanesulfonate (MMS). This is possibly due to endogenous ABH levels being sufficient for repair. We therefore turned to characterization of the *Abh2* and *Abh3* null mice, as compared to wildtype and to another alkylation repair deficient animal, *Aag* null mice. In addition to the primary substrates 1-methyladenine and 3-methylcytosine, AlkB, ABH2, and ABH3 can also repair an important class of damage, the etheno base DNA lesions, which can also be repaired by AAG. Here we have shown in a mouse model that Abh2 and Abh3 overlap with Aag in protecting mice from sensitivity in response to chemically induced chronic inflammation, in which etheno base lesions are readily generated. In addition, we also employed a biochemical approach using a comprehensive library of lesion-containing DNA oligonucleotides to study the redundancy in repair activity between AAG and AlkB. In doing so, we have found new substrates for AAG and in particular, 1-methylguanine, is a new substrate shared between

AAG and AlkB. Thus, although these two proteins employ different mechanisms for repair, our studies established further evidence of the interplay between these proteins and the different repair pathways they represent, underscoring the importance of alkylation damage repair for proper cell homeostasis.

Thesis Supervisor: Leona D. Samson
Title: Professor of Biological Engineering and Biology

Thesis Supervisor: Linda G. Griffith
Title: Professor of Biological and Mechanical Engineering

1. CHAPTER 1 – Introduction and Background

1.1. Types of DNA damaging agents and significance

Alkylating agents are frequently found both endogenously and in our exogenous environment and are commonly used in chemotherapy to treat cancer patients. Because of their clastogenic and cytotoxic effects on tumor cells, they are extremely potent as chemotherapeutic drugs. DNA damage from endogenous sources, mainly spontaneous depurination, oxidation, alkylation, and deamination of bases, leads to about 20,000 lesions per day per cell (*1*).

Alkylating agents can attack DNA at *O*- and N- atoms in the nucleotide bases and *O*-atoms in the phosphodiester bonds and can be divided into S_N1 and S_N2 agents. Both N and *O* alkylations are frequently produced by S_N1 agents while S_N2 agents mainly introduce alkyl adducts at the N positions (*2*). Different alkylation patterns result depending on the alkylating agent, position in the DNA or RNA, and whether the DNA is single- or double-stranded. Monofunctional alkylating agents have one reactive alkyl group that interacts with single nucleophilic centers in DNA whereas bifunctional agents have reactive groups that can interact with two sites. These agents usually attack DNA by simple methylation or more complicated alkylation that can go on to cause crosslink formation (*3*).

1.2. DNA Repair by different mechanisms

Exogenous and endogenous agents are always present to damage DNA and thus, cells have developed several repair mechanisms to protect themselves.

The major DNA repair mechanisms include:

(i) direct reversal of DNA damage
    a. photoreactivation
    b. O^6-methylguanine methyltransferase (MGMT)
    c. oxidative demethylation

(ii) excision repair
    a. base excision repair
    b. nucleotide excision repair
    c. mismatch repair

(iii) tolerance/avoidance
    a. translesion DNA synthesis
    b. DNA recombination

(iv) DNA double-strand break repair
    a. homologous recombination
    b. non-homologous end joining

Excision repair, tolerance/avoidance, and double-strand break repair are multi-step pathways whereas direct reversal of DNA damage, particularly repair by the MGMT and AlkB proteins, involves one step only. Two of the direct reversal repair mechanisms and base excision repair are discussed in the following sections.

1.2.1. Direct reversal of base damage

The simplest form of DNA repair is the direct reversal of damaged bases to normal bases. Mechanisms can involve direct acceptance of the alkyl group to a protein's active site or catalytic demethylation. Direct repair proteins may act alone or involve cofactors and cosubstrates. The O^6-methylguanine methyltransferase (MGMT) and *E. coli* AlkB and the human AlkB homologs (hABH), fall under this class and will be discussed in more detail in later sections.

1.2.2. Base excision repair (BER)

The base excision repair (BER) pathway involves multiple proteins and is quite complex. Single base aberrations or modification by oxidation or alkylation, sites of base loss and strand breaks from chemical attack can be repaired by BER. First, an inappropriate base is removed by a DNA glycosylase; the glycosylase binds to a target base and cleaves the glycosylic bond, leaving an abasic site behind. The abasic site is then recognized by an AP endonuclease that cleaves the phosphodiester bond 5' to the lesion to produce a strand break with a 3' OH and a 5' abasic end. Then short-patch BER utilizes a 5'-deoxyribo-phosphodiesterase (dRpase) DNA to remove the 5' abasic site and Polβ fills in the single nucleotide gap. DNA ligase I or III seals the nick. Long-patch BER replaces more than one nucleotide and is divided into two paths, both involve PCNA, one Polβ-directed and the other Polδ/ε -directed. The type of repair pathways used depends on the substrate to

be repaired and perhaps the cell type. See Figure 1-1 below for a general scheme of BER (*4*).

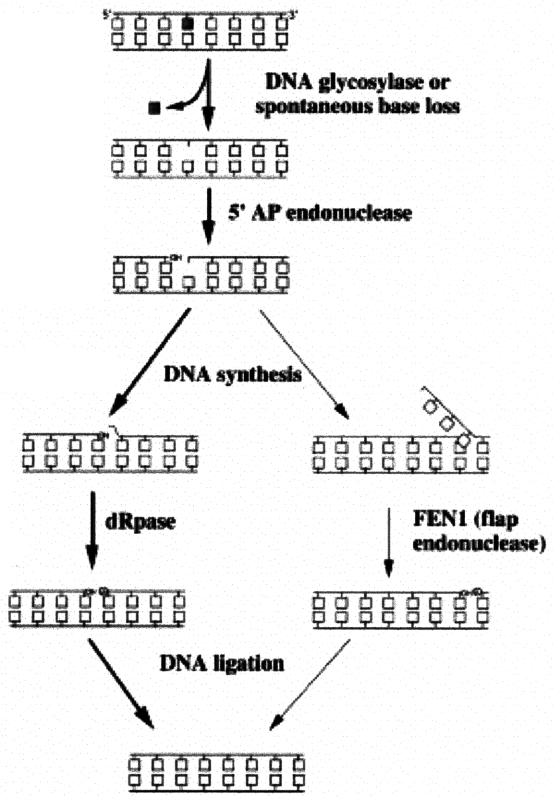

Figure 1-1 General scheme of the base excision repair pathway (left: short-patch; right: long-patch) (Adopted from ref (*4*))

1.3. DNA repair genes

1.3.1. 3-Methyladenine DNA Glycosylase

In *E. coli*, there are two 3MeA DNA glycosylases, the inducible AlkA and the constitutively expressed Tag proteins. Tag and AlkA recognize 3MeA and 3MeG but AlkA also recognizes deamination product of adenine, ring opened purines, some oxidation products like etheno-adducts and also O^2-alkylated pyrimidines (*4-6*). The human 3MeA DNA glycosylase (AAG) differs from AlkA and Tag at both the sequence

and structural level, but it recognizes a wide variety of substrates as does AlkA, with the exception of O^2-alkylated pyrimidines (*7*).

DNA glycosylases act by cleaving the N-glycosylic bond between the damaged base and the deoxyribose sugar to give an abasic site, initiating the base excision repair pathway (see Figure 1-1). One of the main DNA repair genes being extensively investigated in the Samson lab is the 3MeA DNA glycosylase (AAG/Aag), which recognizes a wide range of damaged DNA bases in human and mouse cells, respectively. The release of structurally diverse substrates appears to depend on the weakening of the glycosylic bond (*8*). Base removal by AAG requires that the damaged nucleotide be flipped out from the interior of the helix into the catalytic cavity. Binding and release of the base depends on the shape of the base, hydrogen bonding characteristics, aromaticity and salt bridging between the enzyme and flanking phosphates in DNA (*9*). A water molecule is positioned and deprotonated by Glu125 and the nucleophile attacks the glycosylic bond (*9*).

AAG is needed at an appropriate level to protect cells from the toxicity, clastogenicity, and mutagenicity of alkylating agents. AAG, at appropriate levels, can remove 3MeA that left unrepaired replication block that is toxic to the cell. The biological consequences of modulating the activity of AAG are not always predictable (*10*). Previous studies have shown that increased expression of AAG in many cases did not protect but rather sensitized cells to mutagenic effects or cell death. Inappropriate AAG expression, which can create an imbalance in BER enzymes expression, can cause

accumulation of BER intermediates downstream of the AAG in the form of abasic sites or single-strand breaks that may be more lethal than unrepaired alkyl base lesions (*4*). The resistance or sensitization by AAG (Aag in mice) to the damage induced by alkylating agents is tissue-specific. For example, Aag-deficient mouse bone marrow cells have increased resistance to methyl methanesulfonate (MMS) and methyl lexitropsin (MeLex) compared to wild-type bone marrow cells (*10*). On the other hand, Aag null mouse embroyonic stem cells are sensitive to MMS and MeLex, and also to BCNU and to mitomycin C (*11*). Such complicated effects make the BER enzymes less attractive for straightforward therapy.

Common alkylating agents such as mitomycin-C (MMC), carmustine (BCNU), chloronitrosourea (CNU), and the nitrogen mustards can induce mono-alkyl adducts that go on to cause DNA interstrand cross-links; such crosslinks prevent strand separation during DNA replication and interfere with chromosome segregation. AAG may relieve this toxicity by repairing the mono-alkyl lesions that lead to these interstrand cross-links (*4*).

1.3.2. O^6-Methylguanine DNA Repair Methyltransferase (MGMT)

O^6-methylguanine DNA repair methyltransferase (MGMT), or more generally O^6-alkylguanine DNA alkyltransferase, is a direct reversal repair protein that transfers the methyl (or alkyl) group from the O^6 position of guanine (and to a much smaller extent, from the O^4 position of thymine) to a cysteine residue in its active site; methyltransfer inactivates MGMT in the stoichiometric repair process (Figure 1-2a). In *E. coli*, there are

two genes encoding DNA repair methyltransferases, the constitutively expressed *ogt* (*12*) and the inducible *ada* of the Ada regulon. Both Ada and Ogt repair O^6MeG and O^4MeT while Ada also repairs alkylphosphotriesters. Mammalian MGMT does not repair O^4MeT very efficiently and does not repair methyl phosphotriesters. MGMT not only removes methyl groups but also ethyl-, n-propyl-, n-butyl- and 2-chloroethyl from the O^6-position of guanine (*7*).

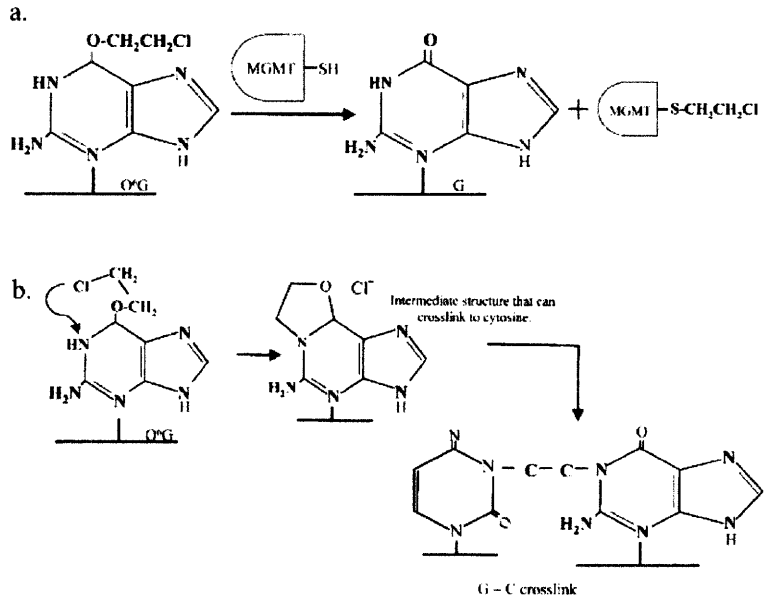

Figure 1-2 a. Chloroethyl adduct removal by MGMT; b. Unrepaired chloroethyl adduct results in interstrand G-C crosslink (Adopted from ref (*13*))

O^6-alkylG and O^4-alkylT lesions can be produced by a wide range of monofunctional and bifunctional alkylating agents including BCNU, cyclophosphamide, dacarbazine, lomustine (CCNU), procarbazine, streptozocin, and temozolomide (*14*), all of which are used in the cancer clinic of chemotherapy.

Alkyl lesions induced by chemotherapeutic agents and cell death

The MGMT protein repairs O^6-alkyl lesions, which can be produced by two classes of alkylating agents, the chloroethylating agents and simple methylating agents. Chloroethylating agents attack the O^6 position of guanine to produce a base lesion that can go on to cause an interstrand crosslink between that guanine and the cytosine on the opposite strand as shown in Figure 1-2b. If such G-C crosslinks do not get repaired efficiently, DNA replication can stall and single- and double-strand breaks can form. These lesions can be toxic enough to cause cell death. However, if the O6-chloroethylguanine lesion is repaired by MGMT, crosslink formation is prevented and toxicity avoided (Figure 1-2a).

The protein inactivates itself during the repair process and acts independently of other proteins. MGMT binds DNA and scans for O^6 alkylation (*15*). The hydrophobic active site accepts the alkyl group and hydrogen-bonds with side-chain residues next to the acceptor Cys145 (*16*). The alkylated inactivated MGMT falls off the DNA quickly and is degraded very rapidly relative to the unalkylated protein (*17*).

Methylating agents, such as procarbazine, temozolomide, streptozotocin, and dacarbazine, are the second class of alkylating agents that produce O^6 alkyl lesions disrupting hydrogen bonding to cytosine but does not cause much distortion. This results in O^6MeG:T mispairs, ultimately leading to a point mutation of G to A. The toxicity of these lesions comes from initiation of mismatch repair. Since mismatch repair targets the

newly synthesized strand, the original O^6-MeG will not get repaired. A thymine will be incorporated opposite to the O^6-MeG and mismatch repair will again recognize and excise the T, leading to iterative and futile repair of the daughter strand (futile cycling). Although O^6-MeG lesions are not as cytotoxic as the interstrand crosslinks induced by chloroethylating agents, the DNA strand breaks from futile mismatch repair can induce apoptosis (*18*). Cells and tissues express MGMT at different levels (*19-21*). Overexpression of MGMT in transgenic mice protects against thymic lymphomas induced by methyl nitrosourea (MNU) (*22*) whereas *Mgmt*-knockout mice are exceedingly sensitive and develop many lymphomas (*23, 24*).

O^6-BG-resistant mutant MGMT

The irreversible inactivation of MGMT upon covalent transfer of the adduct allows any substrate for the protein to be an irreversible inhibitor of MGMT. This has actually been exploited in chemotherapy to increase a tumor's sensitivity to alkylating agents, of which O^6-benzylguanine (O^6-BG) is a candidate. MGMT can be inhibited by O^6-BG, which is used frequently in combination with alkylating agents that produce O^6-MeG to treat solid tumors such as brain tumor, where the endogenous MGMT level is high. The inhibitor O^6-BG inhibits MGMT by the transfer of the benzyl group to the active site cysteine residue of the MGMT protein (*25*).

1.3.3. AlkB/human AlkB Homologs (hABH)

The *E. coli alkB* gene was discovered as early as 1983, 25 years ago, with the isolation of *alkB* mutants specifically sensitive to the S_N2-type methylating agent MMS but not to

S_N1 alkylating agents (*26*). *E. coli* AlkB was also shown to give the same kind of alkylation resistance in human cell lines, as in *E. coli* cells (*27*). However, the human AlkB homolog (hABH) proteins have only been shown in recent years to give *E. coli* cells alkylation resistance, repairing DNA and/or RNA. These proteins have also been a main subject of exploration due to its simple direct repair capability. Sequence alignment showed that the iron-binding and 2-oxoglutarate-binding sites are conserved in the bacterial and the human proteins. In fact, AlkB and its human homologs belong to the 2-oxoglutarate/Fe oxygenase superfamily. These proteins (AlkB, ABH2, and ABH3) are involved in catalyzing oxidative demethylation reactions directly reverting damage primarily reverting 1MeA and 3MeC to A and C, respectively (*28, 29*).

Repair mechanism and preferred substrates

AlkB differs from many other DNA repair proteins in that it depends on unexpected cofactors for activity. In a bioinformatics study by Aravind and Koonin in 2001, AlkB was identified as a member of the superfamily of dioxygenases that require oxygen, 2-oxoglutarate and iron as cofactors (*30*). Based on these findings, two independent studies later showed that AlkB is an oxidative demethylase removing methyl groups from 1-methyladenine and 3-methylcytosine from DNA (*31, 32*). The crystal structure of the AlkB-dsDNA complex reveals an active site where the damaged base (1MeA) is flipped into the active site with the two bases flanking the damage squeezed together, distorting the lesion-containing strand (*33*).

AlkB repairs lesions in the presence of oxygen, Fe^{2+} (a cofactor) and 2-oxoglutarate (or α-ketoglutarate, as a cosubstrate). The methyl group from the methylated substrate is first oxidized to a hydroxymethyl group and then released as formaldehyde. Oxygen is consumed during the reaction and 2-oxoglutarate is converted to succinate and CO_2. AlkB can act alone, independent of other proteins (*34*).

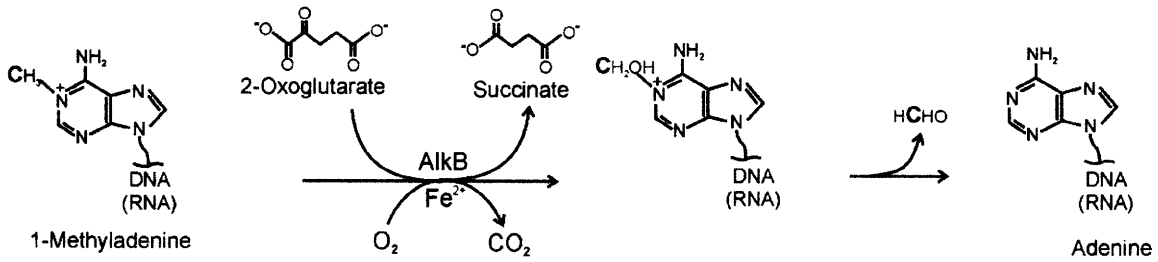

Figure 1-3 AlkB repair mechanism of 1meA (From ref (*35*))

S_N2 type alkylating agents (such as MMS, DMS, and MeI) produce more 1MeA and 3MeC lesions in single-stranded DNA than S_N1 agents (*31*). Most DNA lesions are induced in double-stranded and single-stranded DNA to similar extents by alkylating agents; however, AlkB substrates are preferentially formed in ss-DNA (*36*). The preferred substrates are ss- and ds- DNA and ssRNA for AlkB (*28*).

1MeA and 3MeC are only induced by alkylating agents in low amounts in double-stranded DNA but AlkB can efficiently remove them from both ds- and ss- DNA *in vitro* (*31, 32*). *In vivo*, AlkB may be involved in repairing lesions from transiently single-stranded regions as indicated by its ssDNA repair capacity (during replication and transcription) and in repairing dsDNA in general (*34*). 1MeA and 3MeC are primarily found in single strands because in duplex DNA, the N1 site in adenine and N3 in cytosine (methylation sites) are involved in base pairing and hence are relatively protected from

methylation in double-stranded DNA. Since the AlkB substrates are usually found in single strands and a large amount of RNA in the cell is single-stranded, it would make sense that many of the 1MeA and 3MeC would be in RNA instead of DNA. Therefore, the cell may possibly also have a need for RNA repair (*34*).

In addition to the 1MeA and 3MeC lesions, AlkB has been shown to repair 1-methylguanine (1MeG) (*37, 38*), 3-methylthymine (3MeT) (*37-39*), and 3-ethylcytosine (*37*), although with weaker activity on 1MeG and 3MeT than on 1MeA and 3MeC. It was later shown that AlkB substrates also include exocyclic lesions such as 1,N^6-ethanoadenine (EA) (*40*), 1,N^6-ethenoadenine (εA) (*41, 42*) and 3,N^4-ethenocytosine (εC) (*41*). Etheno adducts are generated by reaction of DNA with lipid oxidation products and also with metabolites of carcinogen in the environment such as chloroacetaldehyde. Etheno lesions have indeed been shown to be repaired efficiently by DNA glycosylases in mammalian, yeast, and bacterial cells (*43-45*).

Mammalian AlkB homologs

In mammals, there appear to be eight different AlkB homologs based on protein sequence similarity (*46, 47*), hABH1-8 in humans (or mAbh1-8 in mice). hABH1 was the homolog first identified and has the most protein sequence similarity with *E. coli* AlkB. ABH1 was shown to be partially active in the complementation of *alkB*-deficient *E. coli* upon treatment with MMS (*48*) although this result was not reproducible in more recent studies (*28, 29*). However, ABH1 has now been shown to demethylate 3MeC (*49*), and as mentioned before, ABH2 and ABH3 were found to demethylate 1meA and 3meC in

DNA and/or RNA (*28, 29*). For the human homologs, only hABH1, hABH2, and hABH3 have been shown to have repair activity on DNA and also RNA (*28, 31, 49-51*). mAbh2 displays i*n vivo* and *in vitro* repair activity on εA (*52*) and *in vitro* activity against εA has been shown for hABH3 (*42*). Similar to AlkB, ABH2 and ABH3 also can act independent of other proteins during the repair process (Figure 1-3).

In a study by Tsujikawa et al., the human *ABH1-ABH8* gene transcripts were detected throughout 16 human tissues examined (*53*). In agreement with previous studies showing localization of ABH2 and ABH3 (*28*), Tsujikawa et al. showed in a comprehensive study that ABH1, ABH3, ABH4, ABH5, ABH6, and ABH7 are expressed in both the cytoplasm and the nucleus and that the full-length hABH2 is in the nucleus (*53*). For hABH5 transfected into HeLa cells, the protein also shows a dot-like pattern in the cytoplasm. The full-length hABH8 newly cloned from testis cDNA that contains the 2OG-Fe(II) oxygenase domain, an RNA-binding motif, and a methyl-transferase domain, was localized exclusively in the cytoplasm in transfected HeLa cells (*53*).

The preferred substrates are ds-DNA for hABH2, and ss-DNA and ss-RNA for hABH3 (*28*). Aas et al. have experimentally shown that in *E. coli*, AlkB and hABH2 repair both ss- and ds-DNA significantly whereas hABH3 shows modest repair of ssDNA and insignificant in dsDNA. Furthermore, AlkB and hABH3 repair ssRNA but hABH2 does not (*28*). It appears that hABH2 and hABH3 complement each other and that together they have the activity of the *E. coli* AlkB protein. The crylstal structure of ABH2-

dsDNA shows that no significant distortion is necessary since the intercalating finger Phe102 fills the space vacated by the flipped out base (*33*).

Table 1-1: Repair preference of AlkB, hABH2, and hABH3

Protein	Preferred substrate
AlkB	ssDNA, ssRNA, some dsDNA
hABH2	dsDNA
hABH3	ssDNA, ssRNA

Significance of RNA repair and *in vivo* repair by ABH2/ABH3

It is likely that RNA methylation damage needs to be repaired to prevent the production of faulty proteins by translation of damaged mRNA, by charged tRNA and damaged ribosomes. However, it remains unknown how the cell distinguishes between RNA alkylation damage and naturally occurring RNA post-transcriptional modifications that are crucial for proper translation. Although RNA methylation damage has not been thoroughly studied, it is known that 1MeA modification in ribosomal RNA can have detrimental effects on binding of the codon-anticodon complex (*54*) and on reverse transcription (*55*). Translation may be affected since the modified bases are involved in direct base-pairing (*28*).

From Northern hybridization studies by Duncan et al., *hABH2* mRNA levels are highest in liver and bladder while *hABH3* mRNA levels are highest in spleen, prostate, bladder, and colon tissues (*29*). For carcinoma cell lines, HeLa cells show high *hABH2* mRNA and very low *hABH3* mRNA levels, which is also almost absent in two of the Burkitt's

lymphomas cell lines (*29*). Furthermore, using mice deficient in Abh2 and/or Abh3, 1MeA lesions were shown to accumulate significantly in the genome of mice deficient in mAbh2 during aging, indicating that mAbh2 is important in repairing such lesions induced by endogenous methylating sources (*35, 56*). However, mAbh3-deficient cells and extracts showed no repair defect of the lesions, although purified hABH3 shows repair activity *in vitro*. The repair of 1MeA and 3MeC by wildtype and mAbh3-deficient mice was very similar (*56*).

1.4. References

(1) Lindahl, T. (1993) Instability and decay of the primary structure of DNA. *Nature 362*, 709-15.

(2) Beranek, D. T. (1990) Distribution of methyl and ethyl adducts following alkylation with monofunctional alkylating agents. *Mutat Res 231*, 11-30.

(3) Gerson, S. L. (2002) Clinical relevance of MGMT in the treatment of cancer. *J Clin Oncol 20*, 2388-99.

(4) Wyatt, M. D., Allan, J. M., Lau, A. Y., Ellenberger, T. E., and Samson, L. D. (1999) 3-methyladenine DNA glycosylases: structure, function, and biological importance. *Bioessays 21*, 668-76.

(5) Krokan, H. E., Standal, R., and Slupphaug, G. (1997) DNA glycosylases in the base excision repair of DNA. *Biochem J 325 (Pt 1)*, 1-16.

(6) Seeberg, E., Eide, L., and Bjoras, M. (1995) The base excision repair pathway. *Trends Biochem Sci 20*, 391-7.

(7) Drablos, F., Feyzi, E., Aas, P. A., Vaagbo, C. B., Kavli, B., Bratlie, M. S., Pena-Diaz, J., Otterlei, M., Slupphaug, G., and Krokan, H. E. (2004) Alkylation damage in DNA and RNA--repair mechanisms and medical significance. *DNA Repair (Amst) 3*, 1389-407.

(8) Berdal, K. G., Johansen, R. F., and Seeberg, E. (1998) Release of normal bases from intact DNA by a native DNA repair enzyme. *Embo J 17*, 363-7.

(9) Lau, A. Y., Wyatt, M. D., Glassner, B. J., Samson, L. D., and Ellenberger, T. (2000) Molecular basis for discriminating between normal and damaged bases by the human alkyladenine glycosylase, AAG. *Proc Natl Acad Sci U S A 97*, 13573-8.

(10) Roth, R. B., and Samson, L. D. (2002) 3-Methyladenine DNA glycosylase-deficient Aag null mice display unexpected bone marrow alkylation resistance. *Cancer Res 62*, 656-60.

(11) Engelward, B. P., Dreslin, A., Christensen, J., Huszar, D., Kurahara, C., and Samson, L. (1996) Repair-deficient 3-methyladenine DNA glycosylase homozygous mutant mouse cells have increased sensitivity to alkylation-induced chromosome damage and cell killing. *Embo J 15*, 945-52.

(12) Sedgwick, B., and Lindahl, T. (2002) Recent progress on the Ada response for inducible repair of DNA alkylation damage. *Oncogene 21*, 8886-94.

(13) Limp-Foster, M., and Kelley, M. R. (2000) DNA repair and gene therapy: implications for translational uses. *Environ Mol Mutagen 35*, 71-81.

(14) Roth, R. B., and Samson, L. D. (2000) Gene transfer to suppress bone marrow alkylation sensitivity. *Mutat Res 462*, 107-20.

(15) Daniels, D. S., and Tainer, J. A. (2000) Conserved structural motifs governing the stoichiometric repair of alkylated DNA by O(6)-alkylguanine-DNA alkyltransferase. *Mutat Res 460*, 151-63.

(16) Wibley, J. E., Pegg, A. E., and Moody, P. C. (2000) Crystal structure of the human O(6)-alkylguanine-DNA alkyltransferase. *Nucleic Acids Res 28*, 393-401.

(17) Srivenugopal, K. S., Yuan, X. H., Friedman, H. S., and Ali-Osman, F. (1996) Ubiquitination-dependent proteolysis of O6-methylguanine-DNA methyltransferase in human and murine tumor cells following inactivation with

O6-benzylguanine or 1,3-bis(2-chloroethyl)-1-nitrosourea. *Biochemistry 35*, 1328-34.

(18) Hickman, M. J., and Samson, L. D. (1999) Role of DNA mismatch repair and p53 in signaling induction of apoptosis by alkylating agents. *Proc Natl Acad Sci U S A 96*, 10764-9.

(19) Gerson, S. L., Miller, K., and Berger, N. A. (1985) O6 alkylguanine-DNA alkyltransferase activity in human myeloid cells. *J Clin Invest 76*, 2106-14.

(20) Gerson, S. L., Trey, J. E., Miller, K., and Berger, N. A. (1986) Comparison of O6-alkylguanine-DNA alkyltransferase activity based on cellular DNA content in human, rat and mouse tissues. *Carcinogenesis 7*, 745-9.

(21) Gerson, S. L., Trey, J. E., Miller, K., and Benjamin, E. (1987) Repair of O6-alkylguanine during DNA synthesis in murine bone marrow hematopoietic precursors. *Cancer Res 47*, 89-95.

(22) Dumenco, L. L., Allay, E., Norton, K., and Gerson, S. L. (1993) The prevention of thymic lymphomas in transgenic mice by human O6-alkylguanine-DNA alkyltransferase. *Science 259*, 219-22.

(23) Sakumi, K., Shiraishi, A., Shimizu, S., Tsuzuki, T., Ishikawa, T., and Sekiguchi, M. (1997) Methylnitrosourea-induced tumorigenesis in MGMT gene knockout mice. *Cancer Res 57*, 2415-8.

(24) Iwakuma, T., Sakumi, K., Nakatsuru, Y., Kawate, H., Igarashi, H., Shiraishi, A., Tsuzuki, T., Ishikawa, T., and Sekiguchi, M. (1997) High incidence of nitrosamine-induced tumorigenesis in mice lacking DNA repair methyltransferase. *Carcinogenesis 18*, 1631-5.

(25) Pegg, A. E., Boosalis, M., Samson, L., Moschel, R. C., Byers, T. L., Swenn, K., and Dolan, M. E. (1993) Mechanism of inactivation of human O6-alkylguanine-DNA alkyltransferase by O6-benzylguanine. *Biochemistry 32*, 11998-2006.

(26) Kataoka, H., Yamamoto, Y., and Sekiguchi, M. (1983) A new gene (alkB) of Escherichia coli that controls sensitivity to methyl methane sulfonate. *J Bacteriol 153*, 1301-7.

(27) Chen, B. J., Carroll, P., and Samson, L. (1994) The Escherichia coli AlkB protein protects human cells against alkylation-induced toxicity. *J Bacteriol 176*, 6255-61.

(28) Aas, P. A., Otterlei, M., Falnes, P. O., Vagbo, C. B., Skorpen, F., Akbari, M., Sundheim, O., Bjoras, M., Slupphaug, G., Seeberg, E., and Krokan, H. E. (2003) Human and bacterial oxidative demethylases repair alkylation damage in both RNA and DNA. *Nature 421*, 859-63.

(29) Duncan, T., Trewick, S. C., Koivisto, P., Bates, P. A., Lindahl, T., and Sedgwick, B. (2002) Reversal of DNA alkylation damage by two human dioxygenases. *Proc Natl Acad Sci U S A 99*, 16660-5.

(30) Aravind, L., and Koonin, E. V. (2001) The DNA-repair protein AlkB, EGL-9, and leprecan define new families of 2-oxoglutarate- and iron-dependent dioxygenases. *Genome Biol 2*, RESEARCH0007.

(31) Falnes, P. O., Johansen, R. F., and Seeberg, E. (2002) AlkB-mediated oxidative demethylation reverses DNA damage in Escherichia coli. *Nature 419*, 178-82.

(32) Trewick, S. C., Henshaw, T. F., Hausinger, R. P., Lindahl, T., and Sedgwick, B. (2002) Oxidative demethylation by Escherichia coli AlkB directly reverts DNA base damage. *Nature 419*, 174-8.

(33) Yang, C. G., Yi, C., Duguid, E. M., Sullivan, C. T., Jian, X., Rice, P. A., and He, C. (2008) Crystal structures of DNA/RNA repair enzymes AlkB and ABH2 bound to dsDNA. *Nature 452*, 961-5.
(34) Falnes, P. O., and Rognes, T. (2003) DNA repair by bacterial AlkB proteins. *Res Microbiol 154*, 531-8.
(35) Falnes, P. O., Klungland, A., and Alseth, I. (2007) Repair of methyl lesions in DNA and RNA by oxidative demethylation. *Neuroscience 145*, 1222-32.
(36) Dinglay, S., Trewick, S. C., Lindahl, T., and Sedgwick, B. (2000) Defective processing of methylated single-stranded DNA by E. coli AlkB mutants. *Genes Dev 14*, 2097-105.
(37) Delaney, J. C., and Essigmann, J. M. (2004) Mutagenesis, genotoxicity, and repair of 1-methyladenine, 3-alkylcytosines, 1-methylguanine, and 3-methylthymine in alkB Escherichia coli. *Proc Natl Acad Sci U S A 101*, 14051-6.
(38) Falnes, P. O. (2004) Repair of 3-methylthymine and 1-methylguanine lesions by bacterial and human AlkB proteins. *Nucleic Acids Res 32*, 6260-7.
(39) Koivisto, P., Robins, P., Lindahl, T., and Sedgwick, B. (2004) Demethylation of 3-methylthymine in DNA by bacterial and human DNA dioxygenases. *J Biol Chem 279*, 40470-4.
(40) Frick, L. E., Delaney, J. C., Wong, C., Drennan, C. L., and Essigmann, J. M. (2007) Alleviation of 1,N6-ethanoadenine genotoxicity by the Escherichia coli adaptive response protein AlkB. *Proc Natl Acad Sci U S A 104*, 755-60.
(41) Delaney, J. C., Smeester, L., Wong, C., Frick, L. E., Taghizadeh, K., Wishnok, J. S., Drennan, C. L., Samson, L. D., and Essigmann, J. M. (2005) AlkB reverses etheno DNA lesions caused by lipid oxidation in vitro and in vivo. *Nat Struct Mol Biol 12*, 855-60.
(42) Mishina, Y., Yang, C. G., and He, C. (2005) Direct repair of the exocyclic DNA adduct 1,N6-ethenoadenine by the DNA repair AlkB proteins. *J Am Chem Soc 127*, 14594-5.
(43) Singer, B., Antoccia, A., Basu, A. K., Dosanjh, M. K., Fraenkel-Conrat, H., Gallagher, P. E., Kusmierek, J. T., Qiu, Z. H., and Rydberg, B. (1992) Both purified human 1,N6-ethenoadenine-binding protein and purified human 3-methyladenine-DNA glycosylase act on 1,N6-ethenoadenine and 3-methyladenine. *Proc Natl Acad Sci U S A 89*, 9386-90.
(44) Saparbaev, M., Kleibl, K., and Laval, J. (1995) Escherichia coli, Saccharomyces cerevisiae, rat and human 3-methyladenine DNA glycosylases repair 1,N6-ethenoadenine when present in DNA. *Nucleic Acids Res 23*, 3750-5.
(45) Saparbaev, M., and Laval, J. (1998) 3,N4-ethenocytosine, a highly mutagenic adduct, is a primary substrate for Escherichia coli double-stranded uracil-DNA glycosylase and human mismatch-specific thymine-DNA glycosylase. *Proc Natl Acad Sci U S A 95*, 8508-13.
(46) Kurowski, M. A., Bhagwat, A. S., Papaj, G., and Bujnicki, J. M. (2003) Phylogenomic identification of five new human homologs of the DNA repair enzyme AlkB. *BMC Genomics 4*, 48.
(47) Osada, N., Hida, M., Kusuda, J., Tanuma, R., Hirata, M., Hirai, M., Terao, K., Suzuki, Y., Sugano, S., and Hashimoto, K. (2002) Prediction of unidentified

human genes on the basis of sequence similarity to novel cDNAs from cynomolgus monkey brain. *Genome Biol 3*, RESEARCH0006.

(48) Wei, Y. F., Carter, K. C., Wang, R. P., and Shell, B. K. (1996) Molecular cloning and functional analysis of a human cDNA encoding an Escherichia coli AlkB homolog, a protein involved in DNA alkylation damage repair. *Nucleic Acids Res 24*, 931-37.

(49) Westbye, M. P., Feyzi, E., Aas, P. A., Vagbo, C. B., Talstad, V. A., Kavli, B., Hagen, L., Sundheim, O., Akbari, M., Liabakk, N. B., Slupphaug, G., Otterlei, M., and Krokan, H. E. (2008) Human AlkB homolog 1 is a mitochondrial protein that demethylates 3-methylcytosine in dna and RNA. *J Biol Chem.*

(50) Ougland, R., Zhang, C. M., Liiv, A., Johansen, R. F., Seeberg, E., Hou, Y. M., Remme, J., and Falnes, P. O. (2004) AlkB restores the biological function of mRNA and tRNA inactivated by chemical methylation. *Mol Cell 16*, 107-16.

(51) Falnes, P. O., Bjoras, M., Aas, P. A., Sundheim, O., and Seeberg, E. (2004) Substrate specificities of bacterial and human AlkB proteins. *Nucleic Acids Res 32*, 3456-61.

(52) Ringvoll, J., Moen, M. N., Nordstrand, L. M., Meira, L. B., Pang, B., Bekkelund, A., Dedon, P. C., Bjelland, S., Samson, L. D., Falnes, P. O., and Klungland, A. (2008) AlkB homologue 2-mediated repair of ethenoadenine lesions in mammalian DNA. *Cancer Res 68*, 4142-9.

(53) Tsujikawa, K., Koike, K., Kitae, K., Shinkawa, A., Arima, H., Suzuki, T., Tsuchiya, M., Makino, Y., Furukawa, T., Konishi, N., and Yamamoto, H. (2007) Expression and sub-cellular localization of human ABH family molecules. *J Cell Mol Med 11*, 1105-16.

(54) Yoshizawa, S., Fourmy, D., and Puglisi, J. D. (1999) Recognition of the codon-anticodon helix by ribosomal RNA. *Science 285*, 1722-5.

(55) Matsugi, J., and Murao, K. (2001) Study on construction of a cDNA library corresponding to an amino acid-specific tRNA and influence of the modified nucleotide upon nucleotide misincorporations in reverse transcription. *Biochim Biophys Acta 1521*, 81-8.

(56) Ringvoll, J., Nordstrand, L. M., Vagbo, C. B., Talstad, V., Reite, K., Aas, P. A., Lauritzen, K. H., Liabakk, N. B., Bjork, A., Doughty, R. W., Falnes, P. O., Krokan, H. E., and Klungland, A. (2006) Repair deficient mice reveal mABH2 as the primary oxidative demethylase for repairing 1meA and 3meC lesions in DNA. *Embo J 25*, 2189-98.

2. CHAPTER 2--AlkB/ABH Expression and Repair Activity in Bacterial and Mammalian Cells

2.1. Introduction

MGMT is an example of a direct DNA repair protein shown to render many cells and organisms alkylation resistant in previous studies and is being tested in combination with the O^6-BG inhibitor drug to treat solid tumors in clinical trials (*1*). It therefore seemed worthwhile to study other direct reversal proteins to determine whether they have the potential for DNA repair in human cells as shown to be true for MGMT. Because the *E. coli* AlkB protein gives alkylation resistance in both *E. coli* and HeLa cells (*2*), we hypothesized that the same could be done with the human AlkB homologs (hABH), another set of proteins involved in the direct reversal of damage in DNA, and in addition RNA (*3*). Early work of this thesis was aimed at determining whether human ABH1, ABH2, and ABH3 expression can confer alkylation resistance in human cells.

2.2. Materials and Methods

2.2.1. Construction of bacterial and mammalian expression vectors containing hABH1, hABH2, or hABH3

Our goal was to express hABH1, hABH2, and hABH3 in human cells. The cDNA fragments encoding the proteins were PCR-amplified from existing vector constructs generated by Thomas Begley in the Samson laboratory (unpublished). To monitor expression of the protein, a hemagglutin (HA) tag was added to either the 5' or 3' end of the gene so that an anti-HA antibody could be used in Western blot analysis. Constructs

without an HA tag were also constructed in case the fused tag interfered with the normal function of the gene product (Figure 2-1).

The vectors used included bacterial expression construct (pET-DEST42 (Invitrogen) for validation of AlkB, ABH1-3 function by MMS gradient plate assay) and mammalian constructs--pMMP-f2-IRES-GFP, p500 (episomal), pCDNA3.2/V5-DEST (constitutive) and pLenti/TO/Puro-DEST (lentiviral, tetracycline-regulated expression system; Eric Campeau, Cooper Lab, LBNL)).

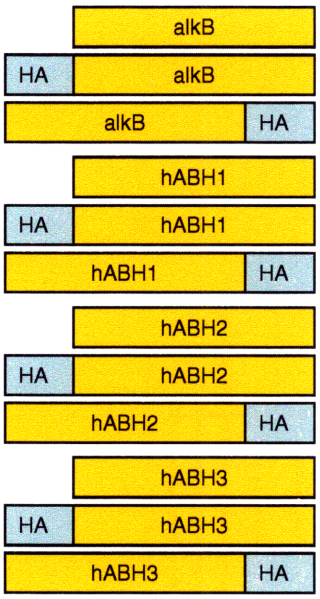

Figure 2-1: Structure of the HA-tagged and untagged hABH constructs

2.2.2. Mammalian expression

Transfection of cell lines

The pMMP-f2-IRES-GFP-alkB/hABH and pcDNA3.2/V5-DEST-alkB/hABH plasmids were transfected into target cells using the lipofectamine transfection reagent (Invitrogen).

Selection of individual clones was performed over a two-week period and expansion of the stable clones over another week. This ensured that the insertion into the genome was stable and not transient. During the cloning and expansion processes, the pMMP-f2-IRES-GFP-alkB/hABH and the pcDNA3.2/V5-DEST-alkB/hABH clones expressed GFP or were geneticin-resistant, respectively, indicating the presence of the plasmids in the cells. Stable clones were then frozen down and harvested for further analysis.

Confirmation -- In vitro transcription and translation

In vitro transcription and translation was done using the alkB/hABH-containing vectors with a T7 RNA polymerase region. After transcription, the transcription product was used in translation using rabbit reticulocyte lysate with ^{35}S-labeled methionine. The labeled protein products translated from the mRNA transcripts of alkB/hABH HA were then detected by SDS-PAGE analysis followed by phosphorimaging. Western blot analysis was also performed to detect the HA-tagged proteins once the labeled bands were seen by phosphorimaging.

2.2.3. MMS gradient assay

Expression constructs containing *alkB, hABH1, hABH2*, and *hABH3* cDNAs, with either no tag, 5'-HA tag, or 3'-HA tag, were transformed into wild-type and alkB-deficient *E. coli* strains. The strains used were HK81(DE3)(wild-type) and HK82(DE3) (alkB-deficient). A gradient of MMS (an S_N2 alkylating agent) was generated across an agar plate containing 1mM IPTG (to induce protein expression) and the appropriate antibiotic. Cultures of HK81(DE3) and HK82(DE3) containing all the different bacterial expression constructs, along with the empty vector as negative controls, were spread across the

gradient. The sensitive phenotype can be seen when the strain dies off whereas resistant strains would survive across most of the plate.

2.2.4. Colony forming survival assay

Cell lines transfected with AlkB/ABH expression vectors were tested for MMS sensitivity using a colony forming survival assay. Stable or transiently transfected cells were both used. To perform the survival assays, cells were treated for 1 hour in 10mL serum-free media with different doses of MMS. After 1 hour of treatment, the media was changed to complete media with serum and the cells were diluted and plated at 500, 5000, or 50000 cells/plate and allowed to grow for 10-14 days for colony formation.

2.2.5. *Ex vivo* bone marrow survival assay

Abh2 and Abh3 knockout mice made by Arne Klungland's group from Norway (*4*) were made available to us. Bone marrow survival experiments using the wild-type and Abh2, Abh3, and Abh2/Abh3 double-mutant mice were performed to test whether Abh2 and/or Abh3 were important in protecting bone marrow from alkylation damage. The femurs were taken from the mice and crushed to extract the bone marrow cells. MMS treatments immediately followed and the bone marrow cells were then resuspended in methocult to allow colony formation of myeloid lineage cells (*5*). Cell colonies were counted after nine days.

2.3. Results

2.3.1. MMS gradient plate assay showed AlkB/ABH activity and no interference from HA tags & detection of HA-tagged AlkB/hABH expression

It was important to ensure that the bacterial expression constructs containing hABH1, hABH2, and hABH3, each with no tag, 5'-HA, and 3'-HA, were functional. Thus, after transforming into wild-type (HK81(DE3)) and alkB-deficient (HK82(DE3)) *E. coli* strains, the MMS gradient plate assay was performed to observe whether the expression of AlkB/ABH in *E. coli* can confer resistance upon alkylation damage. Figure 2-2 shows a representative MMS gradient plate with *E. coli* containing the bacterial expression constructs of AlkB/ABH. Results show that AlkB gave full resistance, hABH1 modest resistance, hABH2 full resistance, and hABH3 little to modest resistance. The HA tags did not appear to interfere with the protein functions since similar activity was observed in the presence or absence of the HA tag, and whether the tag was placed at 5' or 3' end made no difference (results not shown).

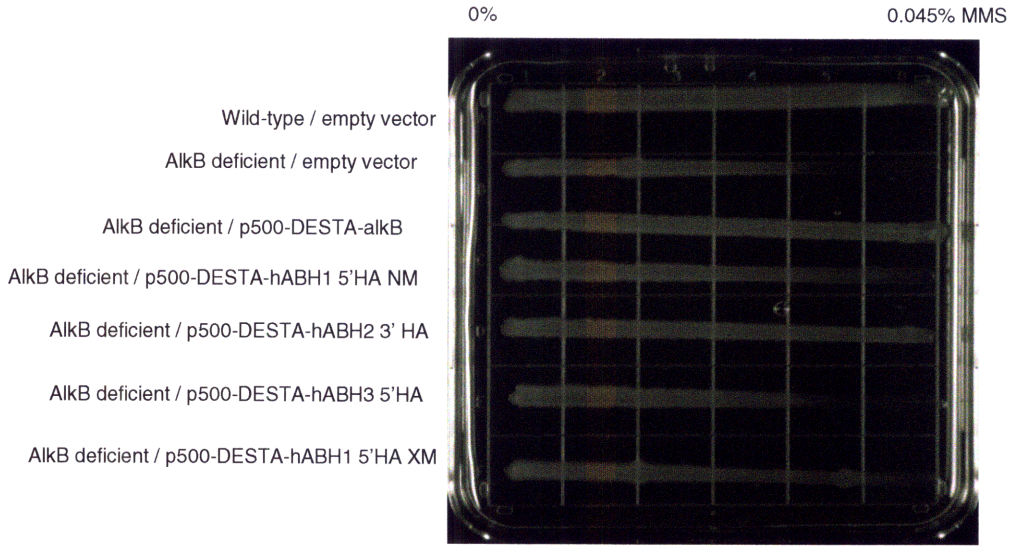

Figure 2-2: MMS gradient plate of p500 -AlkB/hABH HA in AlkB-deficient *E. coli*

The anti-HA antibody (Abcam) was used to detect expression of the HA-tagged constructs in both the *E. coli*. Figure 2-3 shows a Western blot showing expression of the HA-tagged proteins in *E. coli*.

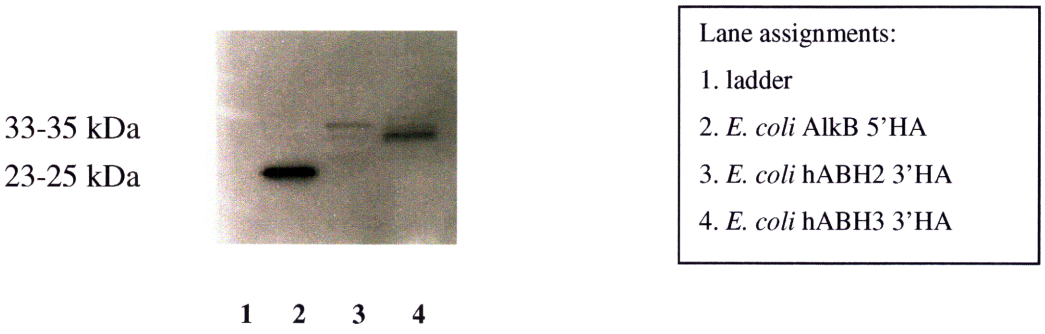

Figure 2-3: Western blot with showing AlkB/ABH expression in *E. coli*

2.3.2. *In vitro* transcription and translation

In order to confirm whether the AlkB/ABH constructs can indeed support transcription and translation, *in vitro* transcription and translation was done using the alkB/hABH-containing vectors with a T7 RNA polymerase region. After transcription, the transcription product was used in translation using rabbit reticulocyte lysate with ^{35}S-labeled methionine. The labeled protein products translated from the mRNA transcripts of alkB/hABH HA were then detected by SDS-PAGE analysis followed by phosphorimaging. Western blot analysis was also performed to detect the HA-tagged proteins once the labeled bands were seen by phosphorimaging.

Radiolabeled bands at the expected product sizes were seen (Figure 2-4), except for ABH2, but somehow could not be detected by Western (data not shown), even with

different anti-HA antibodies. However, based on the fact that the bands on the exposed gel from *in vitro* translation were clean and distinct, it was worthwhile to check for protein functions anyway even if the HA tag could not be detected.

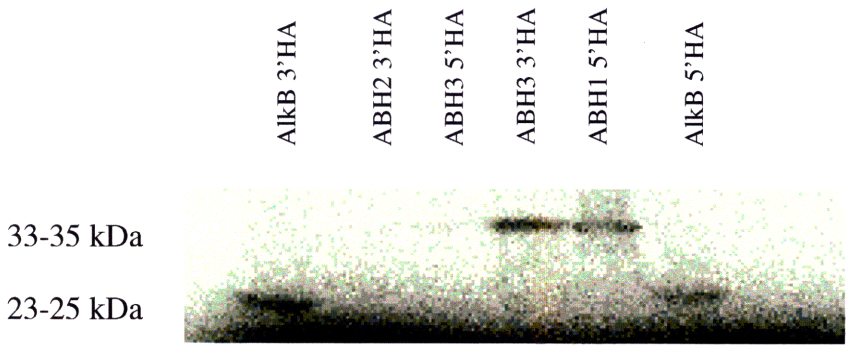

Figure 2-4: *in vitro* translation products from phosphorimaging

(Note: for hABH3 5'HA, the band is too faint to see clearly.)

2.3.3. Mammalian expression and survival assays in human cell lines

Protein expression detection had been problematic in stable populations of human cells, such as K562 and HeLa. It was thought that perhaps long-term growth selects against high level expression of ABH proteins. Hence, HEK293T cells were transiently transfected to see if the proteins could at least be expressed transiently. HEK293T cells are human embryonic kidney cells and are known to allow high transfection efficiency. Cells were harvested 3, 6, and 10 days post-infection. Extracts were prepared for Western blot analysis and growth inhibition assay carried out. Western blots with HA antibody detected AlkB 3'HA in transiently transfected HEK293T cells. (Note that this was the first time that HA-tagged AlkB/hABH proteins were detected in cell extracts.) They were only detected in transiently transfected HEK293T cells and not in stable transfectants, as illustrated with the Western blot below in Figure 2-5.

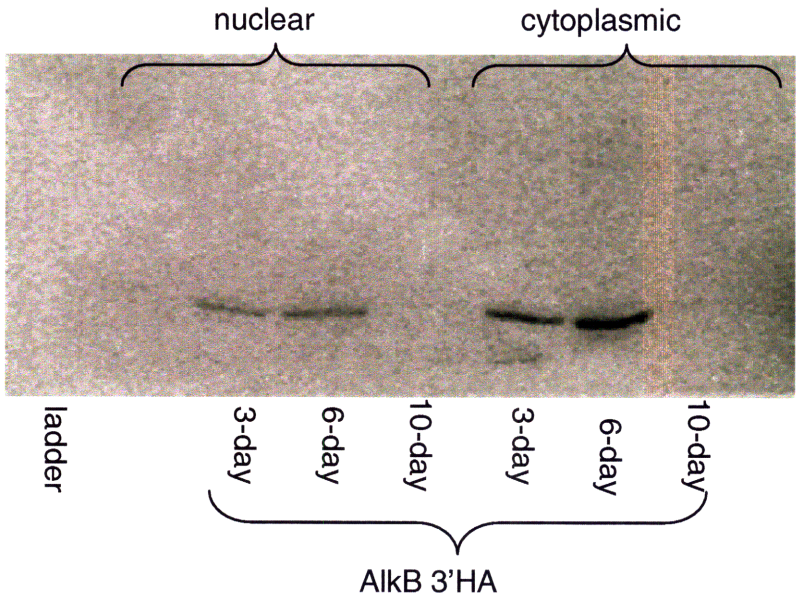

Figure 2-5: Western blot showing AlkB 3'HA in 293T cells 3-, 6-, and 10-day post transfection

After observing the expression of AlkB protein in the transiently transfected HEK293T cells, survival assays were performed. Figure 2-6 shows results from a representative experiment using MMS. Multiple attempts of the assays with different cell lines (such as K562 and HeLa) with different transfection status (transient or stable) showed similar results: the differences in the survival of cell lines transfected with empty vector versus the AlkB/ABH constructs were very small and not statistically significant.

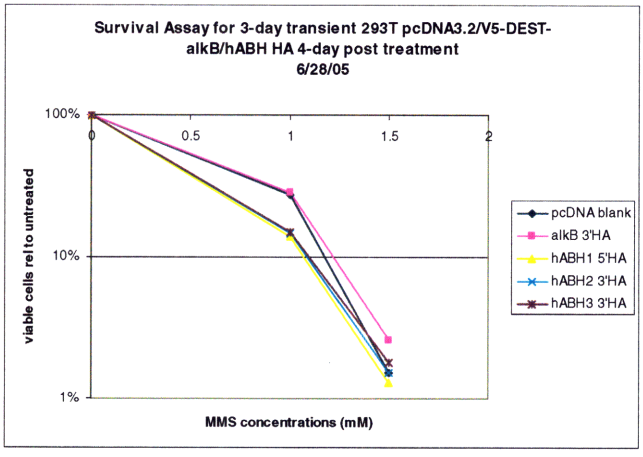

Figure 2-6: MMS survival assay with 3-day transient 293T pcDNA3.2/V5-DEST-alkB/hABH HA 4 days after treatment

2.3.4. Survival in Abh knockout models

To determine the significance of ABH-related repair in mammalian cells, it would be important to check for any sensitivity to damage in ABH-knockout cells compared to wild-type cells. Mouse bone marrow cells were treated with MMS and methyl nitrosourea (MNU), a S_N2 and a S_N1 alkylating agent, respectively. *Ex vivo* bone marrow treatment results with MNU (as negative control) are shown below in comparison with those with MMS (Figure 2-7).

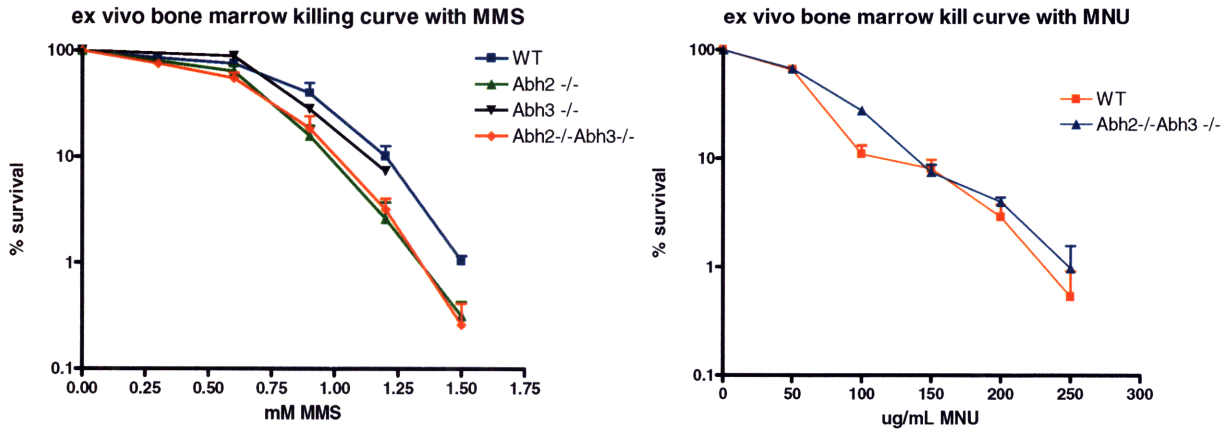

Figure 2-7: *Ex vivo* bone marrow treatment results with MMS and MNU

As seen from above, bone marrow cells from the $Abh2^{-/-}Abh3^{-/-}$ double mutant mice were significantly more sensitive than wild-type cells to MMS damage. $Abh3^{-/-}$ bone marrow cells were not sensitive and $Abh2^{-/-}$ cells were as sensitive as those of the $Abh2^{-/-}Abh3^{-/-}$ to MMS damage. This shows that a deficiency in Abh2 alone (but not Abh3 alone) can cause sensitivity to MMS in the bone marrow. This finding was consistent with that shown by Ringvoll et al (*4*) in mouse embryonic fibroblasts (MEFs) from the $Abh2^{-/-}$ and

Abh3$^{-/-}$ mice. However, the double mutant bone marrow cells were not more sensitive than wild-type against MNU damage. This was within expectation that the AlkB proteins would repair damage induced by S_N2 and not S_N1 alkylating agents, consistent with the findings by Chen et al (*2*). Hence, we saw that Abh2, and not Abh3, appeared to have a protective role against the S_N2 alkylating agent MMS in mouse bone marrow.

2.4. Discussion and summary of chapter

Bacterial expression constructs carrying *E. coli* AlkB and its human homologs were built and sequence verified and protein expression also checked. Subsequently, the expressed proteins were shown to be active as judged by their ability to confer MMS resistance as determined *in vivo* in bacteria on MMS gradient plates. AlkB restored AlkB-deficient *E. coli* strain to wild-type phenotype. Among the human homologs hABH1, hABH2, and hABH3, hABH2 conferred rescue, similar to AlkB levels, while hABH3 and hABH1 showed partial rescue.

In order to verify whether the AlkB protein and its human homologs could confer increased MMS resistance in mammalian cells, mammalian expression constructs were also made. Expression was confirmed by *in vitro* transcription/translation and Western blotting. Numerous attempts to detect increased survival of the human cell lines upon MMS exposure with the different vectors and different cell lines failed. Possible explanations for the failure of transfected AlkB/ABH expression constructs to confer MMS resistance are that the expressed proteins might not be active in the human cells, or that the endogenous hABH activity was already sufficient to rescue the cells from MMS

damage. Furthermore, repair by AlkB/hABH generates toxic formaldehyde and it may be more beneficial to the cells to avoid having the excess formaldehyde byproduct than to have the DNA lesions repaired by the expressed AlkB/hABH. Maintaining the expressed AlkB/hABH proteins could be a burden to the cells. It is also possible that the ABH proteins may need to be in a complex in order to be fully functional, and that the other components of the putative complex were limiting.

However, with *Abh2* and *Abh3* knockout mouse bone marrow, Abh2 appears to play the major role in rescuing the cells from MMS-induced toxicity. This finding was very encouraging and was the first demonstration that Abh2 protects bone marrow against alkylation induced toxicity. It would therefore be interesting to investigate whether Abh2 and/or Abh3 rescue other mouse cell type from alkylation induced toxicity.

2.5. References

(1) Sorrentino, B. P. (2002) Gene therapy to protect haematopoietic cells from cytotoxic cancer drugs. *Nat Rev Cancer 2*, 431-41.

(2) Chen, B. J., Carroll, P., and Samson, L. (1994) The Escherichia coli AlkB protein protects human cells against alkylation-induced toxicity. *J Bacteriol 176*, 6255-61.

(3) Aas, P. A., Otterlei, M., Falnes, P. O., Vagbo, C. B., Skorpen, F., Akbari, M., Sundheim, O., Bjoras, M., Slupphaug, G., Seeberg, E., and Krokan, H. E. (2003) Human and bacterial oxidative demethylases repair alkylation damage in both RNA and DNA. *Nature 421*, 859-63.

(4) Ringvoll, J., Nordstrand, L. M., Vagbo, C. B., Talstad, V., Reite, K., Aas, P. A., Lauritzen, K. H., Liabakk, N. B., Bjork, A., Doughty, R. W., Falnes, P. O., Krokan, H. E., and Klungland, A. (2006) Repair deficient mice reveal mABH2 as the primary oxidative demethylase for repairing 1meA and 3meC lesions in DNA. *Embo J 25*, 2189-98.

(5) Roth, R. B., and Samson, L. D. (2002) 3-Methyladenine DNA glycosylase-deficient Aag null mice display unexpected bone marrow alkylation resistance. *Cancer Res 62*, 656-60.

3. CHAPTER 3 – Chronic inflammation study on animals deficient in Abh2, Abh3, and Aag

3.1. Introduction

Chronic inflammation has been linked to increased cancer risk. One example of such a link is the increased risk of colorectal cancer in patients with inflammatory bowel disease (IBD). One million people per year are affected with IBD which includes ulcerative colitis (UC) and Crohn's disease (*1*). IBD patients have damage to the epithelial layer of the gastrointestinal tract, which serves as a barrier against potentially harmful agents such as acid, enzymes, bacteria, and toxins (*2, 3*). Patients with extended UC are 19 fold more likely to develop colorectal cancer than the general population (*4*). The risk of colon cancer in UC patients increases with the extent of the colon involvement, severity, and duration of the disease (*5*). The link between cancer and inflammation is also supported by the fact that controlling or inhibiting inflammation in IBD patients correlates with a reduced cancer risk. Long-term use of anti-inflammatory drugs such as nonsteroidal anti-inflammatory drugs (NSAIDs) and selective cyclooxygenase-2 (COX2) inhibitors lowers cancer risk significantly (*6*), suggesting similar molecules could be targets for cancer treatment.

Chronic inflammation has also been correlated with increased levels of DNA base damage in the inflamed tissue (*7-9*). Ulcerative colitis patients suffer episodes of active

inflammation (flare-ups) separated by periods of disease inactivity (remission). Active inflammation activates and recruits leukocytes and tissue mast cells (*10*) and leukocytes and phagocytic cells secrete proinflammatory cytokines, chemokines, growth factors, and matrix-degrading enzymes. Furthermore, as a mechanism to fight infection, inflammatory cells such as neutrophils and macrophages generate and release reactive oxygen and nitrogen species (RONS) (*10*). However, uncontrolled inflammation can lead to more RONS and thus, oxidation and deamination of DNA bases. In addition, base alkylation can result indirectly via lipid peroxidation that forms a byproduct that can react with DNA to generate etheno base lesions (*11*). Chronic inflammation has thus been correlated with increased levels of εA, 1,N^2-εG, εC and 8oxoG in the affected tissues (*7-9*).

In a previous study in the Samson lab, it was found that the Aag 3-methyladenine DNA glycosylase can ameliorate colon damage and decrease tumor development in response to chronic colonic inflammation (*9*). Aag initiates the base excision repair (BER) pathway for a wide range of structurally diverse damaged bases, including 3meA, εA, Hx, and 8oxoG. Aag-deficient mice showed a greater increase in oxidized (8oxoG) and etheno DNA base damage (εA and εC) after chronic inflammation in colon tissue compared to wildtype, and this correlated with more pronounced colon tissue damage and increased tumor development in Aag-deficient versus wildtype mice (*9*). These results show that the repair of chronic inflammation-induced DNA lesions is important for colon cancer prevention. Another RONS-related base damage, the εC lesion in DNA, is tightly bound by Aag but not excised (*12*). Thus, the higher accumulation of εC in Aag-deficient

versus WT mice (*9*) seems to suggest that although Aag does not directly excise εC, it can still assist in its repair. This may be an indication that Aag serves to recruit other repair pathway(s) to help rid the DNA of RONS-induced εC DNA lesions.

AlkB (and its mammalian homologs) may be one such alternative pathway since it repairs cyclic etheno lesions such as εA and εC via direct reversal (*13*), in addition to repairing simple alkylated adducts such as 1-methyladenine and 3-methylcytosine (*14, 15*), 1-methylguanine (*15, 16*), 3-methylthymine (*15-17*), and 3-ethylcytosine (*16*). *In vivo* and *in vitro* repair activity on εA (*18*) have been shown for mammalian ABH2 and *in vitro* activity against εA has been shown for hABH3 (*19*). Since both Aag and AlkB efficiently repair etheno DNA lesions, known to be induced during chronic inflammation, we set out to determine whether Abh2 and Abh3, along with Aag, contribute to the amelioration of the response to chronic inflammatory colitis seen in mice.

For IBD and its associated colorectal cancer (CRC), several animal models have been developed and the most widely used involves treatment with dextran sulfate sodium (DSS) (*20*). These models mimic the course of human ulcerative colitis, eventually leading to colorectal tumors with similar pathology to those of humans. Originally developed by Ohkusa (*21*) as a hamster model, the DSS model was later adapted to mice by Okayasu et al. (*20*). DSS is orally administered to the mice in the drinking water, resulting in acute and chronic colitis similar to UC. Following three to five cycles of DSS, mice exhibit signs of colonic mucosal inflammation with ulcerations, body weight loss, and bloody diarrhea (*20*). DSS is toxic to mucosal epithelial cells, which can lead to

dysfunctional mucosal barrier and mucosal inflammation (*22*). The mechanism by which DSS induces colitis is not clear but it is proposed that ingestion of DSS may destroy mucin content or alter macrophage function and cause toxicity in the epithelium, thus increasing exposure to luminal antigens, and activating macrophage inflammatory responses (*20, 23-25*). However, the mouse colitis model using DSS requires an extended and/or repeated cycles of DSS treatment to induce colitis and colitis-related CRC, and the incidence and multiplicity of induced tumors are relatively low (*26*).

Azoxymethane (AOM) is an alkylating agent commonly used in conjunction with DSS in experimental models of colorectal cancer, in conjunction with DSS. Structurally similar to cycasin, a natural compound that strongly induces tumors in colons and rectums of rats and mice (*27, 28*), AOM induces O^6-methylguanine adducts in DNA, causing G→A transition mutations and when given in multiple doses, causes the induction of tumors in the distal colon of rodents (*29*). An initiating single dose of AOM is commonly used in combination with repeated cycles of DSS. The combined treatment enhances tumor formation because AOM acts as a tumor initiator and DSS, by mimicking episodic UC, acts as a tumor promoter (*20*). However, C57BL/6 mice receiving a single dose of AOM do not develop dysplasias/tumors/adenomas, indicating that a single-dose of the colonic carcinogen is insufficient to induce colorectal tumors in the absence of inflammation (*9, 30*).

Here, we set out to examine the effects of deficiency in the DNA repair proteins Abh2 and Abh3 and to assess their roles in tumor development. In addition, we investigated

the genetic interaction of *Abh2* and *Abh3* with *Aag* in susceptibility to chronic inflammation. In order to assess any overlap or interaction between Aag and Abh2/3 activity, we induced chronic inflammatory colitis in single- and double-mutant mice and monitored the phenotypic outcome. Our results show that Aag plays the major role in ameliorating the response to chronic inflammation. Although increased sensitivity to chronic inflammation is apparent in the $Abh2^{-/-}Abh3^{-/-}$ double mutant, niehter of the single mutants showed increased sensitivity.

3.2. Materials and Methods

3.2.1. Animals

All procedures were approved by the MIT Committee on Animal Care. $Abh2^{-/-}$ and $Abh2^{-/-}Abh3^{-/-}$ mice were in 129/SvEv background whereas $Aag^{-/-}$, $Aag^{-/-}Abh2^{-/-}$, and $Aag^{-/-}Abh3^{-/-}$ were in a mixed C57BL/6 and 129/SvEv 50/50 (F1 generation) background. Wild-type (WT) mice in both genetic backgrounds: 129/SvEv and F1 mice from a C57BL/6 x 129/SvEv cross were also included as controls. All animals were 6-8 weeks old at the beginning of experiments. The mice were given a standard diet and housed in the MIT mouse facilities. Note: For simplicity, the strains will be referred to as 129 for 129/SvEv, B6 for C57BL/6, and 129/B6 for the mixed background.

3.2.2. Treatments

To study the effect of chronic inflammation in the absence of Abh2 and Abh3, WT, $Abh2^{-/-}$, and $Abh2^{-/-}Abh3^{-/-}$ mice were given repeated cycles of DSS in the drinking water

to induce episodic colitis. To determine the consequences of a tumor initiation event followed by chronic inflammation in the absence of Aag and/or Abh repair, WT, *Abh2*$^{-/-}$, *Abh2*$^{-/-}$*Abh3*$^{-/-}$, *Aag*$^{-/-}$, *Aag*$^{-/-}$*Abh2*$^{-/-}$, and *Aag*$^{-/-}$*Abh3*$^{-/-}$ mice were treated with AOM prior to the repeated cycles of DSS administration, for tumor initiation.

DSS only

Mice were exposed to seven cycles of DSS. Each cycle consisted of 5 days of 2.5% DSS (MW 36,000-50,000, MP Biomedicals) in the distilled drinking water followed by 16 days of regular tap water, except for the last cycle in which DSS treatment was followed by 4 days of regular tap water. Four days after the 7th DSS cycle, the mice were sacrificed. Figure 3-1A illustrates this treatment scheme.

AOM+DSS

Five days before the first DSS cycle, a single dose of 12.5 mg/kg of AOM (Midwest Research Institute, NCI Chemical Repository) was injected intraperitoneally (i.p.) to the mice. Subsequently, five cycles of DSS were administered (as described above). Treatment scheme is illustrated in Figure 3-1B.

3.2.3. Euthanasia and Tissue Collection

Mice were euthanized by CO_2 inhalation. The whole animal was weighed and colon and spleen collected from each mouse. The colon (from cecum to anus) was removed from each mouse, washed with 1X PBS, cut open lengthwise and length measured.

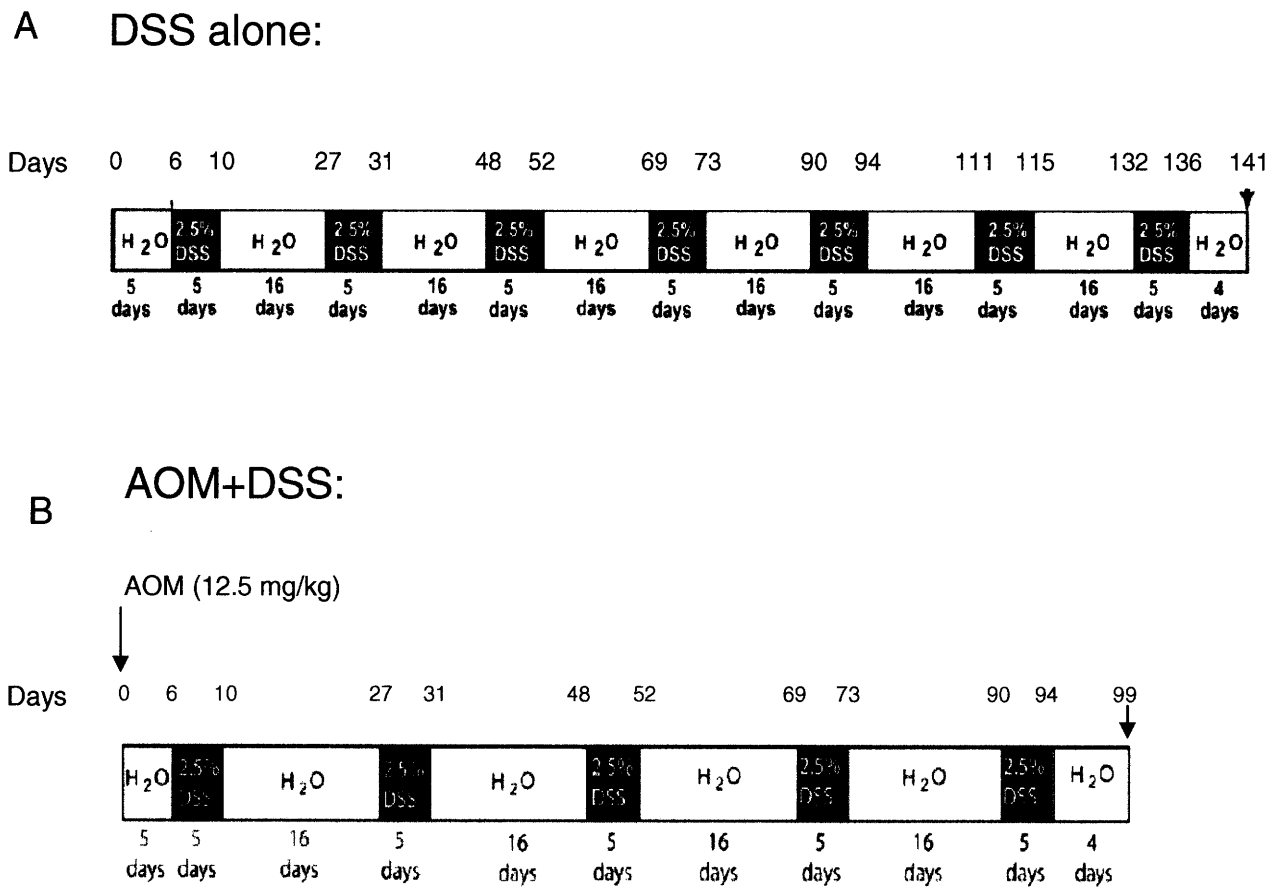

Figure 3-1 Two different treatment schemes were used in this study. (A) Treatment with 7 cycles of DSS (DSS alone). (B) Treatment with an initial dose of AOM followed by 5 cycles of DSS (AOM+DSS). White blocks indicate days of normal water treatment and black blocks indicate 5 days of 2.5% DSS in the drinking water.

Polyps/tumors were counted under a stereomicroscope (magnification, 45X). The colon was then fixed in 10% neutral buffered formalin and transferred to 70% ethanol. The spleens were weighed and fixed in 10% neutral buffered formalin and then transferred to 70% ethanol similar to the colon.

3.2.4. Tissue Processing and Histopathology

The collected spleens and colons in 70% ethanol were processed by the MIT Center for Cancer Research Histology lab where they were embedded in paraffin, sectioned at 5 μm, and Hematoxylin and Eosin (H&E) stained. The H&E stained slides were then scored by Dr. Sureshkumar Muthupalani (Division of Comparative Medicine, MIT) for the following: inflammation; epithelial defects; crypt atrophy; hyperplasia; dysplasia / neoplasia; and area affected by dysplasia/neoplasia. Scoring criteria used by Dr. Muthupalani are shown in the Chapter 3 Appendix.

3.2.5. Statistics

Statistical analyses were done using the GraphPad Prism software. Mann-Whitney test was used to compare data on spleen weights, colon lengths, tumor multiplicities, and pathological scoring. Survival rates on the whole animals were analyzed using Kaplan-Meier survival curves with the Log-Rank test.

3.3. Results

For simplicity, the strains will be referred to as 129, B6, and 129/B6 for the F1 mixed background. In addition, the following graphs showing data on the spleen weight, colon length, tumor incidence, tumor multiplicity, and histopathological scores contain combined data for mice that survived to the end of the treatment regime and for mice that died during the study. The data were very similar from the two sets of mice and so were combined for a more complete representation. Please see tables comparing disease markers of the two sets in the Chapter 3 Appendix.

3.3.1. The 129 and B6 mice respond differently to DSS and to AOM+DSS.

We first examined the susceptibility of the wild-type mice in the 129 versus the B6 genetic backgrounds. Because double knockouts of *Aag*$^{-/-}$*Abh2*$^{-/-}$ and *Aag*$^{-/-}$*Abh3*$^{-/-}$ mice were in a mixed 129/B6 background, the mixed background was also examined. Interestingly, 129 and 129/B6 wild type mice displayed different susceptibility to the treatment, as seen in the survival after an initial AOM treatment followed by 5 cycles of DSS (AOM+DSS) (Figure 3-2A). The 129 mice exhibited a significant decrease in survival compared to mice in the 129/B6 background ($p=0.0174$) and the B6 background ($p=0.0078$). Wild type mice in the three strain backgrounds appeared to have similar spleen weights relative to body weights after AOM+DSS (Figure 3-2B). However, 129 mice trended toward a higher tumor multiplicity than mice in the 129/B6 or in pure B6 (Figure 3-2C). Furthermore, 129 WT mice also showed a significantly greater decrease in colon length ($p=0.0412$) than WT mice in the 129/B6 (Figure 3-2D). The greater susceptibility of 129 versus B6 was also observed in the histopathological scores. The

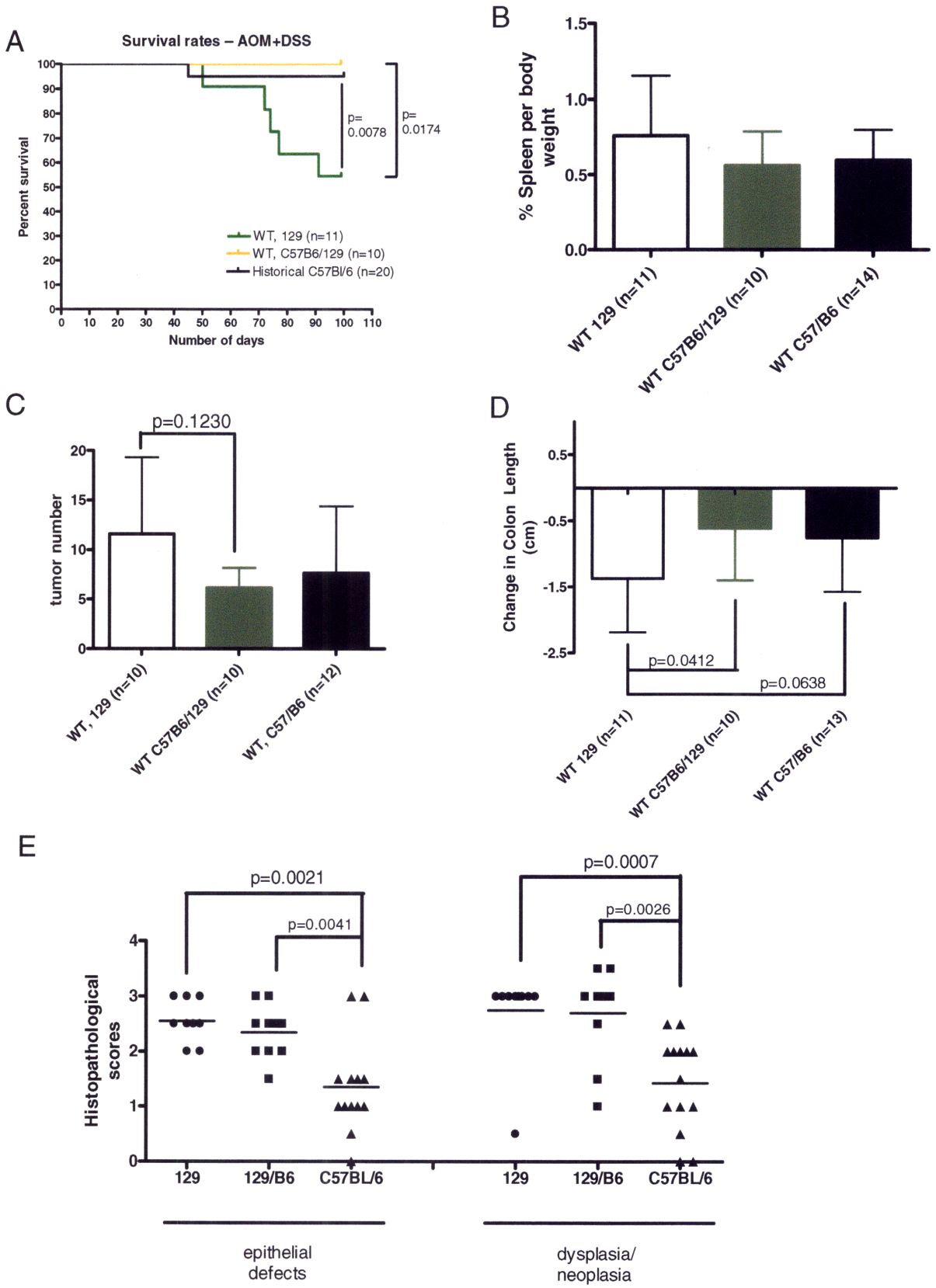

Figure 3-2 WT mice in the different strain backgrounds, 129/SvEv and C57BL/6, exhibit differential susceptibility to colitis induced by AOM+DSS. (A) Kaplan-Meier survival curves for the WT mice in the different backgrounds. (B) Spleen weight as a percentage of body weight. Data are mean ± SD. (C) Tumor multiplicity. Data are mean ± SD. (D) Change in colon length. Data are mean ± SD. (E) Histopathological scores for severity of epithelial defects and dysplasia/neoplasia. Lines indicate mean scores. Data of C57BL/6 mice are historical data from previous study (*11*).

scores were significantly increased for most criteria in 129 WT mice compared to B6 WT from historical data (Figure 3-2E). These data indicate that these two genetic backgrounds exhibit differential susceptibility to colitis and that it was necessary to use appropriate WT controls in our experiments since the genetic background itself confers differences in susceptibility to AOM+DSS.

3.3.2. *Abh2*$^{-/-}$*Abh3*$^{-/-}$ knockout animals suffer more severe general pathologies than WT after DSS-induced colonic inflammation.

Inflammation-induced RONS can directly oxidize and deaminate DNA bases and indirectly alkylate bases via lipid peroxidation that leads to a byproduct that can react with DNA to generate etheno base lesions (*11*). A previous study showed that nuclear extracts lacking Abh2 lacked εA repair activity (*18*), indicating Abh2 is important in the repair of this toxic and mutagenic DNA lesion. We therefore set out to determine whether Abh2 or Abh3 proteins have protective roles in chronic inflammation. Thus, we monitored the sensitivity of Abh-deficient mice to chronic inflammation induced by 7 cycles of DSS (DSS alone), with the treatment scheme as illustrated in Figure 3-1A.

129 WT and 129 *Abh2*$^{-/-}$ mice exhibited similar survival rates during the DSS-alone treatment scheme as shown in Figure 3-3A. The *Abh2*$^{-/-}$*Abh3*$^{-/-}$ mice showed slightly lower survival than the 129 WT and *Abh2*$^{-/-}$ mice that did not reach statistical difference. Overall, these animals did not exhibit any major differences in whole animal lethality in response to episodic colonic inflammation.

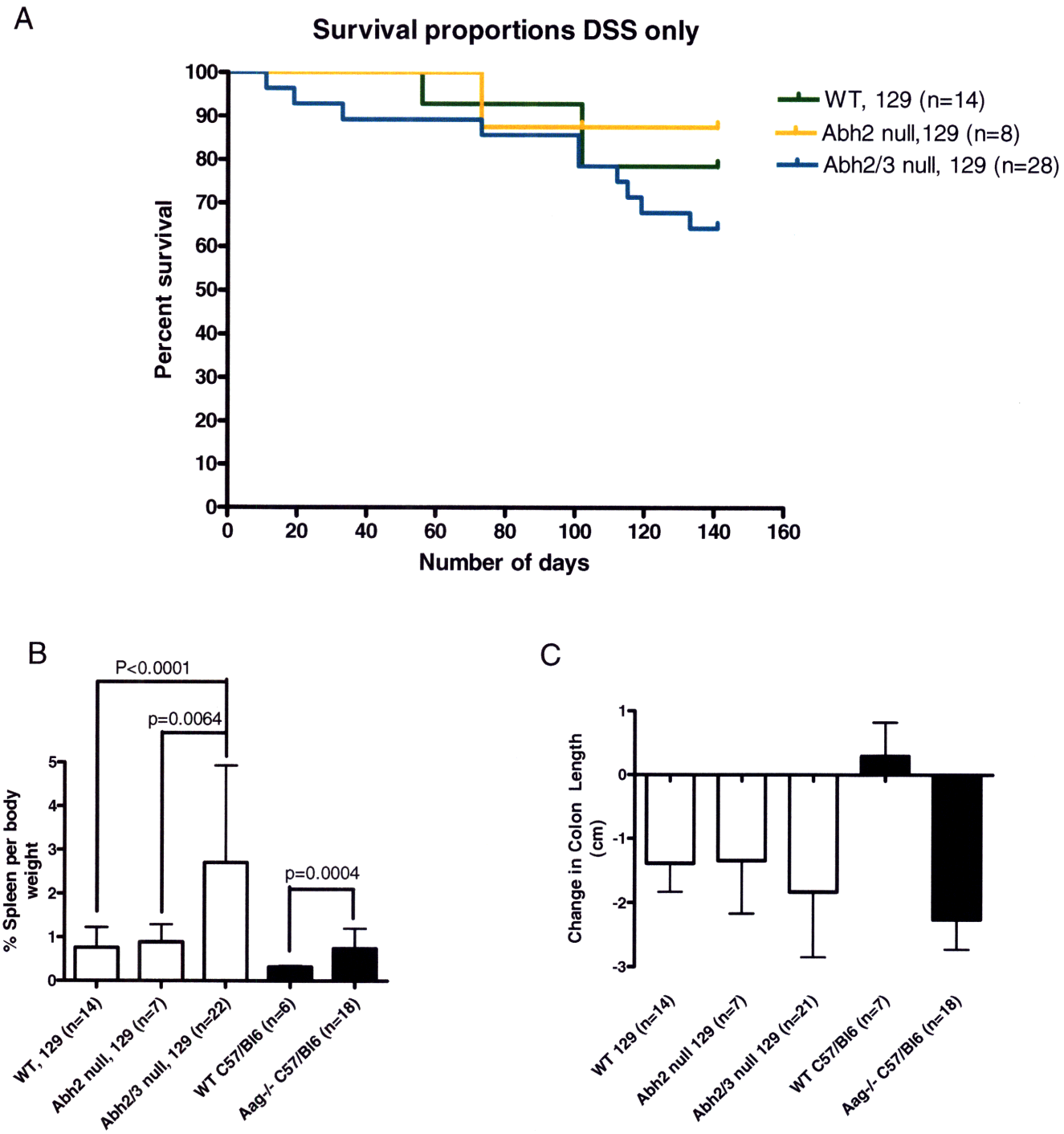

Figure 3-3 *Abh2-/-Abh3-/-* mice appear to be more susceptible than WT and *Abh2-/-* mice in DSS alone treatment. (A) Kaplan-Meier survival curves for the various genotypes in the study. (B) Spleen weight as a percentage of body weight. Data are mean ± SD. (C) Change in colon length. Data are mean ± SD. Black bars represent historical data in C57BL/6 from previous study (*11*).

We next assessed disease markers of colitis including increased spleen weight in 129 WT, 129 *Abh2*$^{-/-}$, and 129 *Abh2*$^{-/-}$*Abh3*$^{-/-}$ animals after DSS-induced chronic inflammation. In colitis, blood is often lost from stools due to tumors or ulcers, leading to splenomegaly associated with extramedullary hematopoiesis (*9*). Figure 3-3B shows *Abh2*$^{-/-}$*Abh3*$^{-/-}$ exhibit significantly greater increase in spleen weight compared to WT ($p<0.0001$) and *Abh2*$^{-/-}$ ($p=0.0064$) animals. These increases were much larger than those observed previously comparing B6 *Aag*$^{-/-}$ to B6 WT animals (*9*) (historical data, Figure 3-3B).

A decrease in colon length is commonly observed in this disease model and is attributed to repeated healing of ulcers and fistulas (*9*). In addition to DNA damage, DSS can also adversely affect protein folding in the endoplasmic reticulum (ER) and cause ER stress in the epithelial cells of the gastrointestinal tract (*20, 23-25*). Such damages lead to cell death and require more healing by the colon, giving rise to a decreased colon length. The 129 *Abh2*$^{-/-}$*Abh3*$^{-/-}$ mice trended towards a greater decrease in colon length than those of 129 WT and 129 *Abh2*$^{-/-}$ mice but this decrease did not reach statistical significance (Figure 3-3C).

DSS-alone treatment did not result in appreciable tumor induction; regardless of genotypes, only 15% of mice developed tumors (Figure 3-4A) and the average number of tumors per colon was less than one (Figure 3-4B), and there was no difference between the genotypes. This is consistent with the histopathological (hyperplasia and dysplasia/neoplasia) scores for these tissues (Figure 3-4C). Colons were scored for inflammation, epithelial defects, crypt atrophy, dysplasia/neoplasia, and area of

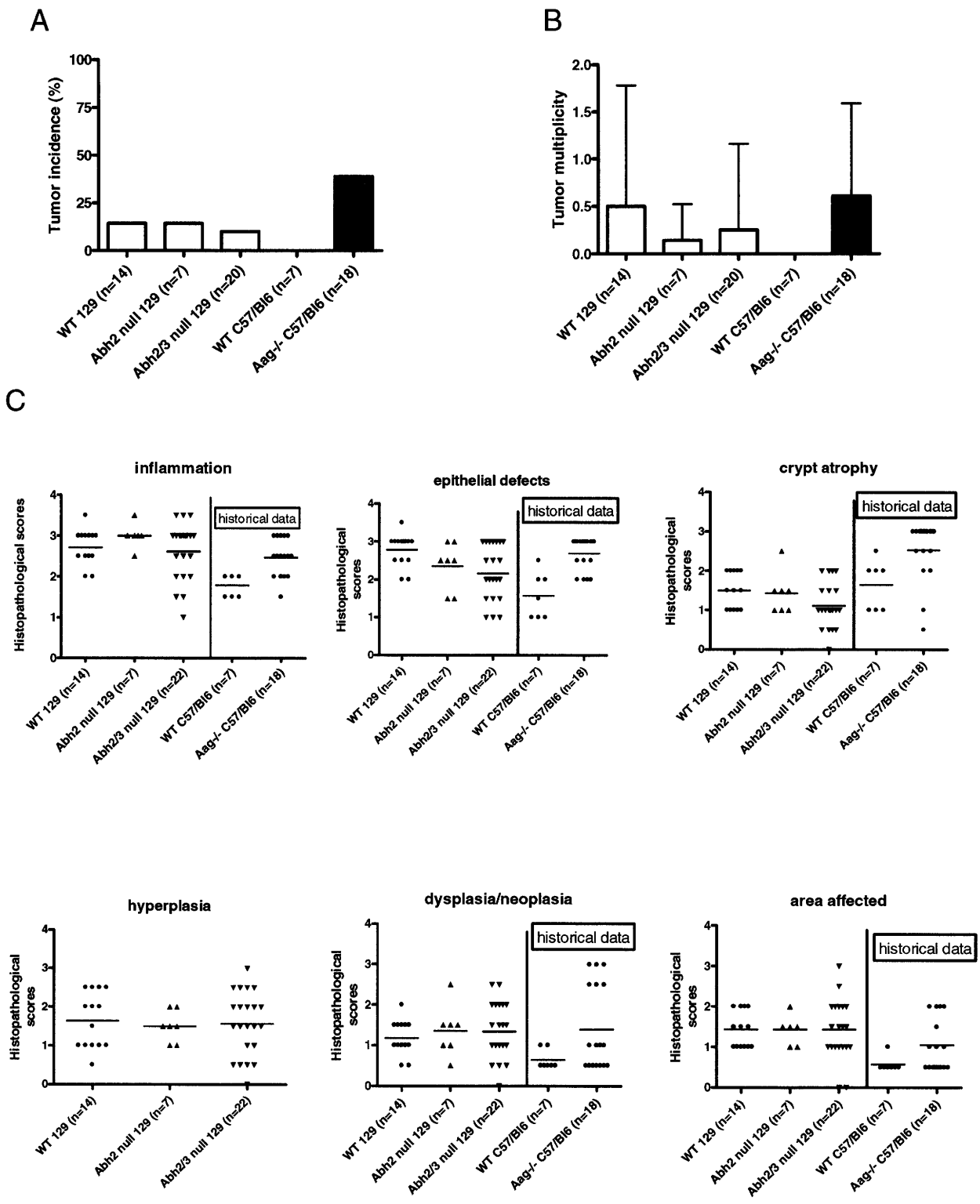

Figure 3-4 Tumor formation is not significant in Abh-deficient and WT animals in DSS alone treatment. (A) Tumor incidence and (B) tumor multiplicity. Data are mean ± SD. Black bars represent historical data in C57BL/6 from previous study (*11*). (C) Histopathological scores for severity of inflammation, epithelial defects, crypt atrophy, hyperplasia, dysplasia/neoplasia, and area affected. Lines indicate mean scores. Histopathological scores of WT and *Aag-/-* animals in C57BL/6 are historical data from previous study (*11*).

dysplasia/neoplasia. Figure 3-4C shows that all animals of the different genotypes experienced similarly high degrees of severity in colon in the different criteria induced by 7 cycles of DSS.

In summary, with 7 cycles of DSS treatment, no significant difference was found in tumor development in any genotype. However, an increase in spleen weight was seen for 129 *Abh2*$^{-/-}$*Abh3*$^{-/-}$ mice compared to 129 WT and 129 *Abh2*$^{-/-}$ mice. Although not statistically significant, the change in colon length for 129 *Abh2*$^{-/-}$*Abh3*$^{-/-}$ mice was slightly larger than that of 129 WT and 129 *Abh2*$^{-/-}$ mice. Tumor incidence and multiplicities were low in all genotypes, consistent with previous studies on B6 *Aag*$^{-/-}$ and B6 WT animals with the same protocols (*9*). Because there was no significant colon tumor formation in the DSS alone treatment scheme, we subsequently adopted another treatment scheme that includes tumor initiation with an initial AOM treatment.

3.3.3. 129 *Abh2*$^{-/-}$ and *Abh3*$^{-/-}$ animals experience greater sensitivity and tumor development than WT animals following AOM+DSS treatment.

The DSS-alone treatment resulted in severe general pathologies but very little tumor formation. Since we are interested in the protective role of DNA repair in chronic inflammation and its relation with cancer, we utilized another treatment scheme. Tumor initiation by the DNA alkylating agent AOM, followed by promotion by DSS-induced inflammation is known to be effective for inducing colon tumors in mice.

In the AOM+DSS treatment scheme (Figure 3-1B), both 129 *Abh2*$^{-/-}$ and 129 *Abh2*$^{-/-}$ *Abh3*$^{-/-}$ mice were slightly more sensitive than the 129 WT mice in terms of survival, although the differences did not reach statistical significance (Figure 3-5A). Moreover, similar to observations in the DSS alone study, *Abh2*$^{-/-}$*Abh3*$^{-/-}$ mice displayed significantly larger spleens than WT (p=0.0021) (Figure 3-5B), whereas *Abh2*$^{-/-}$ mice only showed a slight increase in spleen weight that did not reach statistical significance. Also, as with DSS alone treatment, the change in colon length did not differ for *Abh2*$^{-/-}$ and *Abh2*$^{-/-}$*Abh3*$^{-/-}$ mice compared to WT (Figure 3-5C). As expected, with an initial treatment of a DNA damaging agent, tumor incidence and tumor multiplicity were significantly higher than those in the DSS-alone treatment. In the AOM+DSS treatment scheme, the majority of the mice developed tumors. In fact, 83% of WT in 129 background and 100% of *Abh2*$^{-/-}$ and *Abh2*$^{-/-}$*Abh3*$^{-/-}$ mice developed colon tumors (Figure 3-6A). Similar to the increases in spleen weights observed in both DSS alone and AOM+DSS treatments, *Abh2*$^{-/-}$*Abh3*$^{-/-}$ mice developed significantly more tumors with respect to both WT (p=0.0204) and *Abh2*$^{-/-}$ (p=0.0424) mice (Figure 3-6B). This demonstrates that a deficiency in both Abh2 and Abh3 renders mice slightly more susceptible to the induction of colon tumors by AOM+DSS.

Histopathological scores among these genotypes were similar in most criteria, except where *Abh2*$^{-/-}$*Abh3*$^{-/-}$ animals exhibited significant increase in the amount of hyperplasia found in the colon tissue when compared to WT (p=0.0012), consistent with the increased number of tumors in these animals (Figure 3-6C). As expected, animals treated with AOM+DSS scored higher in dysplasia/neoplasia and the magnitude of its affected

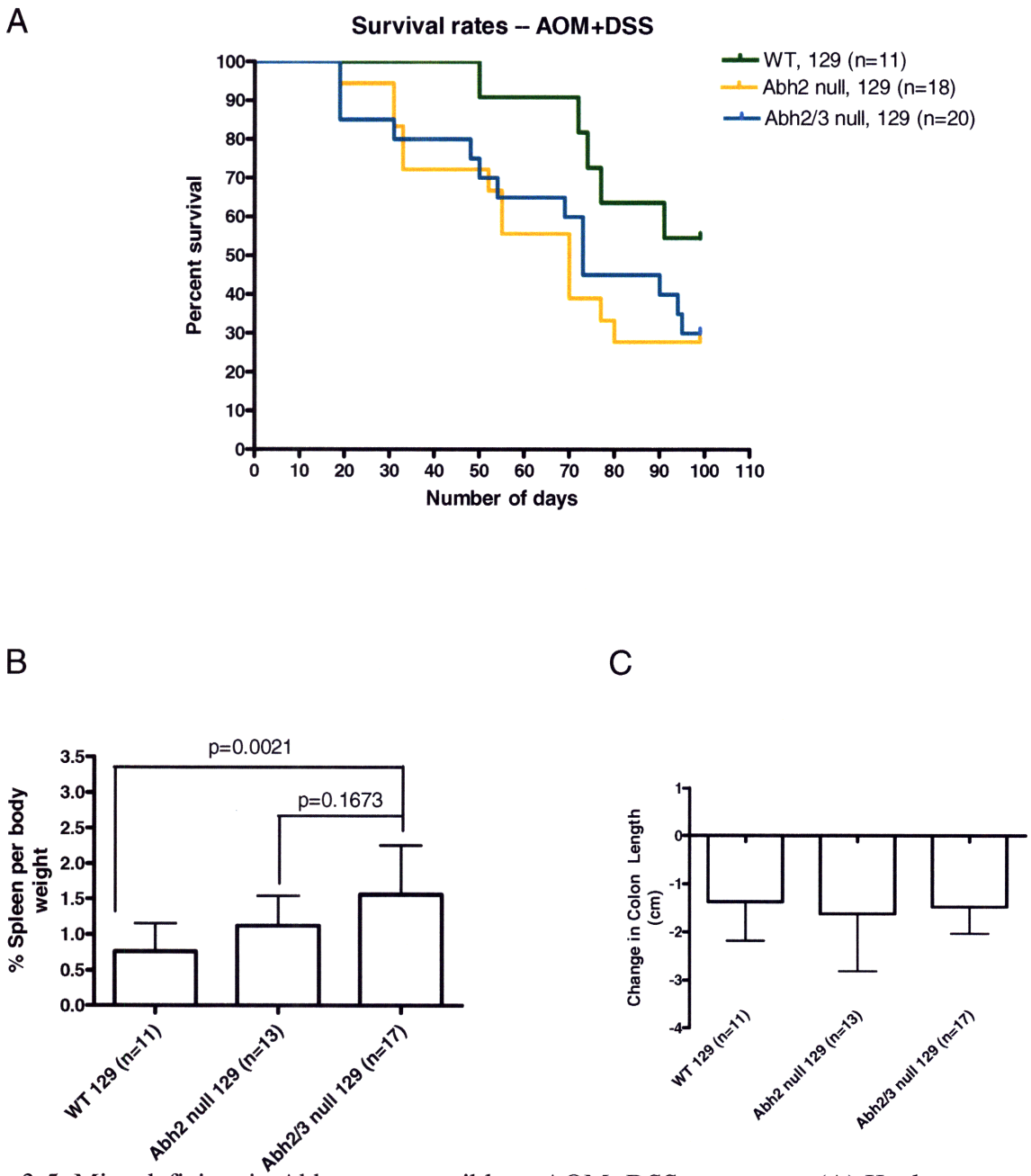

Figure 3-5 Mice deficient in Abh are susceptible to AOM+DSS treatment. (A) Kaplan-Meier survival curves for the various genotypes in the study. (B) Spleen weight as a percentage of body weight. Data are mean ± SD. (C) Change in colon length. Data are mean ± SD.

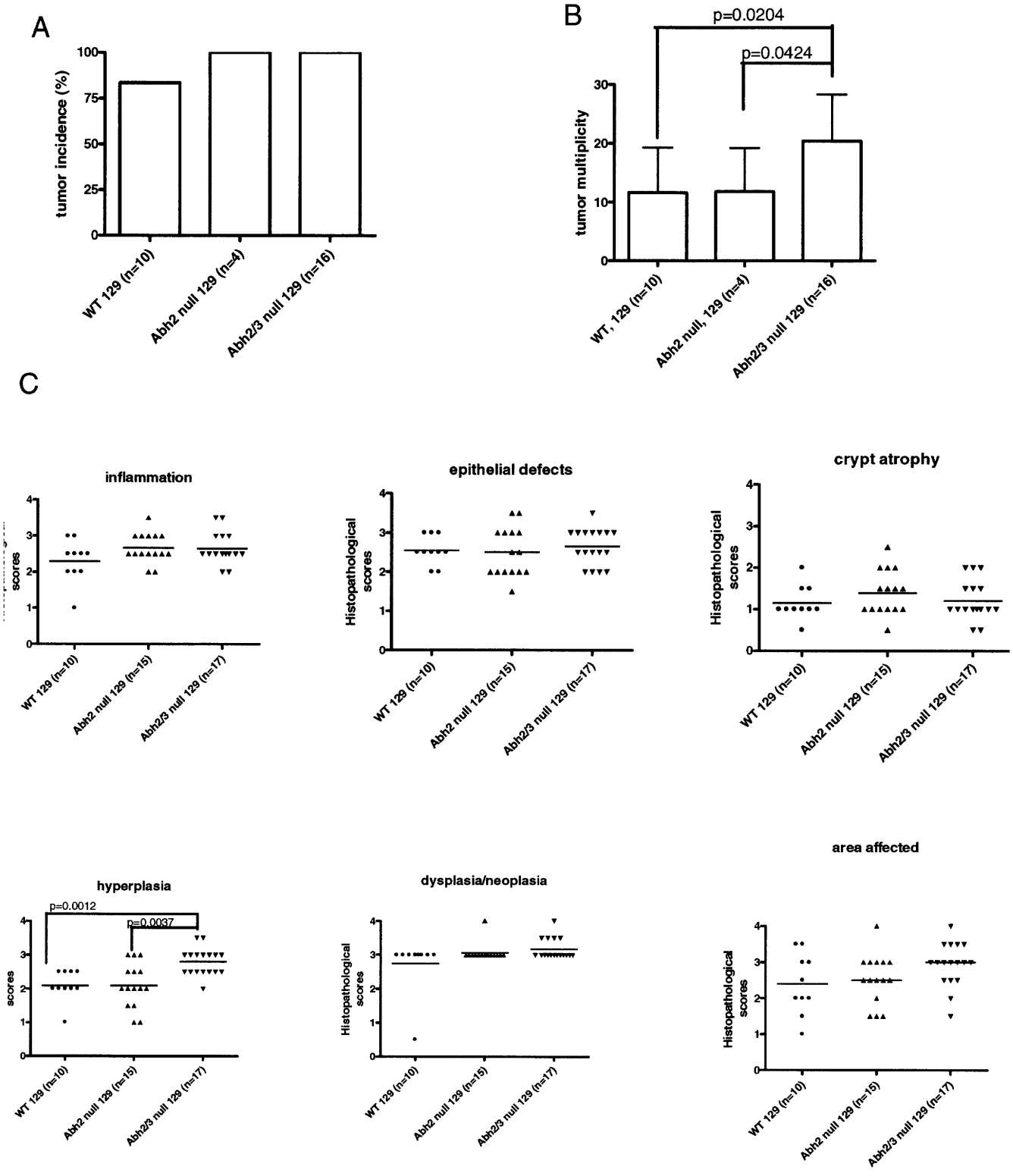

Figure 3-6 Tumor formation is significant for mice deficient in Aag and Abh in AOM+DSS treatment. (A) Tumor incidence and (B) tumor multiplicity. Data are mean ± SD. (C) Histopathological scores for severity of inflammation, epithelial defects, crypt atrophy, hyperplasia, dysplasia/neoplasia, and area affected. Lines indicate mean scores.

area than those in the DSS alone study, confirming that AOM+DSS treatment gives rise to a greater extent of abnormal cell proliferation, consistent with the model leading to higher number of tumors. Taken together, these results show that sensitivity due to the lack of Abh2 is not apparent in the AOM+DSS treatment; however, deficiency in both Abh2 and Abh3 together appears significant in giving rise to a sensitive response to colitis, as with the DSS alone treatment.

3.3.4. *Abh2*$^{-/-}$ or *Abh3*$^{-/-}$ in conjunction with *Aag*$^{-/-}$ mutant mice display more pronounced inflammation phenotype than WT animals following AOM+DSS treatment.

Given the overlap in substrate preference between the Abh2/3 proteins and Aag, we next wanted to determine if the absence of Aag would confer greater sensitivity to Abh-deficient mice. Aag-deficient mice were previously demonstrated to exhibit a significantly more sensitive phenotype than WT animals to AOM+DSS treatment (*9*). We set out to determine whether the absence of Abh2 or Abh3 in an Aag-deficient strain would further increase sensitivity since none was seen for the single Abh2 mutant following AOM+DSS treatment. We treated WT, *Aag*$^{-/-}$, *Aag*$^{-/-}$*Abh2*$^{-/-}$ and *Aag*$^{-/-}$*Abh3*$^{-/-}$ mice with AOM+DSS as described in Figure 3-1B. Note that all the strains in this study were on a mixed 129/B6 strain background. Interestingly, there was a significant decrease in survival (Figure 3-7A) compared to 129/B6 WT mice for 129/B6 *Aag*$^{-/-}$ ($p<0.0001$), 129/B6 *Aag*$^{-/-}$*Abh2*$^{-/-}$ ($p=0.0008$) and 129/B6 *Aag*$^{-/-}$*Abh3*$^{-/-}$ ($p=0.0011$). Consistent with decreased survival, we also observed other disease markers elevated in

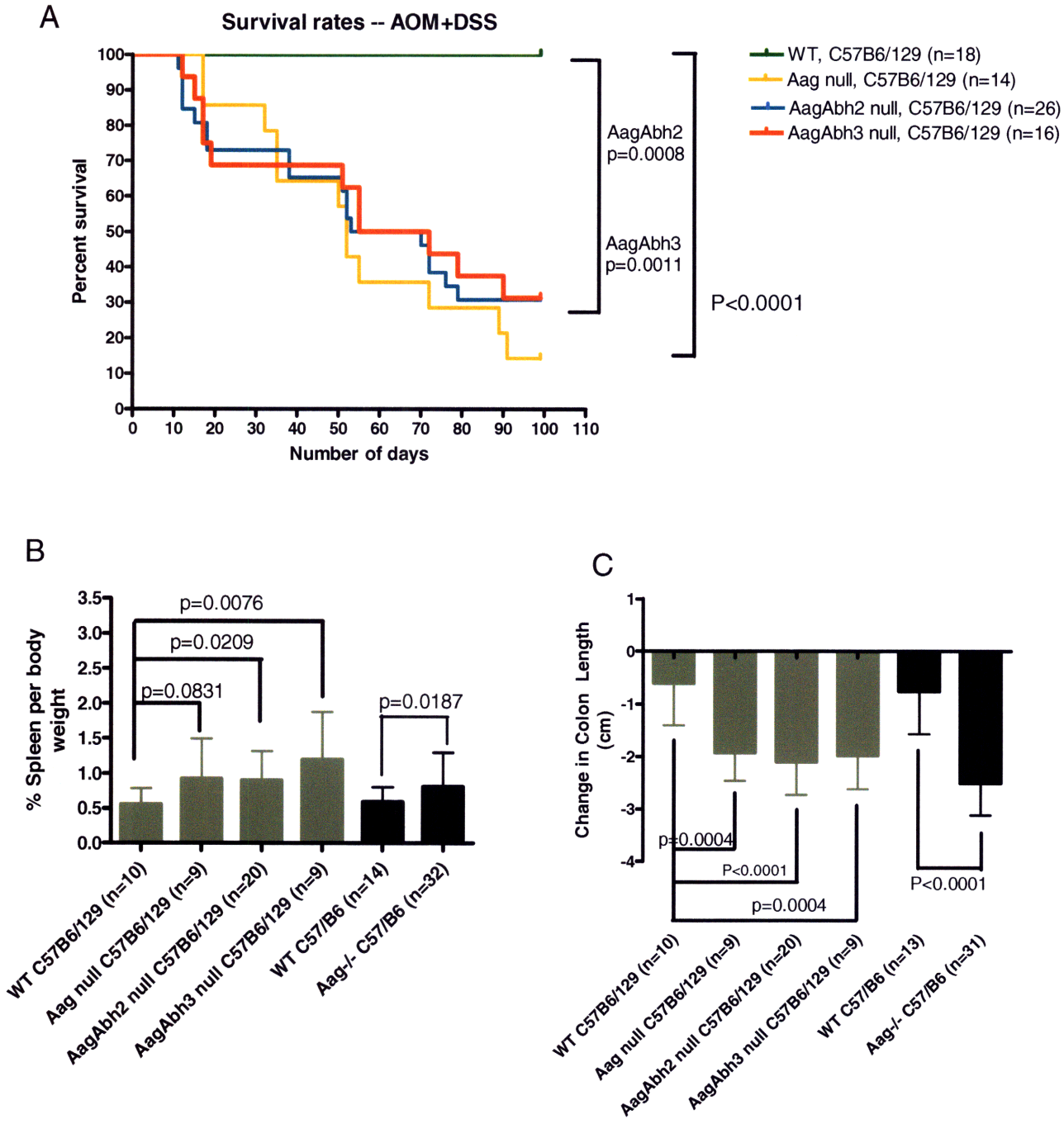

Figure 3-7 Mice deficient in Aag and Abh are susceptible to AOM+DSS treatment. (A) Kaplan-Meier survival curves for the various genotypes in the study. (B) Spleen weight as a percentage of body weight. Data are mean ± SD. (C) Change in colon length. Data are mean ± SD. Black bars represent historical data in C57BL/6 from previous study (*11*).

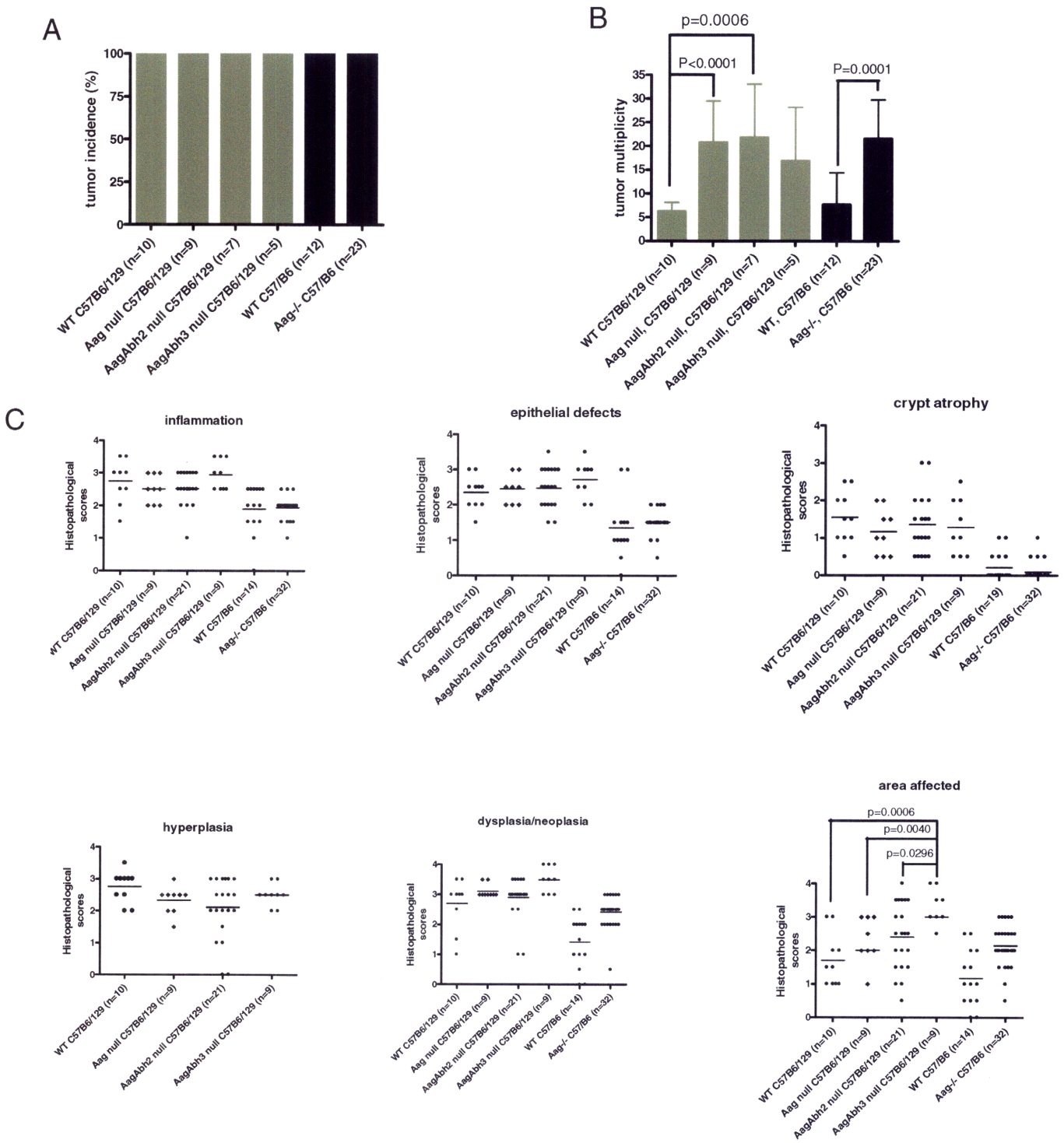

Figure 3-8 Tumor formation is significant for mice deficient in Aag and Abh in AOM+DSS treatment. (A) Tumor incidence and (B) tumor multiplicity. Data are mean ± SD. Black bars represent historical data in C57BL/6 from previous study (*11*). (C) Histopathological scores for severity of inflammation, epithelial defects, crypt atrophy, hyperplasia, dysplasia/neoplasia, and area affected. Lines indicate mean scores. Histopathological scores of WT and *Aag-/-* animals in C57BL/6 are historical data from previous study (*11*).

these repair-deficient mice. For example, spleen weight increases were seen in *Aag*$^{-/-}$ (although not quite significant), *Aag*$^{-/-}$*Abh2*$^{-/-}$ (p=0.0209) and *Aag*$^{-/-}$*Abh3*$^{-/-}$ (p=0.0076) mice when compared to WT (Figure 3-7B). Similarly, *Aag*$^{-/-}$, *Aag*$^{-/-}$*Abh2*$^{-/-}$, and *Aag*$^{-/-}$ *Abh3*$^{-/-}$ all showed significant decreases in colon length compared to 129/B6 WT (Figure 3-7C), indicating severe colon pathology. In the AOM+DSS treatment scheme, all of the mice, regardless of genotypes, developed colon tumors (Figure 3-8A). Figure 3-8B shows tumor multiplicity; compared to WT mice, *Aag*$^{-/-}$ (p<0.0001), *Aag*$^{-/-}$*Abh2*$^{-/-}$ (p=0.0006), and *Aag*$^{-/-}$*Abh3*$^{-/-}$ mice all developed substantially more tumors. However, in the Aag-deficient background, the addition of Abh2 or Abh3 deficiency did not lead to more tumors. In addition to tumor formation, sensitivity in the colon was also evident by histopathological analysis. Figure 3-8C shows the histopathological analysis in the following criteria: inflammation; epithelial defects; crypt atrophy; hyperplasia; dysplasia/neoplasia; and area affected. The histopathological scores in all criteria showed high levels of damage in the colon. These results confirm that Aag has a protective role in preventing the formation of colon tumors and relieving pathology in response to chronic inflammation. Together these data indicate that with the AOM+DSS treatment, the absence of the single Abh2 or Abh3 gene resulted in no additional sensitivity in Aag-deficient mice; thus, Aag appears to be the predominant DNA alkylation repair protein for rescuing mice from the effects of chronic colonic inflammation.

3.4. Discussion

Colorectal cancer is the second most common cancer in the Western world, accounting for about 10% of cancer deaths in the U.S. in 2005 (*27*). Studying inflammation and its

contribution to cancer is important because patients with chronic IBD (ulcerative colitis or Crohn's disease) are at greater risk of developing colorectal cancer (*31, 32*), suggesting chronic inflammation is a major risk factor for this disease (*33, 34*). The risk of colorectal cancer increases with extent of disease and duration, with an increase of 0.5-1% per year after 7 years of colitis (*31*).

In the present study, episodic inflammation (induced by the colonic irritant DSS) was simulated in wild-type and DNA repair-deficient mice lacking Abh2, Abh3, or Aag. As a carcinogen that is used to induce colon cancer in rats and mice, a single dose of AOM alone does not induce colon cancer. Chronic inflammation provoked by repeated cycles of DSS with a preceding treatment with AOM is necessary for cancer since significant tumorigenesis has been seen in previous mouse model studies (*9, 30*). We report here that repair deficiency in Aag, Abh2 and Abh3 contributes to increased disease and pathology in response to DSS-induced chronic inflammation, both in the absence and presence of initial DNA damage by AOM. With treatment of AOM+DSS, increased tumor formation was seen in the absence of alkylation repair proteins Aag and/or Abh2 and Abh3. Tumor formation was significant in AOM+DSS treatment for all animals, regardless of genotype, compared to the treatment with DSS alone, which is not always effective in inducing a robust neoplastic or tumor response.

Because the Abh knockout mice were originally made in the 129 background and Aag knockout mice in the B6 background, Aag and Abh double knockouts are in a mixed 129/B6 background. To generate the double knockout mice in a pure background strain

would require over two years and 10 generations of backcrossing. Therefore, these experiments were carried out in the mixed background. Unfortunately, an unavoidable drawback of this experiment is the difficulty in comparing phenotypes in the different backgrounds. We show that WT 129 mice show increased susceptibility to treatment including lower survival, larger decrease in colon length, higher tumor multiplicity, and higher histopathological scores when compared to the mixed 129/B6 or pure B6 strains. It has been reported that genetically engineered mice in the 129/Sv strain appears susceptible to IBD-like disease while those in the B6 background are more resistant to IBD-related tumorigenesis in comparison with 129 and other genetic backgrounds (*35*). Our results are consistent with previous studies which demonstrated differential susceptibility of inbred mouse strains to DSS-induced colitis (acute inflammation with 1 cycle of DSS) including differences in histological lesions in ceca and colons in terms of severity, ulceration, hyperplasia, and area involved (*36*). Some strains including B6 and 129/SvPas (a different substrain of 129/Sv than the one used in this study) showed different degrees of susceptibility at different anatomical sites in that they were relatively and strongly resistant in the cecum, respectively, but both showed susceptibility in the colon (*36*). Since the B6 strain is known to be more refractory to tumors of epithelial origin (*37*), its resistance compared to the 129 strain is not surprising.

The protective nature of Aag is presumably due to the fact that it can repair DNA from a wide variety of damages. However, an excess of Aag-initiated abasic site intermediates leading to strand breaks would have detrimental effects. Deficiency in repair proteins such as Aag or the direct repair proteins Abh may lead to higher susceptibility to

mutations and cancer, as DNA damage brought about by RONS would be unrepaired. It was shown in this study that during chronic inflammatory colitis, alkylation repair deficient mice are prone to develop more tumors than WT. Using the DSS alone and AOM+DSS model of colitis, the sensitive phenotype of mice deficient in Abh and/or Aag repair was shown in response to chronic inflammation, as seen in the increase in spleen weight, decrease in colon length, and tumor formation. However, lack of either Abh2 or Abh3 alone does not always lead to such sensitivities, likely due to compensation by Aag or other Abh proteins. It is very likely that the interplay and overlap in substrate specificity (etheno base lesions) among Aag, Abh2, and Abh3 allow them to substitute for one another to ensure cancer-free survival.

Significantly increased number of tumors were seen in the AOM+DSS scheme with *Abh2*$^{-/-}$*Abh3*$^{-/-}$, *Aag*$^{-/-}$, *Aag*$^{-/-}$*Abh2*$^{-/-}$, and *Aag*$^{-/-}$*Abh3*$^{-/-}$ mice, when compared to WT mice in the appropriate genetic background. Supported also by increased spleen weight and decreased colon length, these results demonstrate that Abh2 and Abh3 together show combined effects, but that their individual effects are not obvious, in the presence or absence of Aag. It is possible that their individual effects are too small to be observed in this assay by these endpoints. Alternatively, it is also possible that Abh2 and Abh3 can repair inflammation-induced damages that cannot be repaired by Aag. If Abh2 and Abh3 work together to have a protective role and depend on each other for maximal function, it would be important to see whether *Abh3*$^{-/-}$ single mutant would show any measurable phenotype. In protecting animals against chronic inflammation, Aag appears to have a more prominent role. Similarly, since the absence of Aag masks the sensitivity due to the

individual effects of Abh2 or Abh3, and the double knockouts of both Abh2 and Abh3 lead to greater sensitivity than either mutant alone, it would be interesting to examine sensitivity to AOM+DSS in the *Aag*$^{-/-}$*Abh2*$^{-/-}$*Abh3*$^{-/-}$ triple mutant to confirm the combined effects of Abh2 and Abh3. It would be expected that the triple mutant would be much more sensitive than *Aag*$^{-/-}$ alone because *Abh2*$^{-/-}$*Abh3*$^{-/-}$ mice appeared more sensitive than either *Abh2*$^{-/-}$ or *Abh3*$^{-/-}$ single mutant alone from this study.

3.5. References

(1) Eaden, J. A., Abrams, K. R., and Mayberry, J. F. (2001) The risk of colorectal cancer in ulcerative colitis: a meta-analysis. *Gut 48*, 526-35.

(2) Allen, A., Hutton, D. A., Leonard, A. J., Pearson, J. P., and Sellers, L. A. (1986) The role of mucus in the protection of the gastroduodenal mucosa. *Scand J Gastroenterol Suppl 125*, 71-8.

(3) Owen, D. A., and Kelly, J. K. (1995) Inflammatory diseases of the gastrointestinal tract. *Mod Pathol 8*, 97-108.

(4) Gillen, C. D., Walmsley, R. S., Prior, P., Andrews, H. A., and Allan, R. N. (1994) Ulcerative colitis and Crohn's disease: a comparison of the colorectal cancer risk in extensive colitis. *Gut 35*, 1590-2.

(5) Hardy, R. G., Meltzer, S. J., and Jankowski, J. A. (2000) ABC of colorectal cancer. Molecular basis for risk factors. *Bmj 321*, 886-9.

(6) Dannenberg, A. J., and Subbaramaiah, K. (2003) Targeting cyclooxygenase-2 in human neoplasia: rationale and promise. *Cancer Cell 4*, 431-6.

(7) Tardieu, D., Jaeg, J. P., Deloly, A., Corpet, D. E., Cadet, J., and Petit, C. R. (2000) The COX-2 inhibitor nimesulide suppresses superoxide and 8-hydroxy-deoxyguanosine formation, and stimulates apoptosis in mucosa during early colonic inflammation in rats. *Carcinogenesis 21*, 973-6.

(8) Bartsch, H., and Nair, J. (2002) Potential role of lipid peroxidation derived DNA damage in human colon carcinogenesis: studies on exocyclic base adducts as stable oxidative stress markers. *Cancer Detect Prev 26*, 308-12.

(9) Meira, L. B., Bugni, J. M., Green, S. L., Lee, C. W., Pang, B., Borenshtein, D., Rickman, B. H., Rogers, A. B., Moroski-Erkul, C. A., McFaline, J. L., Schauer, D. B., Dedon, P. C., Fox, J. G., and Samson, L. D. (2008) DNA damage induced by chronic inflammation contributes to colon carcinogenesis in mice. *J Clin Invest 118*, 2516-25.

(10) Coussens, L. M., and Werb, Z. (2002) Inflammation and cancer. *Nature 420*, 860-7.

(11) Wiseman, H., and Halliwell, B. (1996) Damage to DNA by reactive oxygen and nitrogen species: role in inflammatory disease and progression to cancer. *Biochem J 313 (Pt 1)*, 17-29.

(12) Gros, L., Maksimenko, A. V., Privezentzev, C. V., Laval, J., and Saparbaev, M. K. (2004) Hijacking of the human alkyl-N-purine-DNA glycosylase by 3,N4-ethenocytosine, a lipid peroxidation-induced DNA adduct. *J Biol Chem 279*, 17723-30.

(13) Delaney, J. C., Smeester, L., Wong, C., Frick, L. E., Taghizadeh, K., Wishnok, J. S., Drennan, C. L., Samson, L. D., and Essigmann, J. M. (2005) AlkB reverses etheno DNA lesions caused by lipid oxidation in vitro and in vivo. *Nat Struct Mol Biol 12*, 855-60.

(14) Trewick, S. C., Henshaw, T. F., Hausinger, R. P., Lindahl, T., and Sedgwick, B. (2002) Oxidative demethylation by Escherichia coli AlkB directly reverts DNA base damage. *Nature 419*, 174-8.

(15) Falnes, P. O., Johansen, R. F., and Seeberg, E. (2002) AlkB-mediated oxidative demethylation reverses DNA damage in Escherichia coli. *Nature 419*, 178-82.
(16) Delaney, J. C., and Essigmann, J. M. (2004) Mutagenesis, genotoxicity, and repair of 1-methyladenine, 3-alkylcytosines, 1-methylguanine, and 3-methylthymine in alkB Escherichia coli. *Proc Natl Acad Sci U S A 101*, 14051-6.
(17) Koivisto, P., Robins, P., Lindahl, T., and Sedgwick, B. (2004) Demethylation of 3-methylthymine in DNA by bacterial and human DNA dioxygenases. *J Biol Chem 279*, 40470-4.
(18) Ringvoll, J., Moen, M. N., Nordstrand, L. M., Meira, L. B., Pang, B., Bekkelund, A., Dedon, P. C., Bjelland, S., Samson, L. D., Falnes, P. O., and Klungland, A. (2008) AlkB homologue 2-mediated repair of ethenoadenine lesions in mammalian DNA. *Cancer Res 68*, 4142-9.
(19) Mishina, Y., Yang, C. G., and He, C. (2005) Direct repair of the exocyclic DNA adduct 1,N6-ethenoadenine by the DNA repair AlkB proteins. *J Am Chem Soc 127*, 14594-5.
(20) Okayasu, I., Hatakeyama, S., Yamada, M., Ohkusa, T., Inagaki, Y., and Nakaya, R. (1990) A novel method in the induction of reliable experimental acute and chronic ulcerative colitis in mice. *Gastroenterology 98*, 694-702.
(21) Ohkusa, T. (1985) [Production of experimental ulcerative colitis in hamsters by dextran sulfate sodium and changes in intestinal microflora]. *Nippon Shokakibyo Gakkai Zasshi 82*, 1327-36.
(22) Kitajima, S., Takuma, S., and Morimoto, M. (1999) Changes in colonic mucosal permeability in mouse colitis induced with dextran sulfate sodium. *Exp Anim 48*, 137-43.
(23) Kitajima, S., Takuma, S., and Morimoto, M. (1999) Tissue distribution of dextran sulfate sodium (DSS) in the acute phase of murine DSS-induced colitis. *J Vet Med Sci 61*, 67-70.
(24) Ni, J., Chen, S. F., and Hollander, D. (1996) Effects of dextran sulphate sodium on intestinal epithelial cells and intestinal lymphocytes. *Gut 39*, 234-41.
(25) Ohkusa, T., Okayasu, I., Tokoi, S., Araki, A., and Ozaki, Y. (1995) Changes in bacterial phagocytosis of macrophages in experimental ulcerative colitis. *Digestion 56*, 159-64.
(26) Okayasu, I., Yamada, M., Mikami, T., Yoshida, T., Kanno, J., and Ohkusa, T. (2002) Dysplasia and carcinoma development in a repeated dextran sulfate sodium-induced colitis model. *J Gastroenterol Hepatol 17*, 1078-83.
(27) Gommeaux, J., Cano, C., Garcia, S., Gironella, M., Pietri, S., Culcasi, M., Pebusque, M. J., Malissen, B., Dusetti, N., Iovanna, J., and Carrier, A. (2007) Colitis and colitis-associated cancer are exacerbated in mice deficient for tumor protein 53-induced nuclear protein 1. *Mol Cell Biol 27*, 2215-28.
(28) Wali, R. K., Skarosi, S., Hart, J., Zhang, Y., Dolan, M. E., Moschel, R. C., Nguyen, L., Mustafi, R., Brasitus, T. A., and Bissonnette, M. (1999) Inhibition of O(6)-methylguanine-DNA methyltransferase increases azoxymethane-induced colonic tumors in rats. *Carcinogenesis 20*, 2355-60.
(29) Reddy, B. S. (2004) Studies with the azoxymethane-rat preclinical model for assessing colon tumor development and chemoprevention. *Environ Mol Mutagen 44*, 26-35.

(30) Clapper, M. L., Cooper, H. S., and Chang, W. C. (2007) Dextran sulfate sodium-induced colitis-associated neoplasia: a promising model for the development of chemopreventive interventions. *Acta Pharmacol Sin 28*, 1450-9.
(31) Itzkowitz, S. H., and Yio, X. (2004) Inflammation and cancer IV. Colorectal cancer in inflammatory bowel disease: the role of inflammation. *Am J Physiol Gastrointest Liver Physiol 287*, G7-17.
(32) Munkholm, P. (2003) Review article: the incidence and prevalence of colorectal cancer in inflammatory bowel disease. *Aliment Pharmacol Ther 18 Suppl 2*, 1-5.
(33) Rhodes, J. M., and Campbell, B. J. (2002) Inflammation and colorectal cancer: IBD-associated and sporadic cancer compared. *Trends Mol Med 8*, 10-6.
(34) Wong, N. A., and Harrison, D. J. (2001) Colorectal neoplasia in ulcerative colitis-recent advances. *Histopathology 39*, 221-34.
(35) Rogers, A. B., and Fox, J. G. (2004) Inflammation and Cancer. I. Rodent models of infectious gastrointestinal and liver cancer. *Am J Physiol Gastrointest Liver Physiol 286*, G361-6.
(36) Mahler, M., Bristol, I. J., Leiter, E. H., Workman, A. E., Birkenmeier, E. H., Elson, C. O., and Sundberg, J. P. (1998) Differential susceptibility of inbred mouse strains to dextran sulfate sodium-induced colitis. *Am J Physiol 274*, G544-51.
(37) Blackwell, B. N., Bucci, T. J., Hart, R. W., and Turturro, A. (1995) Longevity, body weight, and neoplasia in ad libitum-fed and diet-restricted C57BL6 mice fed NIH-31 open formula diet. *Toxicol Pathol 23*, 570-82.

3.6. Appendix

***Colon scoring criteria*:**

Inflammation

0: Normal
1: Small leukocyte aggregates in mucosa and/or submucosa
2: Coalescing mucosal and/or submucosal inflammation
3: Coalescing mucosal inflammation with prominent multifocal submucosal extension +/- follicle formation
4: Severe diffuse inflammation of mucosa, submucosa, & deeper layers

Epithelial defects

0: None
1: Focally dilated glands and/or attenuated surface epithelium, decreased goblet cells
2: Focally extensive gland dilation and/or surface epithelial attenuation
3: Erosions (mucosal necrosis terminating above muscularis mucosae)
4: Ulceration (full-thickness mucosal necrosis extending into submucosa or deeper)

Crypt atrophy (in region most affected)

0: None
1: <25%
2: ~25—50%
3: ~50—75%
4. >75%

Hyperplasia

0: Normal gland length
1: ~1.5 X normal
2: ~2 X; +/- mitotic figures 1/3 way up to surface
3: ~3 X; +/- mitotic figures 1/2 way up to surface
4: ~4X+; +/- mitotic figures >1/2 way up to surface

Dysplasia/Neoplasia

0: Normal
1: Aberrent crypt foci, dysplasia characterized by epithelial cell pleomorphism, plump & attenuated forms, gland malformation with splitting, branching, and infolding
2: Polypoid hyperplasia/dysplasia, moderate dysplasia characterized by pleomorphism, early cellular & nuclear atypia, piling & infolding, occasional cystic dilation, bulging towards muscularis mucosae & projection into lumen, loss of normal glandular, mucous, or goblet cells
3: Adenomatous and/or sessile hyperplasia/dysplasia; gastrointestinal intraepithelial neoplasia (GIN) or carcinoma *in situ*, marked dysplasia confined to mucosa, features as above but greater severity, frequent & sometimes bizarre mitoses
3.5: Intramucosal carcinoma (extension of severely dysplastic regions into muscularis mucosae)

4: Invasive carcinoma: Submucosal invasion (differentiate from herniation) or any demonstrated invasion into blood or lymphatic vessels, regional nodes, or other metastasis.

Note: Dysplastic glands herniated into lymphoid follicles in an otherwise normal mucosa are not scored. Dysplasia is a normal consequence of epithelial cell herniation into GALT.

Area of dysplasia/neoplasia (in affected region of bowel)
0: None
1: <10% surface area
2: 10—25% surface area
3: 25—50% surface area
4: >50% surface area

Table 3-1: Comparison of disease markers in mice that survived to the end of the treatment regime with those that died during study in DSS-alone treatment
Change in colon length is in cm
Spleen per body wt is in %

DSS only			
mean values	WT 129	Abh2 null 129	Abh2/3 null 129
change in colon length			
END	-1.4	-1.3	-1.9
DURING	-1.5		-1.7
% spleen per body wt			
END	0.9	0.9	2.1
DURING	0.4		5.5
tumor multiplicity			
END	0.6	0.1	0.3
DURING	0		0
inflammation			
END	2.7	3	2.7
DURING	2.8		2.1
epithelial defects			
END	2.7	2.4	2.3
DURING	3.0		1.8
crypt atrophy			
END	1.4	1.4	1.1
DURING	1.8		1
hyperplasia			
END	1.8	1.5	1.7
DURING	1.2		1
dysplasia/neoplasia			
END	1.2	1.4	1.3
DURING	1		1.4
area affected			
END	1.5	1.4	1.5
DURING	1.2		1

Table 3-2: Comparison of disease markers in mice that survived to the end of the treatment regime with those that died during study in AOM+DSS treatment
Change in colon length is in cm
Spleen per body wt is in %

AOM+DSS Mean values	WT 129	Abh2 null 129	Abh2/3 null 129	Aag null C57B6/129	AagAbh2 null C57B6/129	AagAbh3 null C57B6/129
change in colon length						
END	-1.1	-0.7	-1.4	-1.5	-2.0	-2.1
DURING	-1.7	-2.1	-1.5	-2.1	-2.1	-1.8
% spleen per body wt						
END	0.5	1.1	1.3	1.1	1.2	0.9
DURING	1.1	1.1	1.7	0.9	0.8	1.6
tumor multiplicity						
END	10.8	10.8	20.0	18.5	21.6	11.8
DURING	12.8	12.3	20.7	21.4	21.7	23.3
inflammation						
END	2.3	2.8	2.6	2	2.7	3.1
DURING	2.3	2.6	2.7	2.6	2.4	2.8
epithelial defects						
END	2.8	2.3	2.6	2	2.1	3
DURING	2.3	2.6	2.7	2.6	2.7	2.4
crypt atrophy						
END	1.2	1.4	1.1	0.8	1.4	1.8
DURING	1.1	1.4	1.3	1.3	1.4	0.6
hyperplasia						
END	2	2.5	2.9	2.5	2.5	2.5
DURING	2.3	1.955	2.8	2.3	1.9	2.5
dysplasia/neoplasia						
END	2.6	3	3.1	3	3	3.6
DURING	3	3.1	3.2	3.1	2.9	3.4
area affected						
END	2.3	2.4	2.7	2.3	2	3.2
DURING	2.5	2.6	3.1	2.3	2.6	3.4

4. CHAPTER 4 – Recognition and Processing of a New Repertoire of DNA Damages by Human 3-Methyladenine DNA Glycosylase (AAG)

4.1. Introduction

DNA damaging agents are ubiquitous and cellular DNA is constantly attacked by a variety of endogenous and exogenous DNA damaging agents. DNA can be deaminated spontaneously or alkylated by endogenous intracellular agents and from environmental exposures. Such damages can interfere with DNA replication and transcription, and may be mutagenic or cytotoxic to the cell. During evolution, multiple DNA repair pathways have evolved to maintain the integrity of DNA in all organisms. Among other pathways, single base aberrations can be repaired by the base excision repair (BER) pathway. BER is initiated by DNA glycosylases that recognize the damaged base in the genome, followed by hydrolysis of the *N*-glycosylic bond, resulting in the release of the damaged base and the generation of an abasic site. The abasic site is then further processed by an AP endonuclease or AP lyase, resulting in a strand break. After trimming of the DNA ends, DNA is resynthesized by a DNA polymerase and a DNA ligase seals the nick to restore undamaged DNA (*1*).

Many DNA glycosylases exhibit strict substrate specificity. The human 3-methyladenine DNA glycosylase (AAG), by contrast, is able to recognize and excise structurally diverse bases, including 3-methyladenine, 7-methylguanine, 1-N^6-ethenoadenine (εA), and hypoxanthine (Hx) from DNA (*2-8*). The crystal structure of AAG bound to DNA

containing εA provides insight into the binding and catalysis by this DNA glycosylase. In the active site complex, the substrate nucleotide is rotated in the plane of the base pair out of the duplex DNA into the active site of the enzyme. Tyr162 of the enzyme is intercalated into the space vacated by the lesion via the DNA minor groove, maintaining proper base stacking and minimizing DNA distortion (*9, 10*). A water molecule is involved in the nucleophilic attack on the *N*-glycosylic bond by an acid-base catalytic mechanism with Glu125 acting as a general base (*9-11*). Equally important, the discrimination against pyrimidines is likely due to the fact that AAG employs an acid-base catalysis that is more suitable for selective excision of purines (*11*). In addition, the possible steric clash of an active site residue side chain (Asn169) with the 2-amino group of guanine plus the inability of adenine to accept a hydrogen bond from His136 may exclude these undamaged purine bases from the binding pocket (*10, 12*).

In contrast to AAG, AlkB is an orthogonal DNA repair protein that can directly reverse alkylation damage catalytically. The *E. coli* AlkB is a direct reversal protein, which was shown in the recent years to repair methylated lesions such as 1-methyladenine (1MeA) and 3-methylcytosine (3MeC) in DNA and RNA (*13, 14*) via oxidative demethylation. Subsequently, 1-methylguanine (1MeG) (*15, 16*), 3-methylthymine (3MeT) (*15-17*), and 3-ethylcytosine (*15*) were also found to be AlkB substrates, although with weaker activity on 1MeG and 3MeT than on 1MeA and 3MeC. Of the human AlkB homologs discovered thus far, only hABH1, hABH2, and hABH3 have been shown to have repair activity on DNA and also RNA (*14, 18-21*). In addition to simple methylated base adducts, AlkB was recently shown to repair 1,N^6-ethanoadenine (EA) (*22*), εA (*23, 24*)

and 3,N^4-ethenocytosine (εC) (*23*). *In vivo* (in mouse) and *in vitro* repair activity on εA have been shown for mammalian ABH2 (*25*).

Although *E. coli* AlkB and the human ABH proteins are able to repair etheno lesions, their chemical mechanism is quite different from AAG-initiated BER, which also serves to repair εA and EA DNA lesions. Etheno base lesions can be formed endogenously by the products of lipid peroxidation, and can be induced by exposure to environmental sources such as vinyl chloride and its metabolites chloroethylene oxide and chloroacetaldehyde (*26-33*). EA is similar to εA with the exception of having a saturated C-C bond in place of the double bond between the two exocyclic carbon atoms bridging the N^6 exocyclic and N1 heterocyclic nitrogens of adenine. EA can be formed from the reaction between DNA and 1,3-bis(2-chloroethyl)-1-nitrosourea (BCNU) (*34*), which is often used to treat brain tumors; EA can be repaired by AAG, albeit inefficiently (*35*). Having two different mechanisms for the repair of such an important class of lesions could be advantageous, and the relative activities of each pathway may differ between tissue and cell types.

Given that AlkB and AAG have overlapping roles in the repair of the clinically relevant exocyclic lesion, 1,N^6-ethenoadenine, we set out to uncover further substrate specificity shared between these two proteins in order to explore the redundancy in their roles. In the present study, we have tested the binding and glycosylase activity of AAG against a library of lesion-containing DNA oligonucleotides (Figure 1) and have identified new substrates for AAG. Both the full-length and a truncated version of AAG missing the N-

terminal 80 amino acids (Δ80) were used in this study, whereas previous studies primarily focused on Δ80AAG because it is more easily purified. We have shown that 1MeG, in addition to the already-known substrates εA and EA, is a substrate shared between AAG and AlkB. To our surprise, we found that both the truncated and full-length AAG excise εA and Hx from single-stranded DNA. Based upon earlier work showing that εA and Hx are refractory to repair when situated opposite a reduced basic site (*36*), it was thought that excision is only possible in duplex DNA. Furthermore, we found that both full-length AAG and Δ80AAG have weak glycosylase activity on 1,N^2-εG. Finally, we found that only full-length AAG, but not Δ80AAG, excises uracil in both ss- and ds-DNA. We demonstrate here, using a comprehensive library of lesion-containing single- and double-stranded DNA oligonucleotides, that AAG has a wide range of substrate specificity including multiple classes of new substrates.

4.2. Materials and Methods

4.2.1. DNA Oligonucleotides.

Oligonucleotides containing 1MeG, 1MeA, 3MeT, and 3MeC were synthesized as described by Delaney and Essigmann (*15*). The synthesis of the oligonucleotide containing EA was described by Frick et al. (*22*), those containing εA and εC by Delaney et al. (*23*), 1,N^2-εG by Zang et al. (*37*), M1G by Wang et al. (*38*), and the synthesis of oligonucleotides containing 3MeU and 3EtU will be published elsewhere. Oligonucleotides containing Hx and U were synthesized using phosphoramidites from Glen Research (Sterling, VA). All of the oligonucleotides were 16-mers with identical sequence (5'GAAGACCTXGGCGTCC3') where the only difference is in the central

lesion, X. The single stranded oligonucleotides were 5'-end-labeled with ^{32}P and purified with a MicroSpin G-25 column (GE Healthcare). For studies involving double-stranded DNA substrates, annealing was performed using a 1:1.5 ratio of modified:unlabeled complement. The base opposite the lesion was chosen to be the natural base-pairing partner of the undamaged base. For U, 3MeU and 3EtU, guanine was used as the opposing base, since the lesions here were assumed to form from deamination of cytosine and 3-alkylcytosine.

4.2.2. AAG protein expression and purification.

The truncated mutant with the first 80 amino acids deleted from the N-terminus, and the full-length AAG protein were both used in this study. The Δ80AAG and full-length AAG proteins were cloned and purified as described (*11*) with and without the gel filtration step, respectively. Previous studies have shown that AAG possessing a truncation of its N-terminal domain has catalytic activity similar to that of the full-length protein (*5, 11*).

4.2.3. DNA Glycosylase Activity Assays.

Glycosylase assays were performed by incubation of 1000 nM AAG protein (10 pmol) and 10 nM of a ^{32}P-labeled DNA substrate (100 fmol) at 37°C in 10 μL assay buffer containing 20 mM Tris-HCl buffer, pH 7.8, 100 mM KCl, 5 mM β-mercaptoethanol, 2 mM EDTA, 1 mM EGTA, and 50 μg/mL BSA. The experiments were carried out under single-turnover conditions where the enzyme concentration (1000 nM) was in large excess of the labeled DNA substrate concentration (10 nM). Initial screening

experiments of AAG glycosylase activity were performed by incubating a 1:100 molar ratio of DNA oligonucleotide : AAG enzyme in the glycosylase buffer for 90 minutes (or 180 minutes for 1,N^2-εG and uracil). For subsequent kinetics experiments, an aliquot of the reaction mixture was removed for quenching at various time points during the course of the incubation. Reaction mixtures were quenched with 0.2 N NaOH, except for εC and 3MeC where 0.2 M piperidine was used to eliminate spontaneous cleavage, and then heated at 75°C for 15 minutes to cleave the DNA at AP sites. Samples were then diluted with formamide loading buffer and cleavage products were resolved on a 20% denaturing polyacrylamide gel. The fraction of uncleaved versus cleaved substrate was determined on a Packard Cyclone PhosphorImager (Packard Instruments, Meridien, CT), analyzed with OptiQuant analysis software (Packard Instruments, Meridien, CT), and quantified with the Kodak 1D scientific imaging software (Eastman Kodak Campany, New Haven, CT).

Enzymatic rate constants were determined by fitting the single-turnover kinetic data into the One Phase Exponential Association equation (Equation 1) in the GraphPad Prism software (GraphPad Software, Inc., La Jolla, CA):

$$y=y_{max}(1-e^{-kobst}) \qquad (1)$$

where y is the amount of substrate cleaved at any particular time point, y_{max} is the maximum amount of cleaved substrate, t is time, and k_{obs} is the observed rate constant. Rate constants for extremely slow reactions where the increase in cleaved substrate amount did not follow an exponential increase were determined using linear regression in the form of $y=k_{obs}t$.

4.2.4. Electrophoretic Mobility Shift (Gel Shift) Assays.

Binding assays were performed in an assay buffer containing 50 mM HEPES, pH 7.5, 100 mM NaCl, 5mM β-mercaptoethanol, 9.5% v/v glycerol, and 0.1 mg/mL BSA. ^{32}P-Labeled DNA substrate (2 nM) was incubated with increasing concentrations of AAG in the binding assay buffer for 30 minutes at 4°C and then directly loaded onto a 6% non-denaturing polyacrylamide gel. After running the gel, it was dried and the fraction of DNA bound by AAG was analyzed as described above for the glycosylase assays. The apparent dissociation constant K_d was calculated by fitting the quantified binding data into the One Site Binding (Hyperbola) equation (Equation 2) in the GraphPad Prism software (GraphPad Software, Inc., La Jolla, CA).

$$y = \frac{B_{\max} x}{K_d + x} \qquad (2)$$

where y is the total amount of bound substrate, B_{max} is the maximum specific binding, x is the concentration of the protein, and K_d is the apparent binding constant.

4.3. Results

4.3.1. AAG recognizes a wide range of substrate structures

In order to investigate thoroughly the substrate specificity of AAG, an extensive library of lesion-containing DNA oligonucleotides was used (Figure 4-1). Substrate binding and glycosylase activity of both the Δ80 and full-length AAG proteins were measured for

single- and double-stranded lesion-containing DNA oligonucleotides. Their identical sequence context allows us to eliminate the possible effects resulting from the flanking base sequence on the protein's binding and excision ability. Lesion recognition and substrate binding was measured by gel-shift assays. Figure 4-2 (left panel) summarizes the binding results at an AAG concentration of 200 nM, with a DNA: protein molar ratio of 1:100 to obtain single-turnover kinetics. Surprisingly, AAG was found to bind a large number of lesions in duplex DNA, but to different extents (Figure 4-2). Note that Δ80AAG binding was only detected for double-stranded DNA and not for single-stranded DNA (data not shown). AAG bound several AlkB substrates; these include simple methylated bases (1MeG, 1MeA, 3MeT and 3MeC), EA, εA and εC. The apparent relative strength of binding was as follows: εA and εC > 3MeC > 1MeA > 3MeT > EA > 1MeG (Figure 4-2). It is also interesting to note that, in addition to εA and εC, AAG showed very strong binding to 3-methyluracil (3MeU) and 3-ethyluracil (3EtU) but not to uracil itself. Very weak binding for 1,N^2-εG was seen, but no binding was

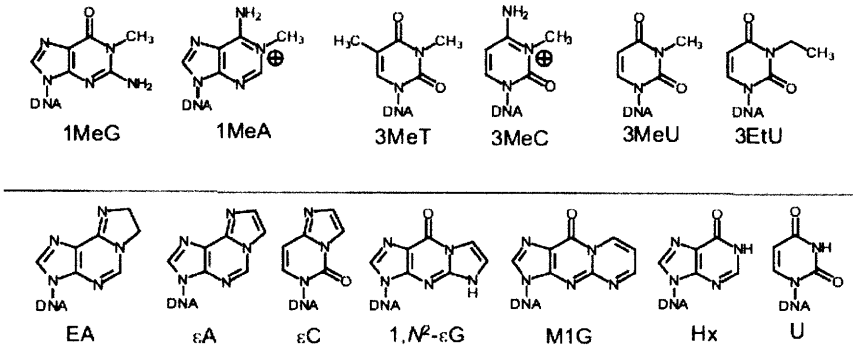

Figure 4-1. Chemical structures and sequence context of the different DNA lesions tested in the present study.

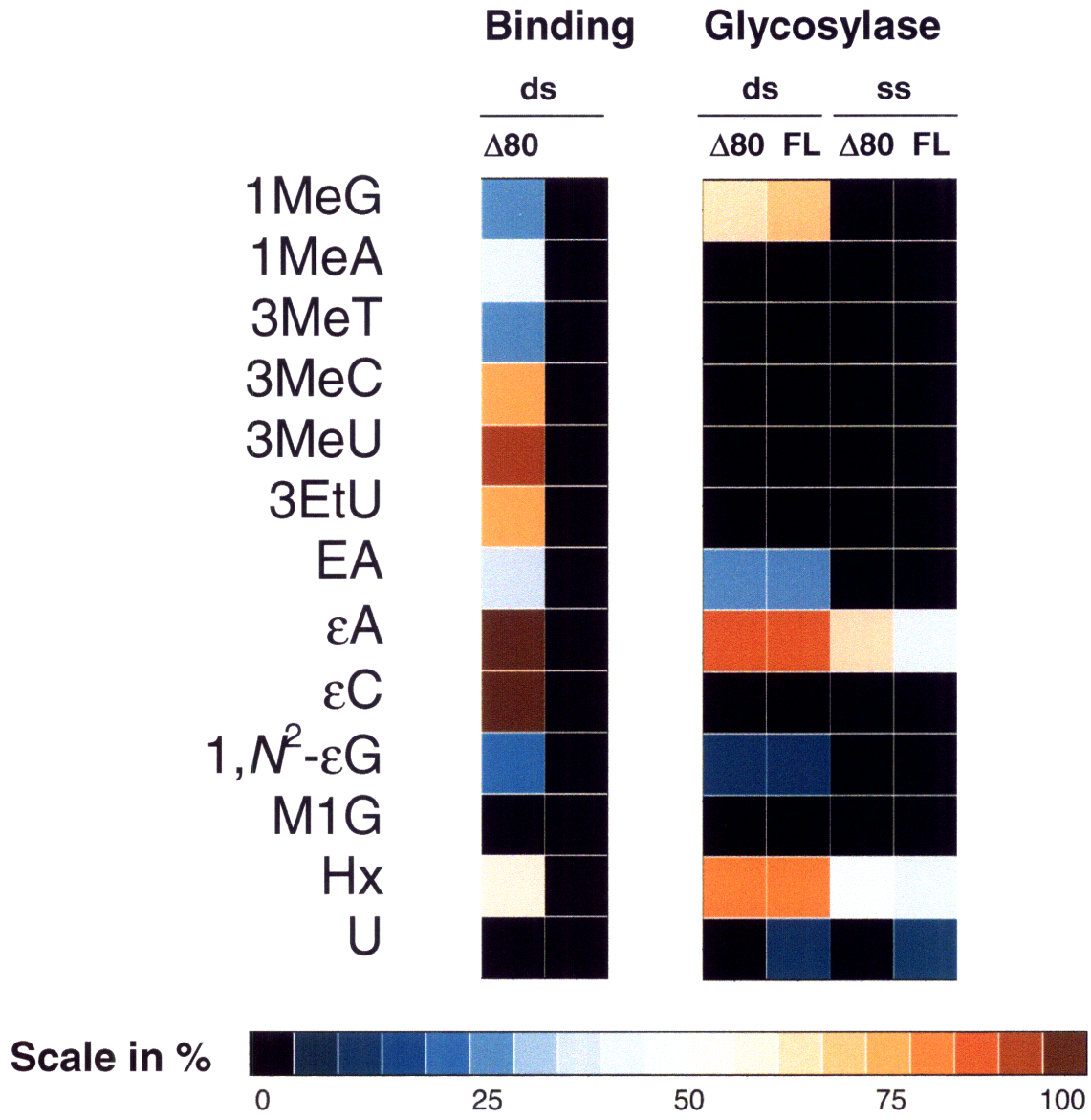

Figure 4-2. AAG binds to a wide range of substrates but excises only a few, as shown in initial screening experiments. Binding and excision are based on % bound (with 2nM substrate and 200nM AAG, a 1:100 molar ratio of substrate to AAG) and % cleavage (at 90 min-incubation for most lesions or 180 min-incubation for 1,N^2-εG and U), respectively. Reaction conditions were as described in "Materials and Methods".

detected for M1G. It is interesting to note the difference in binding affinity of U, 3MeU, and 3MeT in relation to their structural similarity. 3MeU differs from U by the addition of a methyl group on the N3 position, yet this modification is sufficient to increase its binding affinity to AAG significantly to a K_d of ~30 nM compared with no binding shown by U. However, the binding affinity of 3MeT (about 200 nM), which has methyl groups on both the N3 and C5 positions of uracil, was much lower than that of 3MeU. In addition, it is important to note that for all of the lesions tested, band-shifts were only observed for the truncated Δ80AAG (Figure 4-2) and not with the full-length protein. This behavior in gel shift assays was observed before and is likely due to the limitation of this method (unpublished observation). However, using plasmon surface resonance, full-length AAG has been shown to bind to DNA oligonucleotides containing Hx and AP sites (*39*).

To determine the quantitative binding affinity of AAG to the base lesions, shown in Figure 4-1, various concentrations of AAG were incubated with a fixed amount of substrate in duplex DNA. Figure 4-3 shows representative experiments for a weak-binding substrate (1MeG), a moderate binding substrate (3EtU), and a very strong binding substrate (εA) (Figure 4-3A, C, and E), with corresponding quantification of the binding (Figure 4-3B, D, and F), from which the apparent dissociation constants (K_d) were calculated (Table 4-1). AAG showed a wide range of binding affinities to the various lesions. The strongest affinitiy was observed for εA and εC, with a K_d of approximately 10 nM, followed by 3MeU with a K_d ~ 30 nM. AAG exhibited moderate

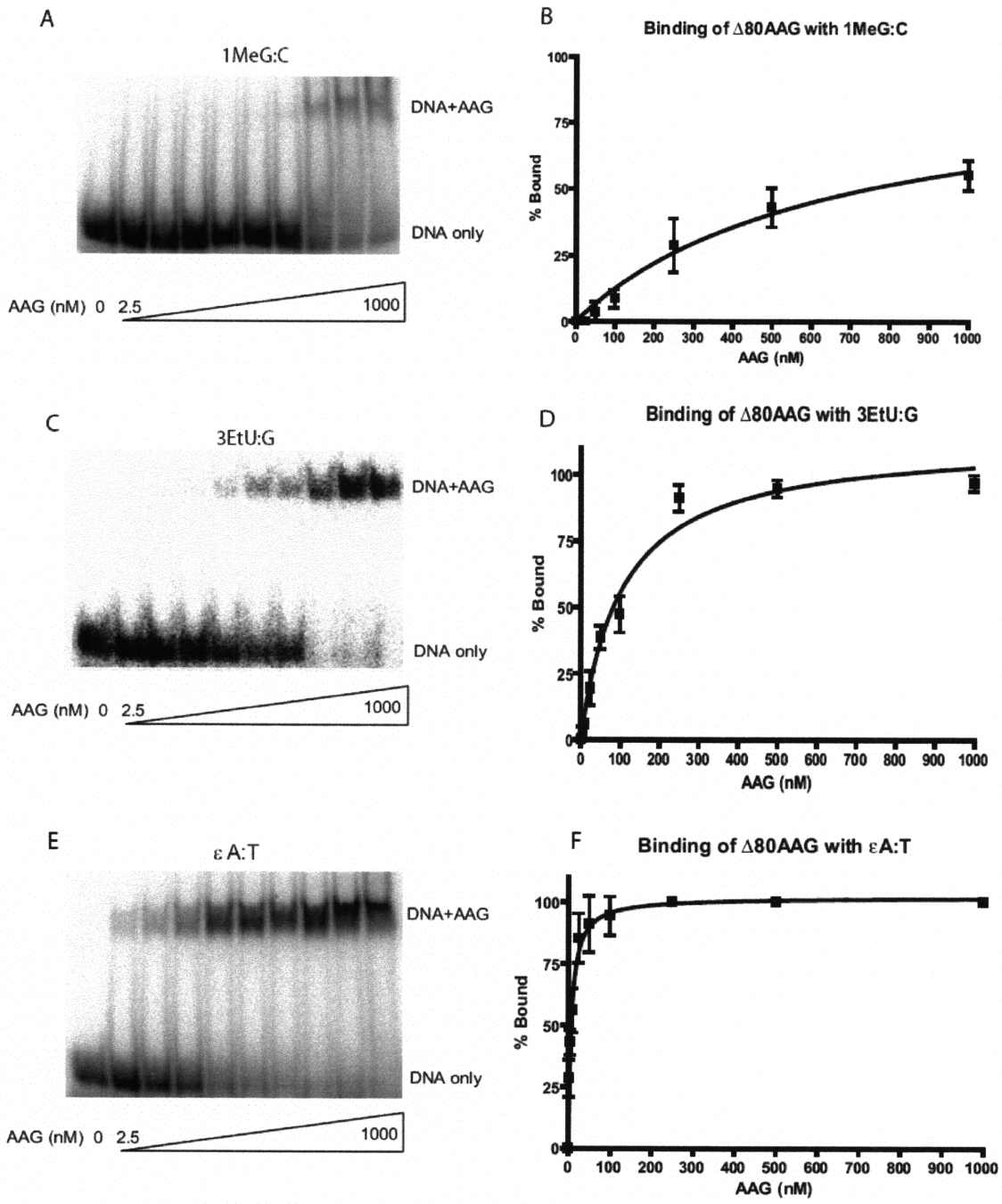

Figure 4-3. AAG binds to different lesions with different affinities. Gel mobility shift assay for the binding of AAG to oligonucleotides containing (A) 1MeG, (C) 3EtU, (E) εA. Graphical representation of the binding of AAG to (B) 1MeG, (D) 3EtU, (F) εA.

binding affinity for 3MeC, Hx, 3EtU, 1MeA, and 3MeT, with apparent K_d's between 60 and 200 nM. Weak to very weak binding was observed for EA (K_d = 340 nM), 1MeG (K_d = 650 nM), and 1,N^2-εG (K_d = 930 nM).

4.3.2. AAG excises only a few of the lesions to which it binds.

We tested the glycosylase activity for both the Δ80 and full-length AAG on the library of lesion-containing oligonucleotides. The glycosylase reactions were carried out under single-turnover conditions where the enzyme was in 100-fold molar excess of the oligonucleotide substrate, such that the reaction kinetics should not be a function of enzyme-substrate binding rates (*12*). Single turnover glycosylase kinetics measure the rate of reaction steps after forming the initial AAG-DNA complex (*12*). From the initial screening of glycosylase activity (Figure 4-2), it seemed that of the damaged bases tested, AAG was active on 1MeG, EA, εA, Hx, 1,N^2-εG, and uracil in double-stranded DNA and also εA, Hx, and uracil in single-stranded DNA. The truncated and full-length AAG appeared to exhibit very similar excision kinetics for most substrates except for U. No glycosylase activity was found toward 1MeA, 3MeT, 3MeC, 3MeU, 3EtU, εC, and M1G (Figure 4-2).

Based on the screening studies (Figure 4-2), we went on to measure detailed base excision kinetics for the substrates that AAG was able to excise. Single-turnover glycosylase activity assays were performed with time courses up to 90 or 180 minutes, depending on the reaction rates. Of the various AlkB substrates tested (1MeG, 1MeA,

3MeT, 3MeC, EA, εA and εC), AAG-mediated excision was only observed for 1MeG, EA, and εA. Thus, among the methylated AlkB substrates, 1MeG was the only lesion to be repaired by AAG, with a fairly fast observed rate constant of ~0.1 min^{-1} for both the Δ80 and full-length AAG (Table 4-1, Figure 4-4A-B). It is interesting that despite AAG's ability to bind to all four methylated lesions, only 1MeG was excised, even though AAG bound 1MeG the least tightly among the four (Table 4-1). Although the purine site of alkylation for 1MeG is identical to 1MeA, AAG could not excise 1MeA (Figure 4-2). 3MeT and 3MeC are pyrimidines and are not expected to be excised by AAG based on the acid-base catalytic mechanism that favors the removal of damaged purines (*11*). Two other AlkB substrates repaired by AAG were EA and εA in duplex DNA. Guliaev et al. (*35*) previously reported that EA is a 65-fold weaker substrate for AAG than εA; however, our present study shows the excision rates of EA and εA to be far less disparate with respective initial rates of 0.5 fmol/min and 2.0 fmol/min (Table 4-1, Figure 4-4C-D, Figure 4-5A-B). No glycosylase activity toward εC was observed despite AAG's very strong binding affinity for this lesion (Figure 4-2, Table 4-1).

4.3.3. Single-turnover kinetics of excision of 1,N^6-ethenoadenine and hypoxanthine from single- and double-stranded DNA

The activity of AAG on its well known εA and Hx substrates was measured in detail for comparison to its activity on the library of substrates within the same sequence context; excision kinetics for Δ80AAG and full-length AAG were monitored for up to 90 minutes (Figure 4-5). The observed rate constant for εA:T was found to be ~0.03 min^{-1} for Δ80

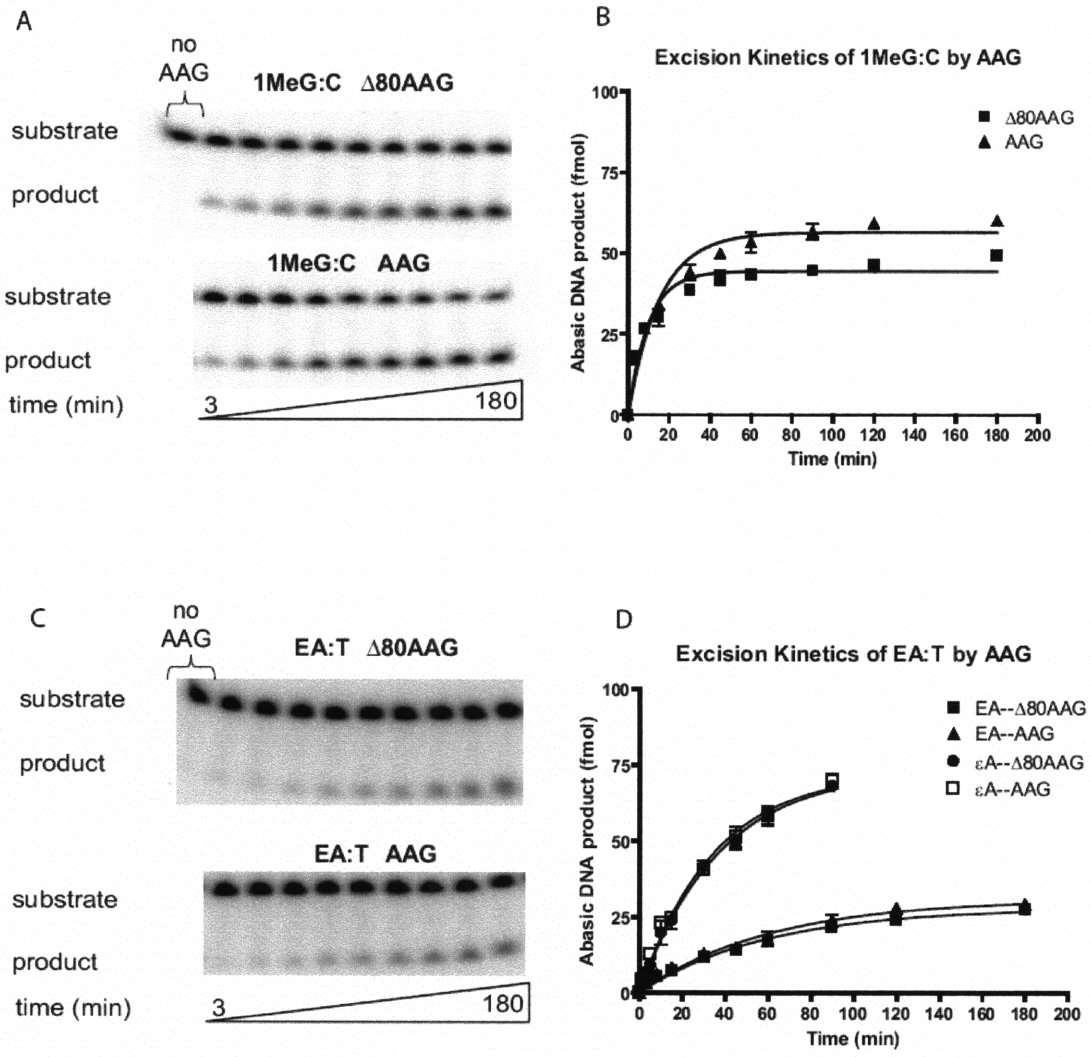

Figure 4-4. 1MeG and EA, known AlkB substrates, are cleaved by AAG when present in double-stranded DNA. Glycosylase activity of AAG toward (A) 1MeG and (C) EA. No AAG represents incubation without AAG for the longest time point of the assay. Graphical representation of the glycosylase activity toward (B) 1MeG and (D) EA by (■) Δ80AAG and (▲) full-length AAG. For comparison with EA, AAG glycosylase activity toward εA from Figure 4-5B is also shown in (D): (•) Δ80AAG and (□) full-length AAG.

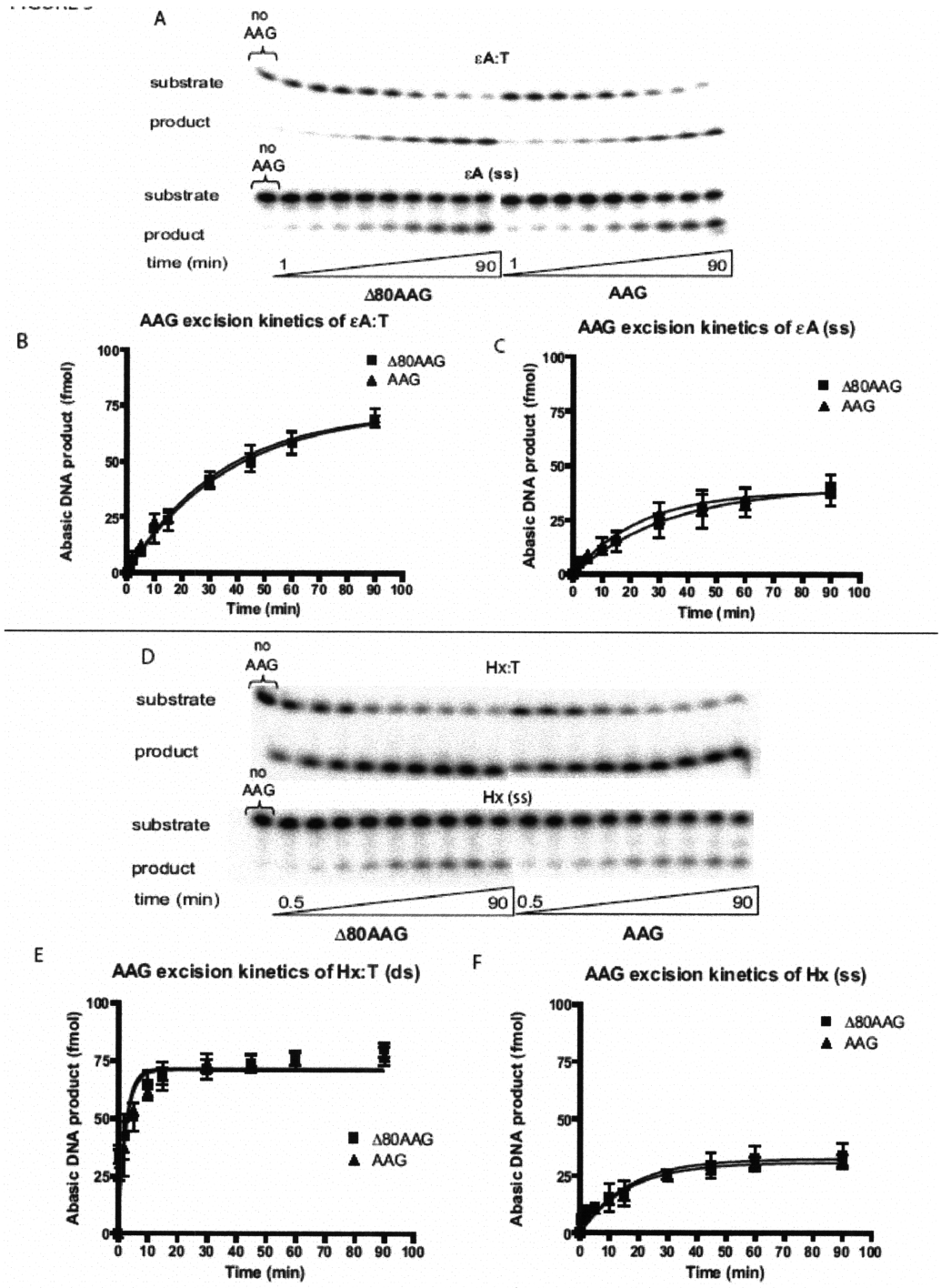

Figure 4-5. AAG cleaves εA and Hx in both double-stranded and single-stranded DNA. Glycosylase activity of AAG toward εA and Hx. Gels showing AAG excision of εA in (A) double- and single-stranded DNA. No AAG represents incubation without AAG for the longest time point of the assay. Graphical representation of the glycosylase activity toward εA in (B) duplex DNA and (C) single-stranded DNA by (■) Δ80AAG and (▲) full-length AAG. Gels showing excision of Hx in (D) double- and single-stranded DNA. Graphical representation of the glycosylase activity toward Hx in (E) duplex and (F) single-stranded DNA by (■) Δ80AAG and (▲) full-length AAG.

and full-length AAG (Table 4-1) and those for Hx:T were about 0.4 min^{-1} (Table 4-1); clearly, the excision rates for the truncated and full-length AAG were very similar. AAG unexpectedly also exhibited catalytic activity against εA and Hx in single-stranded DNA (Figure 4-5A, C, D, F). Although most previous studies have monitored AAG activity on duplex DNA, activity on single-stranded DNA was previously reported for oxanine and εA (*40*). Of all the adducts tested in the present study, the only substrates that could be excised from single-stranded DNA by AAG were εA and Hx (and uracil, which is weakly excised). Interestingly, the observed rate constants for εA in single- and double-stranded DNA were very similar (approximately 0.03-0.04 min^{-1}, Table 4-1) and the initial excision rates were only slightly higher (less than one-fold increase) for duplex DNA than for single-stranded DNA (Table 4-1). On the other hand, the observed rate constants for Hx in single-stranded DNA (~0.06 min^{-1}, Table 4-1) were about seven-fold lower than those in duplex DNA (~0.4 min^{-1}, Table 4-1).

4.3.4. Both Δ80AAG and full-length AAG excise 1,N^2-εG

It was previously shown that glycosylase activity toward 1,N^2-εG in duplex DNA was observed for full-length AAG, but not for the truncated form of AAG lacking the first 73 amino acids (*41*). It was also shown that the inability to excise was not due to an inability to bind, since the truncated form of AAG was observed to bind 1,N^2-εG (*41*); thus, it was concluded that the nonconserved, N-terminal part of AAG was essential for glycosylase activity toward 1,N^2-εG (*41*). However, here we show that both the Δ80AAG and the full-length AAG were able to cleave 1,N^2-εG from double-stranded

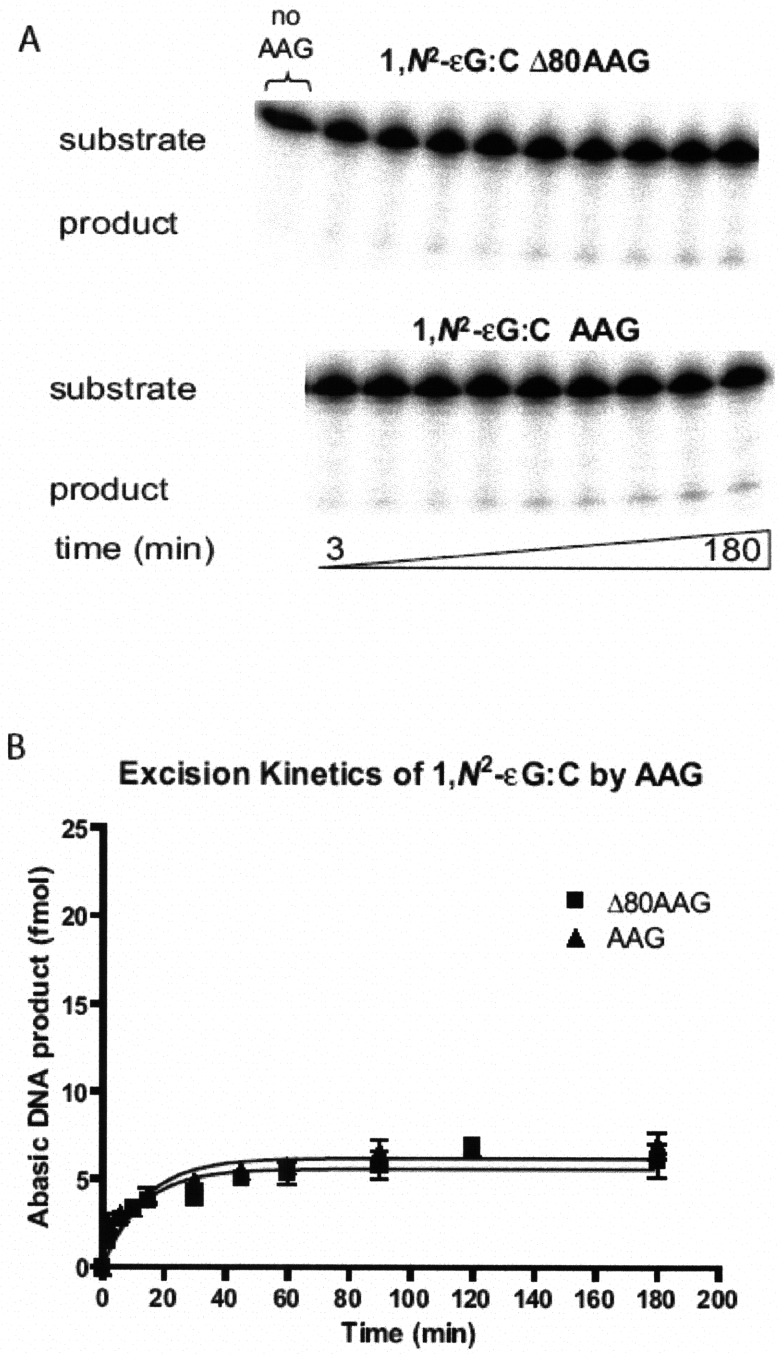

Figure 4-6. 1,N^2-εG in double-stranded DNA is a substrate for both the Δ80 truncated form and the full-length AAG protein. (A) Glycosylase activity of AAG toward 1,N^2-εG by Δ80 and full-length AAG. No AAG represents incubation without AAG for the longest time point of the assay. (B) Graphical representation of the glycosylase activity toward 1,N^2-εG by (■) Δ80AAG and (▲) full-length AAG.

DNA, albeit to a limited extent. As seen from Figure 4-6, both forms of the protein excised about 6% of the 1,N^2-εG base lesion at saturation, with an observed rate constant of 0.08 and 0.07 min^{-1} for Δ80 and full-length AAG, respectively (and initial rates of ~0.5 fmol/min) (Table 4-1). Such rate constants were among the third-highest of the lesions tested in this study, while the corresponding initial excision rates turned out to be very low. However, neither AAG glycosylase activity nor binding was observed for the structurally similar M1G adduct (Figure 4-1, Figure 4-2).

4.3.5. Excision of uracil from single- and double-stranded DNA by AAG.

In addition to hypoxanthine (the deamination product of adenine), AAG has been shown to excise the guanine-derived deaminated bases xanthine (*42*) and oxanine (*40*). Here, we show that deaminated cytosine, namely uracil (U), can also be excised by AAG, although very slowly (Figure 4-7A-C and Table 4-1). Moreover, similar to oxanine, AAG can excise U from both single- and double-stranded DNA; however, only the full-length AAG exhibited such activity. The single-turnover excision with U appeared to be very slow and showed kinetics that followed a linear rather than an exponential fit, yielding initial excision rates (and also observed rate constants) of ~0.06 fmol/min for both single- and double-stranded DNA (Table 4-1), which is about 7-fold lower than those of 1,N^2-εG, whose saturation cleavage was only about 6% (Figure 4-6B). Although uracil can be weakly cleaved by AAG, the alkylated 3MeU and 3EtU (deamination products of 3MeC and e3C, respectively) were not excised despite their significant binding to AAG. In contrast, binding of both forms of AAG to substrates

containing U was not detected. Notably, among the substrates tested in this study, uracil was the only substrate toward which the truncated and full-length AAG showed different activity.

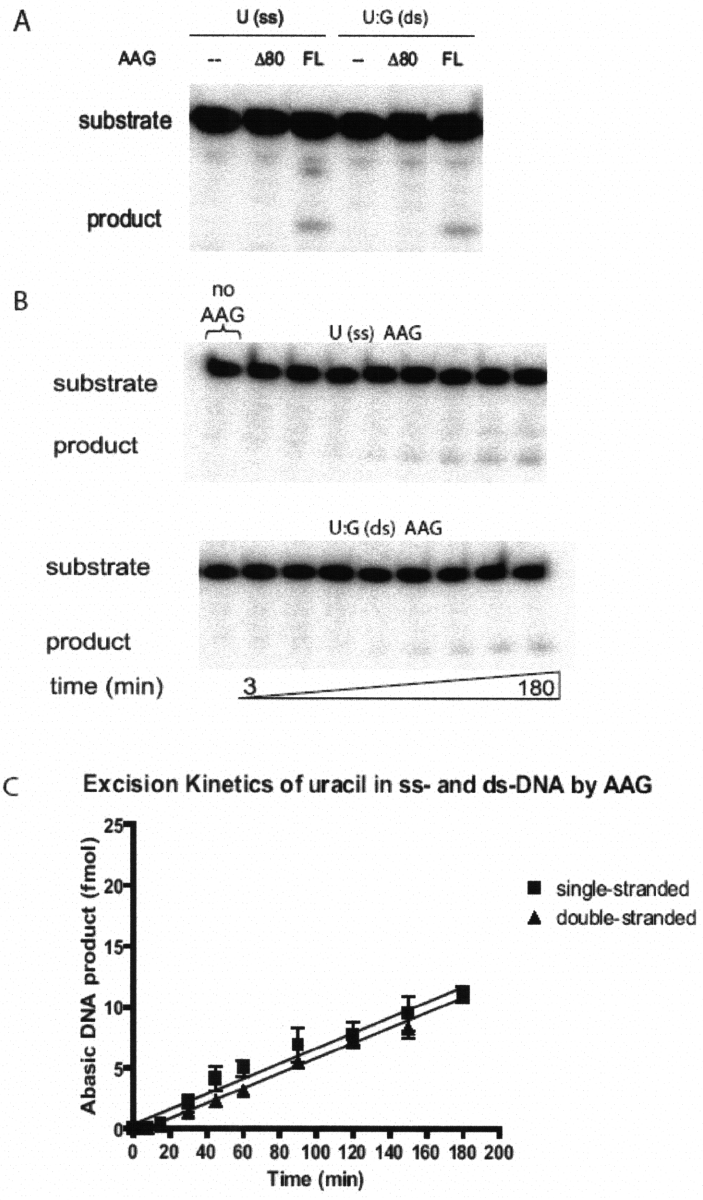

Figure 4-7. Uracil is a substrate for the full-length AAG protein in both single- and double-stranded DNA. (A) Glycosylase activity of Δ80 vs. full-length AAG toward U. (B) Glycosylase activity of full-length AAG toward U. No AAG represents incubation without AAG for the longest time point of the assay. (C) Graphical representation of the glycosylase activity toward U by full-length AAG in (■) single-stranded and (▲) double-stranded DNA.

Table 4-1. Binding and excision kinetic constants of various lesions by AAG.

	Binding	*Glycosylase Activity*				
Base excised : pairing partner	Δ80AAG	Δ80AAG		Full-length AAG		
	K_d±s.d. (nM)	k_{obs}±s.d. (min^{-1})[a]	Initial excision rate (fmol/min)[b]	k_{obs}±s.d. (min^{-1})[a]	k_{obs}±s.d. (fmol/min)[c]	Initial excision rate (fmol/min)[b]
1MeG:C	648 ± 154	0.101 ± 0.010	4.46	0.065 ± 0.005		3.68
1MeA:T	176 ± 28	N.A.	N.A.	N.A.		N.A.
3MeT:A	189 ± 35	N.A.	N.A.	N.A.		N.A.
3MeC:G	61 ± 9	N.A.	N.A.	N.A.		N.A.
3MeU:G	27 ± 4	N.A.	N.A.	N.A.		N.A.
3EtU:G	103 ± 12	N.A.	N.A.	N.A.		N.A.
εA:T	7 ± 1	0.027 ± 0.003	1.98	0.029 ± 0.003		2.12
EA:T	340 ± 129	0.017 ± 0.001	0.47	0.016 ± 0.001		0.51
εC:G	10 ± 1	N.A.	N.A.	N.A.		N.A.
1,N^2-εG:C	928 ± 137	0.079 ± 0.011	0.44	0.074 ± 0.012		0.46
M1G:C	N.B.	N.A.	N.A.	N.A.		N.A.
Hx:T	125 ± 30	0.425 ± 0.070	30.4	0.390 ± 0.061		27.6
U:G	N.B.	N.A.	N.A.		0.062 ± 0.002 [c]	0.062[c]
		k_{obs}±s.d. (min^{-1})[a]		k_{obs}±s.d. (min^{-1})[a]		
εA (ss)	N.B.	0.030 ± 0.006	1.22	0.043 ± 0.005		1.65
Hx (ss)	N.B.	0.062 ± 0.011	2.01	0.061 ± 0.007		1.90
U (ss)	N.B.	N.A.	N.A.		0.063 ± 0.003 [c]	0.063[c]

N.B. or N.A. represents no binding or no activity, respectively.
Full-length AAG was not observed to bind DNA at all in gel-shift assay.
Δ80 AAG was not observed to bind to single-stranded DNA.

[a]Activity rate constants k_{obs} were determined from one-phase exponential association except for U.
[b]Initial rate is the product of the rate constant k_{obs} and the maximum saturation cleavage (maximum amount of abasic product formed), except for U where the initial rate is equal to the rate constant obtained from linear regression.
[c]Rate data for U were fitted with linear regression in the form of y=kt.

4.4. Discussion

The human 3-methyladenine DNA glycosylase (AAG) is known to have a broad substrate specificity for damaged purines including 3-methyladenine, 7-methylguanine, εA, and Hx (*2-8*). In this report, we examined excision kinetics and substrate binding of both truncated Δ80 and full-length AAG, for an extensive library of lesion-containing DNA oligonucleotides in both the single- and double-stranded form. In addition to confirming previous findings, we identified several new substrates for AAG in single- and double-stranded DNA, namely 1MeG (ds), Hx (ss), 1,N^2-εG (ds, excision by truncated Δ80AAG) and uracil in ss- and ds-DNA (excision by full-length AAG).

Although human AAG has been primarily shown to repair lesions in double-stranded DNA, excision activity on single-stranded DNA was previously observed, as shown in repairing εA and oxanine (*40*). Binding and excision of oxanine in duplex DNA appear to be independent of the opposite base; indeed, a complementary strand is not necessary as seen from the similar binding and excision efficiencies for oxanine in 62-mer single- and double-stranded DNA (*40*). In addition to AAG, other DNA glycosylases have been shown to excise damaged bases from single-stranded DNA. For instance, in *E. coli*, the 3-methyladenine glycosylase (AlkA) has been shown to remove 3-methyladenine from single-stranded DNA (*43*) and in mammals, the bovine uracil DNA glycosylase (UDG) (*44*) and human SMUG1 (*45*) also excise uracil from single-stranded DNA substrate. In the present study, we have observed AAG activity on lesion-containing single-stranded

DNA. We found both εA and Hx within single-stranded DNA to be good substrates for AAG. εA was excised with similar observed rate constants in single- and double-stranded DNA, although in single-stranded DNA the initial excision rates were lower (Table 4-1). For Hx, it was previously shown that Hx could only be excised when paired with a base, preferably T rather than C (*36, 40, 46-48*) and not in single-stranded DNA, suggesting that it is the base-pair instead of the damaged base alone that affects the recognition by AAG. However, to our surprise, we observed that Hx can also be repaired in single-stranded DNA, although with observed rate constants of over 6-fold lower (initial rates about 14-fold lower) than those in double-stranded DNA (Table 4-1). Excision on the single strands may be possible because the reduced base stacking and the lack of base-pairing may increase the chances of the damaged bases being captured from the less rigid single-stranded structure. One might argue that the single-stranded DNA may form a secondary structure containing duplex DNA, thus allowing excision to occur. However, other than εA and Hx (and uracil to weak extent), no other substrates were observed to be excised from single strands, indicating that lesion excision from single-stranded DNA may be damage-specific. A previous report showed that AAG did not bind or excise the DNA duplexes with εA or Hx paired opposite to an abasic site (*36*), suggesting that the binding of damaged purine bases by AAG may require an opposite base or an opposite strand. However, we demonstrated catalytic activity toward εA and Hx in single-stranded DNA although no binding of AAG to single-stranded DNA was detected by gel shift mobility assay.

During DNA replication and transcription, transient single-stranded regions may result and expose more potential sites of damage on the DNA bases; therefore, it would be beneficial to the cell if there is a mechanism for repairing damages on single-stranded DNA, especially if they are replication- or transcription-blocking. Although the advantage of base excision in single-stranded DNA is not evident, it is possible that *in vivo,* with an abasic site or strand break, replication or transcription would stop. Polymerase arrest could stimulate recombination and stalled RNA polymerase may trigger transcription-coupled repair.

In addition to the aforementioned εA, we have also found that AAG and AlkB share other classes of DNA damage as substrates such as EA and 1MeG. Formed by chloroethyl nitrosoureas in cancer therapy and structurally similar to εA, ethanoadenine (EA) was recently shown to be metabolized by AlkB (*22*). Unlike εA whose unsaturated exocyclic ring is planar, EA's non-planar saturated ring may give rise to less stable aromatic base-stacking interactions with the active site residues of AAG, possibly leading to the lower binding ability and less efficient repair of EA. Guliaev et al. (*35*) showed that AAG was able to repair EA, but with a 65-fold lower efficiency than for εA. We, however, found only about a four-fold difference in initial excision rates in this study (Table 4-1); this discrepancy could be possibly due to differences in sequence context. AAG bound somewhat weakly to EA, but excised it rather efficiently up to 30% of the substrate (Figure 4-4C and D, Table 4-1). In addition to cyclic lesions (*22-24*), simple methylated lesions such as 1MeG, 3MeT, 1MeA, and 3MeC also interfere with normal Watson-Crick base-pairing and were all shown to be AlkB substrates (*13-17*). However, despite the

observed binding between AAG and these lesions, excision was only seen for 1MeG (Figure 4-2, Table 4-1, Figure 4-3A-B). It is also worth mentioning that binding affinity clearly does not predict excision activity. For instance, AAG exhibited very weak binding to 1MeG (Table 4-1, Figure 4-2, Figure 4-3) and yet it was able to excise ~50% of it at saturation (Figure 4-4A-B), making 1MeG among the top three lesions to be excised. In fact, AAG only bound to Hx:T moderately well (with a K_d of 124.8 nM), but showed the fastest excision rate (Table 4-1). Sometimes, strong binding substrates are weakly excised and vice versa. Indeed, AAG does not excise all of the substrates to which it binds. Hence, it is very difficult to point out any trends relating binding affinity and excision rates.

We questioned why AAG can cleave 1MeG but not the structurally analogous 1MeA. Some main differences between 1MeA and 1MeG include the O^6 atom of 1MeG, which can serve as a hydrogen bond acceptor from the main chain amide of His136 (Figure 4-8) in the enzyme active site, whereas 1MeA has an amino group at the N^6 position and cannot accept the hydrogen bond for stabilization (which is how AAG discriminates against normal adenines (*10*)). Moreover, 1MeA is positively charged whereas 1MeG is neutral and, like guanine, has a 2-amino group that could clash with Asn169 (this 2-amino group is absent on 1MeA). Charge probably has little effect in the assistance of glycosyl bond cleavage in this case, since the positively charged 1MeA is not a better substrate than 1MeG. Perhaps the hydrogen bond between the O^6 position of the 1MeG base and His136 enhances binding in the active site and plays a stronger role in

recognition and binding than the cation-π interaction between the positively charged 1MeA and the aromatic active site residues. The lack of excision of 3MeC and 3MeT

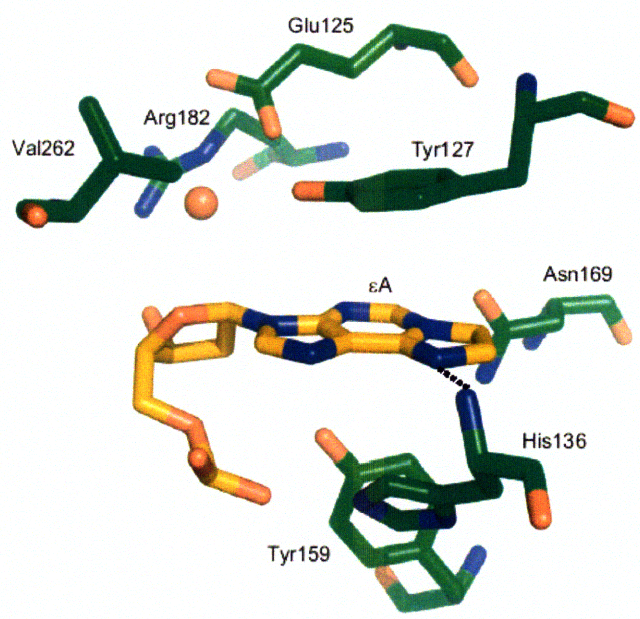

Figure 4-8. Structure of the AAG active site (green) showing the flipped-out εA nucleotide (gold). The dashed line indicates a hydrogen bond between the N^6 of εA (acceptor) and the peptide amide (donor) of His136. This figure is generated using the coordinates of the AAG/εA crystal structure (PDB ID: 1f4r (*10*)) using Pymol.

was expected and may be explained by the fact that protonation of the nucleobase likely occurs at N7 or N3 of purine for AAG-catalyzed excision (*11*) and is more suitable for purines than for pyrimidines, eliminating the likelihood of repairing cytosine or thymine adducts.

Here we also found 1,N^2-εG to be a substrate for AAG, as was reported before (*33, 41*). 1,N^2-εG is a promutagenic and genotoxic product formed from reactions with lipid peroxidation byproducts and along with 1,N^6-ethenoadenine, N^2,3-ethenoguanine, and

3,N^4-ethenocytosine, can result from exposure to industrial chemical pollutants such as vinyl chloride or its metabolite chloroacetaldehyde. The fact that 1,N^2-εG is repaired by MUG (*41*) and AAG (Table 4-1 and Figure 4-6; refs. (*4, 41, 49*)) underscores the importance of its repair for proper cellular homeostasis. Saparbaev et al. (*41*) found that both the full-length and truncated Δ73AAG enzymes were able to bind to 1,N^2-εG, but only the full-length protein was able to release it from duplex DNA. A similar truncated protein lacking the first 70 amino acid residues was slightly active in the repair but was still much less active compared with the full-length protein (*41*). However, in the present study, both the full-length and Δ80AAG excised 1,N^2-εG equally well, albeit weakly (Figure 4-6A and B, Table 4-1). Perhaps the possible conformational change brought about by deletion of the N-terminal tail still allows the protein to bind and excise the shorter 16-mer oligonucleotides (this study) but hinders excision in the longer oligonucleotides (30-31-mer used by Saparbaev et al.(*41*)).

Finally, AAG is known to have an additional role in repairing deaminated bases such as hypoxanthine and oxanine. Uracil arises as a deamination product of cytosine or it can be misincorporated opposite of A from the dNTP pool during DNA synthesis, and is promutagenic like all deaminated base lesions. Efficient repair of this lesion is accomplished by base excision repair involving uracil DNA glycosylases (UDGs), comprised of four families thus far (*45, 50*). In the present study, we have found that the full-length AAG (and not Δ80AAG) can excise uracil to a limited extent with slow excision kinetics, in single- or double-stranded DNA when paired with G (Figure 4-7A-C, Table 4-1), similar to the deaminated bases hypoxanthine (Figure 4-5D-F, Table 4-1) and

oxanine (*40*). The inactivity shown by the truncated Δ80AAG may suggest that the N-terminal tail is necessary in recognizing and excising uracil.

In conclusion, we report significant overlap in substrate specificity between AAG and other repair enzymes such as AlkB, MUG, or UDG. As a genotoxic and mutagenic lesion, 1MeG was known to be a substrate repaired efficiently by the direct reversal protein AlkB, and we now find that it is a good AAG substrate. It would seem advantageous to the cell to have backup DNA repair systems to eliminate this lesion in the event that one system is unavailable. Evaluation of the mutagenic and genotoxic activities of 1MeG in AAG-proficient and AAG-deficient cell lines is a priority based upon this study. As a damaged lesion from the environment and from lipid peroxidation byproducts, 1,N^2-εG is also a shared substrate between MUG and AAG. Although both truncated and full-length AAG showed similar glycosylase activity toward most substrates in this study, it was shown by another study that the N-terminal domain was essential in the excision of 1,N^2-εG. However, we did find that the truncated and full-length AAG protein showed completely different activity toward uracil, highlighting the significance of the N-terminus in the glycosylase activity of AAG. Moreover, our results of AAG activity on εA and Hx-containing single-stranded DNA may underscore the significance of single-stranded DNA repair, in which other repair proteins such as photolyase and AlkB are also involved.

4.5. References

(1) Friedberg, E. C., Graham C. Walker, Wolfram Siede, Richard D. Wood, Roger A. Schultz, and Tom Ellenberger (2006) *DNA Repair and Mutagenesis*, 2nd ed., ASM Press, Washington, DC.

(2) Saparbaev, M., and Laval, J. (1994) Excision of hypoxanthine from DNA containing dIMP residues by the Escherichia coli, yeast, rat, and human alkylpurine DNA glycosylases. *Proc Natl Acad Sci U S A 91*, 5873-7.

(3) Gallagher, P. E., and Brent, T. P. (1982) Partial purification and characterization of 3-methyladenine-DNA glycosylase from human placenta. *Biochemistry 21*, 6404-9.

(4) Singer, B., Antoccia, A., Basu, A. K., Dosanjh, M. K., Fraenkel-Conrat, H., Gallagher, P. E., Kusmierek, J. T., Qiu, Z. H., and Rydberg, B. (1992) Both purified human 1,N6-ethenoadenine-binding protein and purified human 3-methyladenine-DNA glycosylase act on 1,N6-ethenoadenine and 3-methyladenine. *Proc Natl Acad Sci U S A 89*, 9386-90.

(5) O'Connor, T. R. (1993) Purification and characterization of human 3-methyladenine-DNA glycosylase. *Nucleic Acids Res 21*, 5561-9.

(6) Engelward, B. P., Weeda, G., Wyatt, M. D., Broekhof, J. L., de Wit, J., Donker, I., Allan, J. M., Gold, B., Hoeijmakers, J. H., and Samson, L. D. (1997) Base excision repair deficient mice lacking the Aag alkyladenine DNA glycosylase. *Proc Natl Acad Sci U S A 94*, 13087-92.

(7) Hang, B., Singer, B., Margison, G. P., and Elder, R. H. (1997) Targeted deletion of alkylpurine-DNA-N-glycosylase in mice eliminates repair of 1,N6-ethenoadenine and hypoxanthine but not of 3,N4-ethenocytosine or 8-oxoguanine. *Proc Natl Acad Sci U S A 94*, 12869-74.

(8) Miao, F., Bouziane, M., and O'Connor, T. R. (1998) Interaction of the recombinant human methylpurine-DNA glycosylase (MPG protein) with oligodeoxyribonucleotides containing either hypoxanthine or abasic sites. *Nucleic Acids Res 26*, 4034-41.

(9) Lau, A. Y., Scharer, O. D., Samson, L., Verdine, G. L., and Ellenberger, T. (1998) Crystal structure of a human alkylbase-DNA repair enzyme complexed to DNA: mechanisms for nucleotide flipping and base excision. *Cell 95*, 249-58.

(10) Lau, A. Y., Wyatt, M. D., Glassner, B. J., Samson, L. D., and Ellenberger, T. (2000) Molecular basis for discriminating between normal and damaged bases by the human alkyladenine glycosylase, AAG. *Proc Natl Acad Sci U S A 97*, 13573-8.

(11) O'Brien, P. J., and Ellenberger, T. (2003) Human alkyladenine DNA glycosylase uses acid-base catalysis for selective excision of damaged purines. *Biochemistry 42*, 12418-29.

(12) O'Brien, P. J., and Ellenberger, T. (2004) Dissecting the broad substrate specificity of human 3-methyladenine-DNA glycosylase. *J Biol Chem 279*, 9750-7.

(13) Trewick, S. C., Henshaw, T. F., Hausinger, R. P., Lindahl, T., and Sedgwick, B. (2002) Oxidative demethylation by Escherichia coli AlkB directly reverts DNA base damage. *Nature 419*, 174-8.

(14) Falnes, P. O., Johansen, R. F., and Seeberg, E. (2002) AlkB-mediated oxidative demethylation reverses DNA damage in Escherichia coli. *Nature 419*, 178-82.
(15) Delaney, J. C., and Essigmann, J. M. (2004) Mutagenesis, genotoxicity, and repair of 1-methyladenine, 3-alkylcytosines, 1-methylguanine, and 3-methylthymine in alkB Escherichia coli. *Proc Natl Acad Sci U S A 101*, 14051-6.
(16) Falnes, P. O. (2004) Repair of 3-methylthymine and 1-methylguanine lesions by bacterial and human AlkB proteins. *Nucleic Acids Res 32*, 6260-7.
(17) Koivisto, P., Robins, P., Lindahl, T., and Sedgwick, B. (2004) Demethylation of 3-methylthymine in DNA by bacterial and human DNA dioxygenases. *J Biol Chem 279*, 40470-4.
(18) Ougland, R., Zhang, C. M., Liiv, A., Johansen, R. F., Seeberg, E., Hou, Y. M., Remme, J., and Falnes, P. O. (2004) AlkB restores the biological function of mRNA and tRNA inactivated by chemical methylation. *Mol Cell 16*, 107-16.
(19) Aas, P. A., Otterlei, M., Falnes, P. O., Vagbo, C. B., Skorpen, F., Akbari, M., Sundheim, O., Bjoras, M., Slupphaug, G., Seeberg, E., and Krokan, H. E. (2003) Human and bacterial oxidative demethylases repair alkylation damage in both RNA and DNA. *Nature 421*, 859-63.
(20) Falnes, P. O., Bjoras, M., Aas, P. A., Sundheim, O., and Seeberg, E. (2004) Substrate specificities of bacterial and human AlkB proteins. *Nucleic Acids Res 32*, 3456-61.
(21) Westbye, M. P., Feyzi, E., Aas, P. A., Vagbo, C. B., Talstad, V. A., Kavli, B., Hagen, L., Sundheim, O., Akbari, M., Liabakk, N. B., Slupphaug, G., Otterlei, M., and Krokan, H. E. (2008) Human AlkB homolog 1 is a mitochondrial protein that demethylates 3-methylcytosine in dna and RNA. *J Biol Chem.*
(22) Frick, L. E., Delaney, J. C., Wong, C., Drennan, C. L., and Essigmann, J. M. (2007) Alleviation of 1,N6-ethanoadenine genotoxicity by the Escherichia coli adaptive response protein AlkB. *Proc Natl Acad Sci U S A 104*, 755-60.
(23) Delaney, J. C., Smeester, L., Wong, C., Frick, L. E., Taghizadeh, K., Wishnok, J. S., Drennan, C. L., Samson, L. D., and Essigmann, J. M. (2005) AlkB reverses etheno DNA lesions caused by lipid oxidation in vitro and in vivo. *Nat Struct Mol Biol 12*, 855-60.
(24) Mishina, Y., Yang, C. G., and He, C. (2005) Direct repair of the exocyclic DNA adduct 1,N6-ethenoadenine by the DNA repair AlkB proteins. *J Am Chem Soc 127*, 14594-5.
(25) Ringvoll, J., Moen, M. N., Nordstrand, L. M., Meira, L. B., Pang, B., Bekkelund, A., Dedon, P. C., Bjelland, S., Samson, L. D., Falnes, P. O., and Klungland, A. (2008) AlkB homologue 2-mediated repair of ethenoadenine lesions in mammalian DNA. *Cancer Res 68*, 4142-9.
(26) Leonard, N. J. (1984) Etheno-substituted nucleotides and coenzymes: fluorescence and biological activity. *CRC Crit Rev Biochem 15*, 125-99.
(27) el Ghissassi, F., Barbin, A., and Bartsch, H. (1998) Metabolic activation of vinyl chloride by rat liver microsomes: low-dose kinetics and involvement of cytochrome P450 2E1. *Biochem Pharmacol 55*, 1445-52.
(28) Guengerich, F. P., Crawford, W. M., Jr., and Watanabe, P. G. (1979) Activation of vinyl chloride to covalently bound metabolites: roles of 2-chloroethylene oxide and 2-chloroacetaldehyde. *Biochemistry 18*, 5177-82.

(29) Guengerich, F. P. (1992) Roles of the vinyl chloride oxidation products 1-chlorooxirane and 2-chloroacetaldehyde in the in vitro formation of etheno adducts of nucleic acid bases [corrected]. *Chem Res Toxicol 5*, 2-5.
(30) Guengerich, F. P., Persmark, M., and Humphreys, W. G. (1993) Formation of 1,N2- and N2,3-ethenoguanine from 2-halooxiranes: isotopic labeling studies and isolation of a hemiaminal derivative of N2-(2-oxoethyl)guanine. *Chem Res Toxicol 6*, 635-48.
(31) Kusmierek, J. T., and Singer, B. (1982) Chloroacetaldehyde-treated ribo- and deoxyribopolynucleotides. 1. Reaction products. *Biochemistry 21*, 5717-22.
(32) Kusmierek, J. T., and Singer, B. (1992) 1,N2-ethenodeoxyguanosine: properties and formation in chloroacetaldehyde-treated polynucleotides and DNA. *Chem Res Toxicol 5*, 634-8.
(33) Dosanjh, M. K., Chenna, A., Kim, E., Fraenkel-Conrat, H., Samson, L., and Singer, B. (1994) All four known cyclic adducts formed in DNA by the vinyl chloride metabolite chloroacetaldehyde are released by a human DNA glycosylase. *Proc Natl Acad Sci U S A 91*, 1024-8.
(34) Ludlum, D. B. (1990) DNA alkylation by the haloethylnitrosoureas: nature of modifications produced and their enzymatic repair or removal. *Mutat Res 233*, 117-26.
(35) Guliaev, A. B., Hang, B., and Singer, B. (2002) Structural insights by molecular dynamics simulations into differential repair efficiency for ethano-A versus etheno-A adducts by the human alkylpurine-DNA N-glycosylase. *Nucleic Acids Res 30*, 3778-87.
(36) Abner, C. W., Lau, A. Y., Ellenberger, T., and Bloom, L. B. (2001) Base excision and DNA binding activities of human alkyladenine DNA glycosylase are sensitive to the base paired with a lesion. *J Biol Chem 276*, 13379-87.
(37) Zang, H., Goodenough, A. K., Choi, J. Y., Irimia, A., Loukachevitch, L. V., Kozekov, I. D., Angel, K. C., Rizzo, C. J., Egli, M., and Guengerich, F. P. (2005) DNA adduct bypass polymerization by Sulfolobus solfataricus DNA polymerase Dpo4: analysis and crystal structures of multiple base pair substitution and frameshift products with the adduct 1,N2-ethenoguanine. *J Biol Chem 280*, 29750-64.
(38) Wang, H., Marnett, L. J., Harris, T. M., and Rizzo, C. J. (2004) A novel synthesis of malondialdehyde adducts of deoxyguanosine, deoxyadenosine, and deoxycytidine. *Chem Res Toxicol 17*, 144-9.
(39) Adhikari, S., Uren, A., and Roy, R. (2007) N-terminal extension of N-methylpurine DNA glycosylase is required for turnover in hypoxanthine excision reaction. *J Biol Chem 282*, 30078-84.
(40) Hitchcock, T. M., Dong, L., Connor, E. E., Meira, L. B., Samson, L. D., Wyatt, M. D., and Cao, W. (2004) Oxanine DNA glycosylase activity from Mammalian alkyladenine glycosylase. *J Biol Chem 279*, 38177-83.
(41) Saparbaev, M., Langouet, S., Privezentzev, C. V., Guengerich, F. P., Cai, H., Elder, R. H., and Laval, J. (2002) 1,N(2)-ethenoguanine, a mutagenic DNA adduct, is a primary substrate of Escherichia coli mismatch-specific uracil-DNA glycosylase and human alkylpurine-DNA-N-glycosylase. *J Biol Chem 277*, 26987-93.

(42) Wuenschell, G. E., O'Connor, T. R., and Termini, J. (2003) Stability, miscoding potential, and repair of 2'-deoxyxanthosine in DNA: implications for nitric oxide-induced mutagenesis. *Biochemistry 42*, 3608-16.
(43) Bjelland, S., and Seeberg, E. (1996) Different efficiencies of the Tag and AlkA DNA glycosylases from Escherichia coli in the removal of 3-methyladenine from single-stranded DNA. *FEBS Lett 397*, 127-9.
(44) Eftedal, I., Guddal, P. H., Slupphaug, G., Volden, G., and Krokan, H. E. (1993) Consensus sequences for good and poor removal of uracil from double stranded DNA by uracil-DNA glycosylase. *Nucleic Acids Res 21*, 2095-101.
(45) Haushalter, K. A., Todd Stukenberg, M. W., Kirschner, M. W., and Verdine, G. L. (1999) Identification of a new uracil-DNA glycosylase family by expression cloning using synthetic inhibitors. *Curr Biol 9*, 174-85.
(46) Dianov, G., and Lindahl, T. (1991) Preferential recognition of I.T base-pairs in the initiation of excision-repair by hypoxanthine-DNA glycosylase. *Nucleic Acids Res 19*, 3829-33.
(47) Saparbaev, M., Mani, J. C., and Laval, J. (2000) Interactions of the human, rat, Saccharomyces cerevisiae and Escherichia coli 3-methyladenine-DNA glycosylases with DNA containing dIMP residues. *Nucleic Acids Res 28*, 1332-9.
(48) Wyatt, M. D., and Samson, L. D. (2000) Influence of DNA structure on hypoxanthine and 1,N(6)-ethenoadenine removal by murine 3-methyladenine DNA glycosylase. *Carcinogenesis 21*, 901-8.
(49) Elder, R. H., Jansen, J. G., Weeks, R. J., Willington, M. A., Deans, B., Watson, A. J., Mynett, K. J., Bailey, J. A., Cooper, D. P., Rafferty, J. A., Heeran, M. C., Wijnhoven, S. W., van Zeeland, A. A., and Margison, G. P. (1998) Alkylpurine-DNA-N-glycosylase knockout mice show increased susceptibility to induction of mutations by methyl methanesulfonate. *Mol Cell Biol 18*, 5828-37.
(50) Pearl, L. H. (2000) Structure and function in the uracil-DNA glycosylase superfamily. *Mutat Res 460*, 165-81.

5. CHAPTER 5 -- Summary and Conclusions

5.1. Summary and Conclusions

In this thesis, we explored the repair of DNA damages by a set of direct reversal DNA repair proteins, namely AlkB and two of its mammalian homologs (ABH2 and ABH3), and any interaction and overlap with the base excision repair protein AAG, particularly in response to pathology involving etheno base lesions. To approach this study, we first examined whether expression of the AlkB and ABH proteins in *E. coli* and established human cell lines could confer resistance upon alkylation damage. We demonstrated that AlkB and ABH expression in AlkB-deficient *E. coli* strain enhance survival upon MMS treatment. However, no phenotypic difference was observed in several human cell lines with expressed AlkB/ABH when compared to wild-type cells. It is possible that the protein levels are tightly regulated in order to minimize the generation of the toxic formaldehyde byproduct from the repair reaction by AlkB, which must be further processed by the cell. We also hypothesize that endogenous ABH proteins are likely maintained at sufficient levels for repair of the small amounts of 1meA and 3meC induced by MMS in double-stranded DNA due to their involvement in base-pairing. Therefore, expressed ABH proteins may not be needed and eventually degraded. Also, it is possible that the ABH proteins need to interact with each other for maximal function so that singly expressed ABH proteins may not enhance the repair.

We next focused on mice deficient in Abh2 and/or Abh3 in order to investigate whether using knockout cells would eliminate the possibility of sufficient repair by endogenous

Abh proteins. This also allowed us to determine any interaction between the Abh2 and Abh3 proteins. Following treatment of bone marrow cells *ex vivo* with MMS, we observed that *Abh2*$^{-/-}$ or *Abh2*$^{-/-}$*Abh3*$^{-/-}$ bone marrow cells exhibited increased sensitivity compared to WT or *Abh3*$^{-/-}$ bone marrow cells. These results are consistent with a previous finding in mouse embryonic fibroblasts (*1*), indicating a protective role of the Abh2 protein upon MMS exposure in a knockout background.

Results thus far led us to further explore the role of the Abh2 and Abh3 proteins in a knockout background. Using the Abh2/Abh3 knockout mice, we examined not only the genetic interaction between Abh2 and Abh3, but also how they relate to the Aag DNA glycosylase enzyme that can initiate BER at a variety of alkylated DNA bases. To this end, we studied the response to chronic inflammation in mice deficient for Aag and/or Abh2 and Abh3, because all three proteins repair etheno base lesions, common lesions induced by chronic inflammation. Using the mouse model of AOM and DSS to mimic episodic colitis, we found that either in the absence of Aag, or in the absence of both Abh2 and Abh3, an increased sensitivity was observed including increased colon tumors and more severe spleen and colon pathology.

The effects of Abh2 and Abh3 proteins appear to lead to differences in sensitivity in different cell types. Unlike in the mouse embryonic fibroblasts (*1*) and bone marrow, where the deficiency in Abh2 alone (but not Abh3 alone) leads to sensitivity against MMS damage, the absence of Abh2 alone does not result in measurable sensitivities in the spleen and colon, or tumor formation in response to chronic inflammation, in the

presence or absence of Aag. Only sensitivity from a combined effect of Abh2 and Abh3 together was observed, indicating that absence of Abh2 alone does not significantly alter the response to chronic inflammation. Although it is necessary to determine whether *Abh3*$^{-/-}$ single knockout mice exhibit increased sensitivity, it is possible that either Abh2 does not contribute to repair or it needs to work in a complex with Abh3 together for maximal activity in fighting the DNA damage induced by inflammation. We found that in the response to chronic inflammation, base excision repair initiated by Aag remains as the more dominant pathway in alleviating the effects of the inflammation-induced DNA damage as deficiency in Aag tends to mask any possible sensitivity from the absence of Abh2 or Abh3.

To further examine the genetic interaction of Aag, Abh2, and Abh3 *in vivo*, it will be necessary to examine the response of the *Abh3*$^{-/-}$ single mutant and *Aag*$^{-/-}$*Abh2*$^{-/-}$*Abh3*$^{-/-}$ triple mutant to DSS-induced chronic colonic inflammation in order to determine whether individual effects of Abh3 are detectable in the presence of Aag. The triple mutant would aid in determining whether the single effect of Aag plus the combined effect of Abh2 and Abh3 would greatly sensitize the mice. Moreover, molecular analysis measuring the levels of accumulated base lesions, such as εA, εC, and 8oxoG, in the AOM + DSS-induced chronic inflammation model in the different genotypes would confirm whether sensitivities and tumorigenesis were indeed caused by unrepaired RONS-induced DNA damage in the repair-deficient animals, as we have shown in *Aag*$^{-/-}$ mice (*2*). This would be particularly informative for *Abh2*$^{-/-}$*Abh3*$^{-/-}$, *Aag*$^{-/-}$, *Aag*$^{-/-}$*Abh2*$^{-/-}$, and *Aag*$^{-/-}$*Abh3*$^{-/-}$, in which increased tumorigenesis was significant. It would also be interesting to determine

which lesions increased in these mice, and whether the lesion accumulations correlate to the substrate preference by Aag versus Abh2/3.

To further understand the overlap in repair activity between AlkB and AAG, we examined the kinetics of AAG activity on an extensive library of lesion-containing DNA oligonucleotides. From these experiments, we observed multiple novel findings, including a new substrate shared between AlkB and AAG, namely 1-methylguanine. This strengthens the overlap in substrates repaired by these two proteins, in addition to the already known substrates εA, EA (repaired robustly by AlkB), and 1,N^2-εG (repaired weakly by AlkB).

To follow up on these findings, it would be interesting to examine any possible physical interactions between AlkB and AAG. Because AAG was found to bind to a wide range of substrates but only to excise a few, it would be interesting to examine whether AAG can serve as an inhibitor in the repair reaction by AlkB on substrates that are tightly bound by AAG but not repaired. Indeed, Fu and Samson have unpublished data indicating that this is the case. Similarly, we can test whether AlkB can inhibit repair of the shared substrates by AAG in reaction conditions optimized for AAG. In order to assess whether these proteins compete for the same binding site on DNA, DNA footprinting assays could also be performed. Furthermore, competition studies with both AlkB and AAG acting on their shared substrates may allow us to determine which protein is preferred for repair.

In addition to studying inflammation in colon induced by a chemical irritant, we could examine other mouse models of chronic inflammation. For example, one such approach is to use a model involving mice deficient in interleukin-10 (IL-10). IL-10 inhibits production of pro-inflammatory cytokines and its deficiency can lead to spontaneous colitis (*3*) in response to gut flora (*4*). Thus, examining the effects of colitis on double or triple mutants of *IL-10*$^{-/-}$, *Abh2*$^{-/-}$, *Abh3*$^{-/-}$, and *Aag*$^{-/-}$ mice would allow us to determine whether Aag and/or Abh2/3 proteins can also suppress colon tumorigenesis and the sensitive phenotype from colitis not induced chemically.

Other than models of inflammation in the colon, we can examine chronic inflammation in different tissues to determine whether this protective effect of Aag and/or Abh2/3 proteins is a global effect. For example, chronic inflammation of the liver (hepatitis) is associated with the development of hepatocellular carcinoma (HCC). One established mouse model of inflammation-associated HCC model is the *Mdr2*$^{-/-}$ mice. These mice are deficient in the liver-specific P-glycoprotein that transports phosphatidylcholine across the bile canalicular membrane, giving rise to accumulation of bile acids and portal inflammation (*5-7*). Liver inflammation leads to hepatocyte dysplasia and a high incidence of liver tumors in *Mdr2*$^{-/-}$ mice as early as 16 months (*5*). Studying mutants of *Mdr2*$^{-/-}$ with *Aag*$^{-/-}$ and/or *Abh*$^{-/-}$ will allow us to determine whether these repair proteins also have protective roles in another model of inflammation.

5.2. References

(1) Ringvoll, J., Nordstrand, L. M., Vagbo, C. B., Talstad, V., Reite, K., Aas, P. A., Lauritzen, K. H., Liabakk, N. B., Bjork, A., Doughty, R. W., Falnes, P. O., Krokan, H. E., and Klungland, A. (2006) Repair deficient mice reveal mABH2 as the primary oxidative demethylase for repairing 1meA and 3meC lesions in DNA. *Embo J 25*, 2189-98.

(2) Meira, L. B., Bugni, J. M., Green, S. L., Lee, C. W., Pang, B., Borenshtein, D., Rickman, B. H., Rogers, A. B., Moroski-Erkul, C. A., McFaline, J. L., Schauer, D. B., Dedon, P. C., Fox, J. G., and Samson, L. D. (2008) DNA damage induced by chronic inflammation contributes to colon carcinogenesis in mice. *J Clin Invest 118*, 2516-25.

(3) Kuhn, R., Lohler, J., Rennick, D., Rajewsky, K., and Muller, W. (1993) Interleukin-10-deficient mice develop chronic enterocolitis. *Cell 75*, 263-74.

(4) Madsen, K. L. (2001) Inflammatory bowel disease: lessons from the IL-10 gene-deficient mouse. *Clin Invest Med 24*, 250-7.

(5) Katzenellenbogen, M., Mizrahi, L., Pappo, O., Klopstock, N., Olam, D., Jacob-Hirsch, J., Amariglio, N., Rechavi, G., Domany, E., Galun, E., and Goldenberg, D. (2007) Molecular mechanisms of liver carcinogenesis in the mdr2-knockout mice. *Mol Cancer Res 5*, 1159-70.

(6) Fickert, P., Fuchsbichler, A., Wagner, M., Zollner, G., Kaser, A., Tilg, H., Krause, R., Lammert, F., Langner, C., Zatloukal, K., Marschall, H. U., Denk, H., and Trauner, M. (2004) Regurgitation of bile acids from leaky bile ducts causes sclerosing cholangitis in Mdr2 (Abcb4) knockout mice. *Gastroenterology 127*, 261-74.

(7) De Vree, J. M., Ottenhoff, R., Bosma, P. J., Smith, A. J., Aten, J., and Oude Elferink, R. P. (2000) Correction of liver disease by hepatocyte transplantation in a mouse model of progressive familial intrahepatic cholestasis. *Gastroenterology 119*, 1720-30.